VNIVERSITAT DE VALÈNCIA

Departamento de Física Teórica, Facultad de Física
Doctorado en Física

Dynamical gluon mass generation in pure Yang-Mills theories.

PhD dissertation by

David Ibáñez Gil de Ramales

Thesis director

Joannis Papavassiliou

Valencia, Spain; June, 2012

Joannis Papavassiliou, Profesor Titular de la Universidad de Valencia,

CERTIFICA:

Que la presente memoria,

"Dynamical gluon mass generation in pure Yang-Mills theories"
ha sido realizada bajo su dirección en el Departamento de Física Teórica de la Universidad de Valencia-IFIC, por **David Ibáñez Gil de Ramales** y constituye su Tesis para optar al grado de Doctor en Física.

Y para que así conste, en cumplimiento de la legislación vigente, presenta en el Departamento de Física Teórica la referida Tesis Doctoral y firma el presente certificado en Valencia, a 25 de junio de 2012.

Firma del director de tesis

Joannis Papavassiliou

Agradecimientos

En fin, va siendo hora de terminar esta tesis y cerrarla escribiendo, quizás, la sección más difícil y complicada, los agradecimientos. Es complicada porque a lo largo de estos últimos cuatro años muchísimas buenas personas han pasado por mi vida. Por este motivo, mis agradecimientos empiezan con un *agradecimiento general* hacia todas ellas.

Pero desde luego, si hay una persona que debe encabezar estos agradecimientos, esa es Joannis Papavassiliou, mi director de tesis. La razón de ello es muy clara. Esta tesis nunca hubiera existido (al menos escrita por mí), si Joannis no hubiera supervisado y dirigido mi trabajo de investigación. Pero más allá de ello, le debo un agradecimiento mucho más profundo, porque no ha sido solo un nombre sobre el documento de turno que lo acredita como mi director de tesis. Desde el principio hasta el final de esta tesis ha estado implicado y siempre disponible para discutir ideas y para formarme como investigador. Por supuesto, también para enfadarse de vez en cuando. Así pués, considero que la presente tesis es tanto suya como mía.

Junto con Joannis, hay dos personas también importantísimas sin las cuales esta tesis tampoco hubiera sido nunca escrita. Daniele Binosi y Cristina Aguilar. A ellos les debo muchísimo y les agradezco enormemente haber estado ahí.

Bueno, no menos importantes son las personas que aparecen a continuación. Como dijo un buen amigo ellos son "los grandes físicos que te han inspirado y ayudado en los momentos más difíciles (sin hablar de los momentos difíciles que gracias a ellos has vivido)". Diego Milanés, Jorge Martín, Daniel Gamerman, Fabio Bernardoni y Oliver Valero, que aunque no sea físico le gustan las partículas que viajan a más velocidad que la luz. Decir que son amigos es poco. Son como hermanos para mí y, aunque ahora estamos dispersos por el mundo, siempre hay lugar para el reencuentro y nunca podré agradecer lo suficiente todo lo que hemos compartido juntos (y seguimos compartiendo).

Y como este mundo de la investigación es tan dinámico y las personas vienen y van, llegaron Javier Rasero, Joaquín Ruiz y Juan Herrero. Además de Alberto Aparici, que ya estaba por aquí. También se han ganado su merecido agradecimiento explícito.

Parece mentira que hasta el momento no haya aparecido ninguna mujer, salvo Cristina, pero el que es físico sabe muy bien que es difícil conocerlas en este ámbito. Sin embargo, por suerte, también hay algunas amigas por ahí a las que tengo que mencionar aquí. Clarilla Panea, Carmen Moret,

Bibiana Pérez, Aurora Courtoy, Adela Lope y Mira Minges.

Finally I should also mention the members of my thesis evaluation committee. They are Vicente Vento, Nick Mavromatos, Teresa Mendez and Pedro González. Thanks for doing the effort of read almost 200 pages about the gluon mass generation mechanism.

Por último unas líneas para tres amigas a las que tengo un cariño muy especial. Olivia Jüestel, Eva Koch y Laura Lopera.

This work has been supported by the Spanish MEYC under Grant No. FPA2011-23596.

A mi yaya Carmen y a mi tío Antonio.
A mi hermanita Mariana y a mis padres Paco y Vicki.
A toda la familia Gil de Ramales.
Y por supuesto, a mi mismo.

CONTENTS

1. INTRODUCTION (INTRODUCCIÓN).

Nowadays Quantum Chromodynamics (QCD) is without any doubt the accepted quantum field theory used to describe the behavior of the strong interactions from the point of view of their fundamental constituents, quarks and gluons, in the entire range of energies. As is well known, the running of the strong coupling constant is such that, in the ultraviolet regime (high energies), the theory exhibits the property of asymptotic freedom [1], allowing for a perturbative treatment of the physics at this scale of energies. However, in the infrared regime (low energies), the strong interaction becomes truly strong, thus invalidating any attempt to employ perturbation theory. For this reason one is forced to appeal to nonperturbative methods.

The most widely used framework for studying in the continuum various dynamical questions that lie beyond perturbation theory are the Schwinger-Dyson equations (SDEs) [2, 3]. This infinite system of coupled non-linear integral equations for all Green's functions of the theory is inherently non-perturbative, and captures the full content of the quantum equations of motion. Even though these equations are derived by an expansion about the free-field vacuum, they finally make no reference to it, or to perturbation theory, and can be used to address problems related to chiral symmetry breaking, dynamical mass generation, formation of bound states, and other non-perturbative effects [4, 5].

Specifically, the generation of mass gaps in QCD is one of the most fundamental problems in particle physics. In part the difficulty lies in the fact that the symmetries governing the QCD Lagrangian prohibit the appearance of mass terms at tree-level for all fundamental fields and, provided that these symmetries are not violated through the procedure of regularization, this masslessness persists to all orders in perturbation theory. Thus, mass generation in QCD becomes an inherently non perturbative problem, whose tackling requires the use of rather sophisticated calculational tools and approximation schemes.

Whereas the generation of quark masses is intimately connected with

the breaking of chiral symmetry [6], Cornwall argued long ago [7] that an effective gluon mass can be generated dynamically, while preserving the $SU(3)_C$ invariance of QCD, in close analogy to what happens in QED_2 (Schwinger model), where the photon acquires a mass without violating the Abelian gauge symmetry (see Chapter 4). This is possible thanks to the famous Schwinger mechanism, which exploits the fact that the gauge invariance of a vector field does not necessarily imply zero mass for the associated particle, if the current vector coupling is sufficiently strong [8]. Schwinger's fundamental observation was that (if for some reason) the vacuum polarization tensor $\Pi_{\mu\nu}(q)$ acquires a pole at zero momentum transfer, then the vector field becomes massive, even if the gauge symmetry forbids a mass at the level of the fundamental Lagrangian [9].

Perhaps the most salient feature of the Schwinger mechanism is that the appearance of the required massless pole may happen for purely dynamical reasons, and, in particular, without the need to introduce fundamental scalar fields in the Lagrangian. Therefore, in the seventies, the Schwinger mechanism has been extensively studied, as an appealing alternative to the Higgs mechanism [10–14], employed in the electroweak sector.

The general philosophy adopted when applying the Schwinger mechanism to pure Yang-Mills theories (without matter fields), such as quarkless QCD, is the following [15]. One assumes that, in a strongly-coupled gauge theory, longitudinally coupled, zero-mass bound-state excitations are dynamically produced. To be sure, the demonstration of the existence of a bound-state, and in particular a zero-mass bound-state, in realistic field theories is a difficult dynamical problem usually studied by means of integral equations, known as Bethe-Salpeter (BS) equations (see, e.g., [16]). Thus, it is clear that a vital ingredient for this scenario is strong coupling, which can only come from the infrared instabilities of a non-Abelian gauge theories. The aforementioned excitations are like dynamical Nambu-Goldstone bosons [17–21], in the sense that they are massless, composite, and longitudinally coupled; but at the same time, they differ from Nambu-Goldstone bosons as far as their origin is concerned: they do not originate from the spontaneous breaking of any global symmetry. The main role of these excitations is to trigger the Schwinger mechanism, i.e., to provide the required pole in the gluon self-energy $\Pi_{\mu\nu}(q)$. In addition they preserve the form of the Ward identities (WIs) and the Slavnov-Taylor identities (STIs) of the theory in the presence of a mass (e.g., [22]), thus furnishing a gauge-invariant gluon mass generation mechanism.

To understand why such poles must be introduced in the massive theory, we turn to the following simplified situation. Consider then the tree-level value for the conventional three-gluon vertex (see Appendix A),

$$\Gamma_{\alpha\mu\nu}(q,r,p) = (r-p)_\alpha g_{\mu\nu} + (p-q)_\mu g_{\nu\alpha} + (q-r)_\nu g_{\alpha\mu}. \tag{1.1}$$

It is elementary to verify that this vertex satisfy the following WI

$$q^\alpha \Gamma_{\alpha\mu\nu}(q,r,p) = d^{-1}(p)P_{\mu\nu}(p) - d^{-1}(r)P_{\mu\nu}(r), \tag{1.2}$$

where the rhs is the difference of two inverse tree-level propagators in the Landau gauge, since the quantity $d^{-1}(q) = q^2$ is the inverse of the tree-level form factor appearing in the gluon propagator, whereas

$$P_{\mu\nu}(q) = g_{\mu\nu} - \frac{q_\mu q_\nu}{q^2} \tag{1.3}$$

is the usual transverse projector. Supposing now that the gluon propagator develops a mass $m^2(q)$, how must one modify the three-gluon vertex in order for the WI to continue been valid, which is tantamount to saying that the gauge invariance remains intact? Thus, replace the $d^{-1}(q)$ by $d_m^{-1}(q) = q^2 - m^2(q)$ and substitute it in the rhs of Eq. (1.2). In order to maintain the validity of the WI one must simultaneously replace the three-gluon vertex on the lhs by the vertex

$$\Gamma'_{\alpha\mu\nu}(q,r,p) = \Gamma_{\alpha\mu\nu}(q,r,p) + V_{\alpha\mu\nu}(q,r,p), \tag{1.4}$$

where the new part V must be such that it satisfies the following WI

$$q^\alpha V_{\alpha\mu\nu}(q,r,p) = m^2(r)P_{\mu\nu}(r) - m^2(p)P_{\mu\nu}(p). \tag{1.5}$$

Evidently, a solution of Eq. (1.5) is given by

$$V_{\alpha\mu\nu}(q,r,p) = \frac{q_\alpha}{q^2}[m^2(r)P_{\mu\nu}(r) - m^2(p)P_{\mu\nu}(p)]. \tag{1.6}$$

So, the new vertex V has, as mentioned above, terms with longitudinally-coupled massless poles.

From this simple example one learns that the composite excitations must be incorporated at the level of the Green's functions adding a new kind of nonperturbative vertices, denoted generically by V and referred to as "pole vertices". They contain massless poles and satisfy very specific

STIs, completely determined by the requirement of preserving the gauge invariance of the theory in the presence of a mass.

At this point, the study of the gluon mass generation mechanism in pure Yang-Mills theories may be tackled following two rather distinct procedures. The difference between them lies in how the V vertices are employed in order to extract information about the effective gluon mass. Specifically, in the first procedure, one assumes from the beginning that the strong interaction favors the dynamical formation of the necessary massless bound-states required for the existence of the pole vertices. Then, these special vertices are incorporated into the SDE of the gluon propagator and one operates at this level to derive a mass equation, which describes the evolution of the effective momentum-dependent gluon mass. Interestingly enough, this can be accomplished without knowledge of the explicit closed form of the nonperturbative vertices, relying only on their general features, most notably their longitudinal nature and the STIs that they satisfy. Using this procedure we will be able to obtain the all-order equation of the effective gluon mass, Eq. (6.68), as well as the solutions of this equation in the entire range of momenta [section 6.5 in chapter 6]. Thus, in this approach, the pole vertices are used in an "effective" way, i.e., without appealing to the dynamical origin of their fundamental components.

In the second procedure we take a closer look at the "microscopic" structure and composition of these vertices, as well as their actual dynamical formation. To that end, we introduce two crucial nonperturbative ingredients, namely, the transition amplitude Fig. 7.9, which connects the massless bound-state with a gluon, and certain effective vertices allowing the mixing between the massless bound-state and gluons or ghosts Fig. 7.4. At this level, one needs to demonstrate that none of these new ingredients is zero, otherwise the entire construction collapses. This is accomplished by proving the existence of the massless bound-states through a detailed BS analysis. Indeed, a preliminary mumerical study of the BSE is reported in section 5.5 of chapter 5, which confirms the existence of the aforementioned massless bound-states. Finally, once this is proved, in chapter 7, the gluon mass will be expressed through a very simple formula, Eq. (7.30), in terms of the transition amplitude, which in turn has a clear physical interpretation in terms of bound-state exchanges.

We conclude this introduction by presenting a roadmap of the topics discussed in the several chapters of this thesis.

Chapter 2. We present the recent results obtained in large-volume lattice sim-

ulations for the gluon propagator and the ghost dressing function, signaling that both are infrared finite. These lattice results and their possible explanation in terms of an effective gluon mass, motivate the detailed study of the phenomenon of dynamical (gluon) mass generation in the context of pure Yang-Mills theories.

Chapter 3. The exclusively nonperturbative nature of the mass generation mechanism forces us to employ for its description the formalism of the SDEs. This complicated set of integral equations will be analyzed throughout this thesis in the framework of the PT-BFM scheme, provided by the synthesis of the Pinch Technique (PT) [23, 24] and the Background Field Method (BFM) [25]. Here we outline the basic features and properties that make so advantageous the use of the PT-BFM scheme when dealing with the SDE.

Chapter 4. In this chapter we formulate the general statement of the Schwinger mechanism and we show how this mechanism generates a mass term for gauge bosons, without interfering with the gauge-invariance of the theory. Specifically, we will study briefly the Schwinger model and the Jackiw-Johnson model, where the Schwinger mechanism is applied in Abelian gauge theories.

Chapter 5. The aim of this chapter is two-fold. Provide a preliminary analysis on how the Schwinger mechanism is realized in a non Abelian context and show, through a detailed numerical study, that the dynamics of pure Yang-Mills theories support indeed the formation of the aforementioned massless bound-states.

Chapter 6. This chapter contains the general derivation of the full non-perturbative equation describing the evolution of the dynamically generated gluon mass in the Landau gauge. The mass equation is then scrutinized in a detailed numerical analysis, revealing the existence of monotonically decreasing solutions for the effective momentum-dependent gluon mass.

Chapter 7. The objective of this final chapter is to realize a general description of the mass generation mechanism in the language of bound-state excitations. After a precise definition of the required ingredients, the effective gluon mass is expressed by means of an exact and simple mass formula. Then, in a decisive self-consistency check, we show

that the above mass formula reproduces the mass equation obtained in chapter 6, thus proving that both approaches are totally equivalent.

The thesis ends with some concluding remarks in Chapter 8 about the problem of confinement and its possible relation with the gluonic mass generation mechanism, and two appendices where the QCD Lagrangian and the BFM are briefly discussed.

1. Introducción.

Actualmente, la Cromodinámica cuántica (QCD, por supuesto las siglas no coinciden cuando se escribe en español) es sin lugar a duda la teoría cuántica de campos aceptada para describir el comportamiento de las interacciones fuertes desde el punto de vista de sus constituyentes fundamentales, quarks y gluones, en todo el rango de energías. Como es bien conocido, la dependencia de la constante de acoplamiento fuerte con la energía es tal que, en el régimen ultravioleta (altas energías), la teoría exhibe la propiedad de libertad asintótica [1], permitiendo un tratamiento perturbativo de la física de las interacciones fuertes en esta escala de energías. Sin embargo, en el régimen infrarrojo (bajas energías), la interacción fuerte se hace "verdaderamente" fuerte invalidando, por tanto, el empleo de teoría de perturbaciones. Por este motivo, uno se ve forzado a recurrir a los métodos no perturbativos.

El esquema de trabajo comúnmente usado para estudiar en el continuo varios problemas dinámicos que escapan a la teoría de perturbaciones, recibe el nombre de ecuaciones de Schwinger-Dyson [2, 3]. Este sistema infinito de ecuaciones integrales acopladas no lineales para todas las funciones de Green de la teoría es inherentemente no perturbativo y captura el contenido completo de las ecuaciones de movimiento cuánticas. A pesar de que estas ecuaciones se derivan realizando una expansión alrededor de un vacío libre de campos, finalmente no hacen referencia a dicho vacío, o a la teoría de perturbaciones, y pueden utilizarse para abordar problemas relacionados con la ruptura de simetría quiral, la generación dinámica de masas, la formación de estados ligados, y otros efectos no perturbativos [4, 5].

Específicamente, la generación de masas en QCD es uno de los problemas más fundamentales en física de partículas. En parte, la dificultad radica en el hecho de que las simetrías que gobiernan el lagrangiano de QCD prohíben la aparición de términos de masas para todos los campos fundamentales que aparecen en él y, dado que dichas simetrías no son violadas por ningún proceso de regularización, los campos continúan siendo no masivos a todos los órdenes en teoría de perturbaciones. Por tanto, la generación de masas en QCD se manifiesta como un fenómeno puramente no perturbativo, cuyo estudio requiere el uso de técnicas más sofisticadas.

Mientras la generación de masas de quarks esta íntimamente conectada con la ruptura de simetría quiral [6], Cornwall argumentó [7] que se puede generar dinámicamente una masa efectiva para el gluon al mismo tiempo que se preserva la invariancia $SU(3)_C$ de QCD, análogamente a lo

que ocurre en QED_2 (modelo de Schwinger), donde el fotón adquiere una masa sin violar la simetría gauge Abeliana (ver Capítulo 4). Esto es posible gracias al famoso mecanismo de Schwinger, el cual explota el hecho de que la invariancia gauge de un campo vectorial no implica necesariamente masa cero para el campo asociado, si la corriente vectorial es suficientemente fuerte [8]. La observación fundamental de Schwinger fue que, si por alguna razón, el tensor de polarización del vacío $\Pi_{\mu\nu}(q)$ adquiere un polo cuando la transferencia de momento es cero, entonces el campo vectorial se hace masivo, aun cuando la simetría gauge prohíba una masa a nivel del lagrangiano [9].

Quizás, la característica más sobresaliente del mecanismo de Schwinger es que la aparición del polo requerido puede ocurrir debido a motivos puramente dinámicos y, en particular, sin la necesidad de introducir campos escalares fundamentales en el lagrangiano. Debido a ello, el mecanismo de Schwinger fue extensivamente estudiado en los setenta como una firme alternativa al mecanismo de Higgs [10–14], empleado en el sector electrodébil.

La filosofía general adoptada cuando se aplica el mecanismo de Schwinger al estudio de teorías puras de Yang-Mills (sin campos de materia), como es el caso de QCD sin quarks, se puede esbozar de la siguiente manera [15]. Uno asume que, en una teoría gauge con una constante de acoplamiento fuerte, es posible la producción dinámica de estados ligados excitados de masa cero, que se acoplan longitudinalmente. La demostración de la existencia de un estado ligado en teorías de campos realistas, y en particular un estado ligado de masa cero, es un difícil problema dinámico que se estudia a través de ecuaciones integrales conocidas como ecuaciones de Bethe-Salpeter (BSEs) (consultar, por ejemplo, [16]). Así pues, uno de los ingredientes vitales para que se realice el escenario anterior es el acoplamiento fuerte, que sólamente puede aparecer como consecuencia de las inestabilidades infrarrojas de teorías gauge no Abelianas. Las mencionadas excitaciones actúan como bosones de Nambu-Goldstone dinámicos [17–21], en el sentido de que son no masivas, compuestas y se acoplan longitudinalmente. Pero al mismo tiempo, difieren de los bosones de Nambu-Goldstone debido a que su origen no es la ruptura espontánea de ninguna simetría global. El papel principal de estas excitaciones es el de activar el mecanismo de Schwinger, es decir, proporcionar el polo requerido en la auto-energía del gluon. Además, dichas excitaciones preservan la forma de las identidades de Ward (WIs) y de las identidades de Slavnov-Taylor (STIs) de la teoría

en presencia de masas (ver, por ejemplo, [22]), porporcionando por tanto un mecanismo de generación dinámica de masa gluónica invariante gauge.

Para comprender el motivo por el cual se deben introducir tales polos en la teoría masiva analicemos la siguiente situación simplificada. Consideremos el vértice de tres gluones convencional (ver Apendice A), dado por la expresión

$$\Gamma_{\alpha\mu\nu}(q,r,p) = (r-p)_\alpha g_{\mu\nu} + (p-q)_\mu g_{\nu\alpha} + (q-r)_\nu g_{\alpha\mu}. \tag{1.7}$$

Es elemental verificar que este vértice satisface la siguiente WI

$$q^\alpha \Gamma_{\alpha\mu\nu}(q,r,p) = d^{-1}(p)P_{\mu\nu}(p) - d^{-1}(r)P_{\mu\nu}(r), \tag{1.8}$$

donde la parte derecha de la identidad contiene la diferencia de dos propagadores inversos a nivel árbol en el gauge de Landau, dado que la cantidad $d^{-1}(q) = q^2$ es el inverso del factor de forma a nivel árbol del propagador del gluon, mientras que

$$P_{\mu\nu}(q) = g_{\mu\nu} - \frac{q_\mu q_\nu}{q^2} \tag{1.9}$$

es el proyector transversal. Suponiendo ahora que el propagador del gluon adquiere una masa efectiva $m^2(q)$, la pregunta que debemos responder sería cuál es la manera en la que debe modificarse el vértice de tres gluones para que la WI continue siendo válida, lo que es equivalente a decir que la invariancia gauge permanece intacta después de la generación de la masa efectiva. Para contestar a esta pregunta reemplacemos la cantidad $d^{-1}(q) = q^2$ por $d^{-1}(q) = q^2 - m^2(q)$ y substituyámosla en la parte derecha de la identidad Eq. (1.8). Puede verse entonces que, para mantener la validez de la WI, uno debe reemplazar simultáneamente el vértice de tres gluones en el miembro izquierdo por el vértice

$$\Gamma'_{\alpha\mu\nu}(q,r,p) = \Gamma_{\alpha\mu\nu}(q,r,p) + V_{\alpha\mu\nu}(q,r,p), \tag{1.10}$$

donde la nueva pieza del vértice V debe ser tal que satisfaga la siguiente WI

$$q^\alpha V_{\alpha\mu\nu}(q,r,p) = m^2(r)P_{\mu\nu}(r) - m^2(p)P_{\mu\nu}(p). \tag{1.11}$$

Evidentemente, un solucion de la Eq. (1.11) viene dada por

$$V_{\alpha\mu\nu}(q,r,p) = \frac{q_\alpha}{q^2}[m^2(r)P_{\mu\nu}(r) - m^2(p)P_{\mu\nu}(p)]. \tag{1.12}$$

Así pues, el nuevo vértice V tiene, como mencionamos anteriormente, términos con polos no masivos acoplados longitudinalmente.

De este simple ejemplo se aprende que las excitaciones compuestas deben incorporarse al nivel de las funciones de Green añadiendo un nuevo tipo de vértices no perturbativos, designados genéricamente por V y llamados "vértices polo". Estos vértices contienen los polos no masivos y satisfacen unas STIs muy específicas, completamente determinadas por el requerimiento de que la invariancia gauge de la teoría se preserve intacta en presencia de masas.

Llegados a este punto, el estudio del mecanismo de generación de la masa gluónica en teorías puras de Yang-Mills puede ser abordado siguiendo dos procedimientos diferentes. La diferencia entre ellos radica en la manera en la cual se emplean los vértices V para obtener información sobre la masa efectiva del gluon. Específicamente, en el primer procedimiento, se asume desde el principio que la interacción fuerte favorece la formación dinámica de los estados ligados no masivos necesarios para la existencia de los vértices polo. Asumida entonces su existecia, estos vértices especiales se introducen en la SDE del propagador del gluon y se opera a este nivel para derivar una *ecuación de masa*, la cual describirá la evolución de la dependencia de la masa gluónica efectiva con la energía. Resulta entonces interesante observar que este procedimiento puede llevarse a cabo sin la necesidad de conocer la forma cerrada de los vértices no perturbativos. De hecho, notablemente, sólamente es necesario tener en cuenta su naturaleza longitudinal y las STIs que satisfacen. Usando este procedimiento seremos capaces de derivar, a todos los órdenes, la ecuación de la masa gluónica efectiva [Eq. (6.68)], así como de obtener las soluciones de esta ecuación en el rango completo de energías [sección 6.5 en el capítulo 6]. Por tanto, en este enfoque, los vértices polo son usados de una manera "efectiva", es decir, sin apelar al origen dinámico de sus componentes fundamentales.

En el segundo procedimiento se estudia la estructura "microscópica" y la composición de estos vértices, atendiendo a su formación dinámica. Para llevar a cabo este estudio se deben introducir dos ingredientes no perturbativos cruciales. El primero de ellos recibe el nombre de amplitud de transición [ver Fig. 7.9] y conecta los gluones con los estados ligados no masivos. El segundo ingrediente es un conjunto de vértices efectivos que permiten el acoplamiento entre el estado ligado no masivo y gluones y/o "ghosts" [ver Fig. 7.4]. A este nivel es necesario demostrar que ninguno de estos ingredientes es cero ya que, si así lo fueran, la construcción entera

colapsaría. Tal demostración se lleva a cabo probando la existencia de los estados ligados no masivos mediante un analisis de las BSEs que satisfacen. De hecho, en la sección 5.5 del capítulo 5, se presenta un estudio numérico preliminar de la BSE para los estados ligados no masivos que demuestra su existencia. Finalmente, una vez se ha probado la existencia de estados ligados no masivos, en el capítulo 7, la masa gluónica se podrá relacionar con la amplitud de transición a través de una simple formula Eq. (7.30) que, a su vez, tiene una clara interpretación física en términos de intercambio de estados ligados.

Vamos entonces a concluir esta introducción presentando un pequeño resumen de los contenidos de cada capítulo de la tesis.

Capítulo 2. En este capítulo se presentan los recientes resultados obtenidos en las simulaciones del lattice para el propagador del gluon y la función "vestida" del "ghost". Dichos resultados señalan que ambas funciones de Green son finitas en el infrarrojo, lo cual puede explicarse en términos de una masa gluónica efectiva. Este aspecto es una de los razones que motivan el estudio del fenómeno de generación dinámica de masas en el contexto de teorías puras de Yang-Mills.

Capítulo 3. La exclusiva naturaleza no perturbativa del mecanismo de generación de masas nos obliga e emplear el formalismo de las SDEs para su descripción. Este complicado conjunto de ecuaciones integrales será analizado en el llamado esquema PT-BFM, el cual surge como una síntesis de la Técnica de Pinch (PT) [23,24] con el Método del Campo de Fondo (BFM) [25]. Estableceremos entonces las características básicas y las propiedades que hacen del esquema PT-BFM un ventajoso formalismo cuando se trabaja con las SDEs.

Capítulo 4. En este capítulo se formula el enunciado básico del mecanismo de Schwinger y se muestra como este mecanismo genera un término de masa para los bosones sin interferir con la invariancia gauge de la teoría. En particular, estudiaremos brevemente los modelos de Schwinger y Jackiw-Johnson donde el mecanismo de Schwinger se aplica a teorías gauge Abelianas.

Capítulo 5. El objetivo de este capítulo es doble. Proporcionar un análisis preliminar de cómo se realiza el mecanismo de Schwinger en el contexto de una teoría gauge no Abeliana y demostrar, a través de un detallado

estudio numérico, que la dinámica de las teorías puras de Yang-Mills contempla la formación de estados ligados no masivos.

Capítulo 6. Este capítulo contiene la derivación general de la ecuación completa (a todos los órdenes) que describe la evolución de la masa gluónica generada dinámicamente en el gauge de Landau. La *ecuación de masa* será entonces estudiada en un detallado análisis numérico que revelará la existencia de soluciones monotónicamente decrecientes para la masa gluónica efectiva.

Capítulo 7. El objetivo de este capítulo final es realizar una descripción general del mecanismo de generación de masas en el lenguaje de estados ligados excitados. Después de una precisa definición de los ingredientes necesarios, la masa gluónica efectiva podrá ser expresada a través de una simple *fórmula de masa*. Posteriormente, en una decisiva comprobación de auto-consistencia, vamos a demostrar que la *fórmula de masa* reproduce la *ecuación de masa* obtenida en el capitulo 6, probando que ambos formalismos son totalmente equivalentes.

La tesis concluye con algunas referencias en el capítulo 8 acerca del problema de confinamiento y su (más que) posible conexión con el mecanismo de generación de la masa gluónica. Además se incluyen dos apéndices en los cuales el lagrangiano de QCD y el BFM se discuten brevemente.

2. RECENT LARGE-VOLUME LATTICE RESULTS.

The main theoretical tool for quantitative calculations in the infrared region of QCD, aside from the SDEs, is the lattice. Thanks to the enormous progress realized in this field during the last years, lattice simulations have been revealed as a powerful instrument, which can be combined with the SDEs in order to study the Green's functions of QCD, as has been done in a series of recent works (see, e.g., [26–28]).

In this framework, QCD is approximated by a lattice gauge theory with a non-zero lattice spacing and a finite space-time volume. In this way, one reduces the infinite functional integrals to a finite number of finite integrations, thus allowing the computation of correlation functions by numerical evaluations of these integrals via Monte-Carlo methods. Using these methods the gluon and ghost propagators (in various gauges) have been studied extensively on the lattice [29–31] and a large body of recent high-quality lattice results for these Green's functions, both in $SU(3)$ [32–35] and in $SU(2)$ [36–38], have been computed in the conventional Landau gauge. The results obtained in these large-volume lattice simulations have firmly established that the gluon propagator and the ghost dressing function of pure Yang-Mills theories are infrared (IR) finite and they saturate at zero momentum transfer ($q^2 = 0$).

Specifically, on the left panel of Fig.2.1 are shown the lattice data for the gluon propagator $\Delta(q^2)$ obtained in [32], corresponding to a $SU(3)$ quenched lattice simulation renormalized at $\mu = 4.3$ GeV. On the right panel of the same figure are reported the quenched $SU(2)$ lattice data obtained in [36], renormalized at $\mu = 2.2$ GeV. Both sets of lattice data can be accurately fitted in terms of a IR finite gluon propagator of the form

$$\Delta^{-1}(q^2) = M^2(q^2) + q^2\left[1 + \frac{13C_A g_1^2}{96\pi^2}\ln\left(\frac{q^2 + \rho_1 M^2(q^2)}{\mu^2}\right)\right], \qquad (2.1)$$

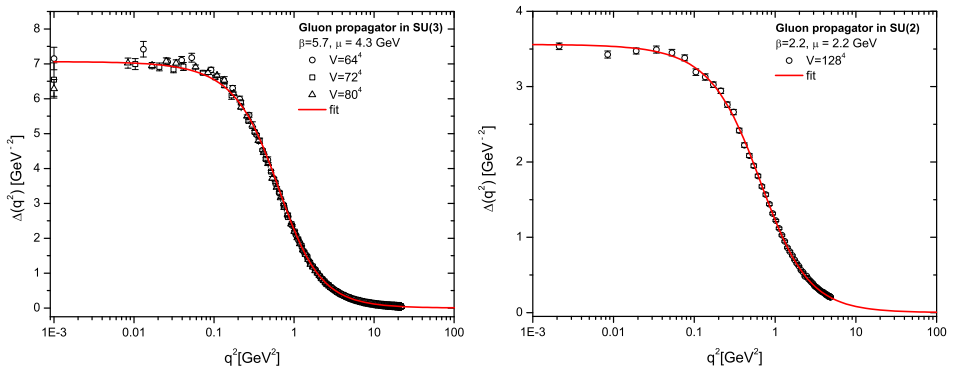

Fig. 2.1: Lattice results for the $SU(3)$ (left) and $SU(2)$ (right) gluon propagator, renormalized at $\mu = 4.3$ GeV and $\mu = 2.2$ GeV respectively. The red continuous lines represents the best fits to the data obtained from Eq. (2.1).

where the function $M^2(q^2)$ given by

$$M^2(q^2) = \frac{m_g^4}{q^2 + \rho_2 m_g^2} \tag{2.2}$$

controls the value of the gluon propagator at the origin,

$$\Delta^{-1}(0) = M^2(0) = m_g^2/\rho_2. \tag{2.3}$$

Turning next to the ghost dressing function, on the left panel of Fig.2.2, are shown the $SU(3)$ lattice results of [32], renormalized as before at $\mu = 4.3$ GeV. On the right panel are plotted instead the results for the $SU(2)$ case [36], renormalized at $\mu = 2.2$ GeV. These data can be fitted in terms of the expression

$$F^{-1}(q^2) = 1 + \frac{9}{4}\frac{C_A g_2^2}{48\pi^2}\ln\left(\frac{q^2 + \rho_3 M^2(q^2)}{\mu^2}\right), \tag{2.4}$$

with $M^2(q^2)$ given by Eq. (2.2), but changing the parameter $\rho_2 \to \rho_4$ and $m_g^2 \to m^2$. The best values for the fitting parameters in expressions Eq. (2.1) and Eq. (2.4) can be found in various recent articles [22, 39, 40],

- $SU(3)$ case: $m_g^2 = m^2 = 520$ MeV, $g_1^2 = 5.68$, $g_2^2 = 8.57$, $\rho_1 = 8.55$, $\rho_2 = 1.91$, $\rho_3 = 0.25$, $\rho_4 = 0.68$.

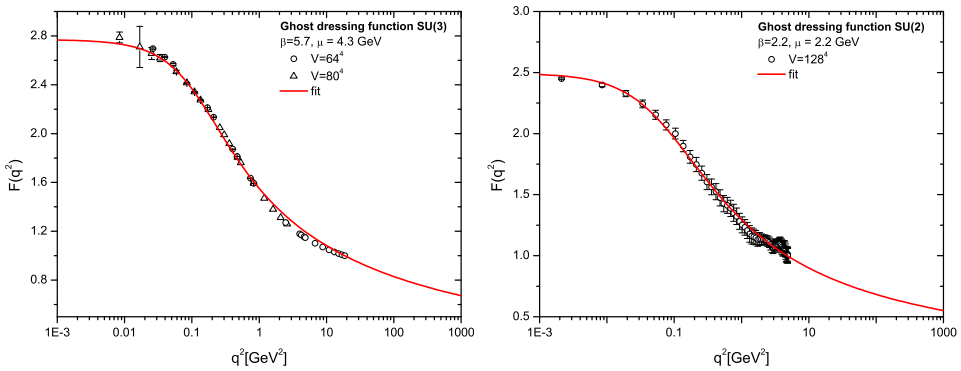

Fig. 2.2: Lattice results for the $SU(3)$ (left) and $SU(2)$ (right) ghost dressing function, renormalized at $\mu = 4.3$ GeV and $\mu = 2.2$ GeV respectively. The red continuous lines represent the best fits to the data obtained from Eq. (2.4).

- $SU(2)$ case: $m_g^2 = 867$ MeV, $m^2 = 523$ MeV, $g_1^2 = 10.80$, $g_2^2 = 15.03$, $\rho_1 = 1.96$, $\rho_2 = 2.68$, $\rho_3 = 0.21$, $\rho_4 = 0.78$.

Notice that the mass M^2 appearing in this fits acts as an infrared cutoff keeping finite the gluon propagator and the ghost dressing function.

These lattice results suggest the study of the gluon mass generation mechanism as a possible explanation of the IR finiteness of the gluon propagator and the ghost dressing function. Indeed, expressions Eq. (2.1) and Eq. (2.4) will be extensively used in the numerical analysis of the analytical results obtained throughout this thesis. However, the reader should be advised about the limitations of the lattice results. Principally, the effects of the non-zero lattice spacing and the finite space-time volume used in the simulations, are translated into numerical errors in the physical data predicted by lattice. Also, the process of fixing the gauge in the lattice is quite subtle and involved. Thus, although these lattice results motivate physically our study, the analytical results presented in this thesis complement and supplement the deficiencies and limitations of the lattice.

3. A BRIEF OVERVIEW OF THE PINCH TECHNIQUE-BACKGROUND FIELD METHOD FORMALISM.

The lattice results presented in the previous chapter indicate clearly that the gluon propagator and the ghost dressing function are IR finite in the conventional Landau gauge, both in $SU(2)$ and in $SU(3)$. These important results have sparked a renewed interest in the important issue of dynamical mass generation in non-Abelian gauge theories, and especially in QCD. The reason is that perhaps the most physical way of explaining the observed finiteness of these quantities is the generation of a non-perturbative, momentum-dependent gluon mass [7, 22, 26, 41–43], which acts as a natural IR cutoff.

Given the non-perturbative nature of this mechanism, the usual starting point in the continuum is the SDEs governing the Green's functions under scrutiny. In the framework provided by the synthesis of the PT [7,23,44–46] with the BFM [25,47], known in the literature as the PT-BFM scheme, these complicated integral equations are endowed with a variety of important properties, which allow a much tighter control on the truncations adopted and the approximation schemes employed. Therefore, we set up in this chapter the necessary notation and review some of the most salient features of the PT-BFM scheme, putting particular emphasis on the form of the SDE for the gluon propagator, and the various field-theoretic ingredients appearing in it.

In a general renormalizable R_ξ gauge, defined through a linear gauge fixing function of the Lorentz type ($\mathcal{F}^a = \partial^\mu A^a_\mu$), the all-order gluon propagator $\Delta^{ab}_{\mu\nu}(q) = \delta^{ab}\Delta_{\mu\nu}(q)$ and its inverse read

$$i\Delta_{\mu\nu}(q) = -i\left[P_{\mu\nu}(q)\Delta(q^2) + \xi\frac{q_\mu q_\nu}{q^4}\right], \tag{3.1}$$

$$\Delta^{-1}_{\mu\nu}(q) = i\left[P_{\mu\nu}(q)\Delta^{-1}(q^2) + \frac{1}{\xi}q_\mu q_\nu\right], \tag{3.2}$$

where ξ denotes the gauge fixing parameter and

$$P_{\mu\nu}(q) = g_{\mu\nu} - q_\mu q_\nu / q^2, \tag{3.3}$$

is the dimensionless transverse projector. The choice $\xi = 0$ corresponds to the Landau gauge giving raise to the totally transverse gluon propagator

$$\Delta_{\mu\nu}(q) = -iP_{\mu\nu}(q)\Delta(q^2). \tag{3.4}$$

The scalar form factor $\Delta(q^2)$ appearing above is related to the all-order gluon self-energy $\Pi_{\mu\nu}(q)$ through

$$\Delta^{-1}(q^2) = q^2 + i\Pi(q^2) = q^2 J(q^2), \tag{3.5}$$

where we have defined the dimensionless function $J(q^2)$, which coincides with the inverse of the gluon dressing function, frequently considered in the literature [48]. As a direct consequence of the gauge invariance of the theory, which after the gauge-fixing is encoded into the BRST symmetry [49, 50], we know that the gluon self-energy is transverse to all-orders in perturbation theory, as well as non perturbatively, at the level of the corresponding SDE. One has then

$$q^\mu \Pi_{\mu\nu}(q) = 0 \quad ; \quad \Pi_{\mu\nu}(q) = \Pi(q^2) P_{\mu\nu}(q). \tag{3.6}$$

The non-perturbative dynamics of the gluon propagator in the continuum is governed by the corresponding SDE. It reads

$$\Delta^{-1}(q^2) P_{\mu\nu}(q) = q^2 P_{\mu\nu}(q) + i \sum_{i=1}^{5} (a_i)_{\mu\nu}, \tag{3.7}$$

where the diagrams (a_i) are shown in Fig. 3.1. The main theoretical problem one encounters when dealing with the SDE given above is the fact that it cannot be truncated in a physically meaningful way. The most direct manifestation of this drawback is the following: after the truncation the fundamental Eq. (3.6) is violated and one cannot truncate Eq. (3.7) in any obvious way without violating the transversality of the resulting gluon self-energy. For example, keeping only graphs (a_1) and (a_2) is not correct even perturbatively, since the ghost loop is crucial for the transversality of $\Pi_{\mu\nu}$ already at one-loop; adding (a_3) is still not sufficient for a SD analysis, because (beyond one-loop) $q^\mu[(a_1) + (a_2) + (a_3)]_{\mu\nu} \neq 0$.

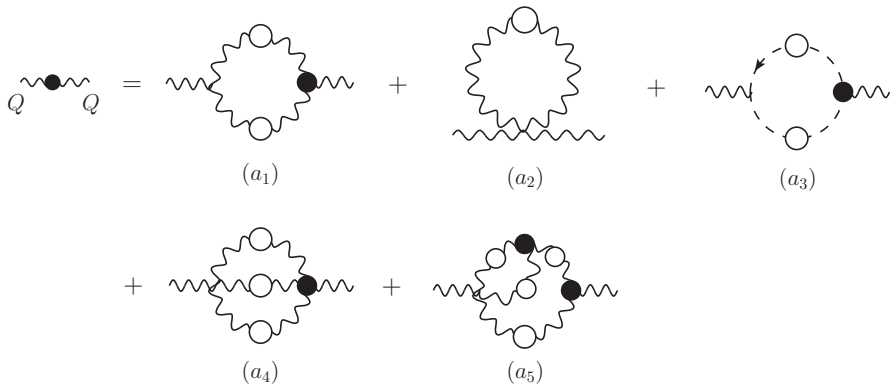

Fig. 3.1: SDE satisfied by the conventional gluon self-energy with two quantum gluons entering. The symmetry factors of the diagrams are $S(a_1, a_2, a_5) = 1/2$, $S(a_3) = -1$, $S(a_4) = 1/6$. White blobs will represent connected Green's functions while black bobs will correspond to fully-dressed one particle irreducible (1PI) vertices.

In order to devise a truncation scheme for the SDE that preserves manifestly the gauge-invariance of the answer at every step one needs to resort to the PT. It is a particular algorithm for rearranging the perturbative series in such a way as to obtain new Green's functions that are independent of the gauge-fixing parameter, and satisfy to all orders ghost-free WIs, instead of the usual STIs. When the PT is formulated at the SD level one operates on a handful of classes of diagrams (each one containing an infinite number of individual graphs) and the rearrangements are collectively implemented through the systematic use of the STIs satisfied by certain Green's functions and kernels. Specifically, the implementation of the PT at the level of the SDE of the gluon self-energy [51, 52] gives rise dynamically to a new kind of SD series (see Fig. 3.2 and Fig. 3.3) in which we have graphs that are made out of new vertices, but contain inside them the same gluon propagator as before, namely $\Delta_{\mu\nu}(q)$. The new vertices, see Appendix B, correspond precisely to the Feynman rules of the BFM, i. e., it is as if the external quantum gluon (Q) had been converted dynamically into a background gluon (B). So, Fig. 3.2 represents the SDE of a propagator connecting a quantum gluon with a background gluon,

$$\widetilde{\Delta}^{-1}(q^2)P_{\mu\nu}(q) = q^2 P_{\mu\nu}(q) + i\sum_{i=1}^{6}(a_i)_{\mu\nu}, \tag{3.8}$$

while Fig. 3.3 contains the SDE of a propagator connecting two background gluons,

$$\widehat{\Delta}^{-1}(q^2)P_{\mu\nu}(q) = q^2 P_{\mu\nu}(q) + i\sum_{i=1}^{10}(a_i)_{\mu\nu}. \tag{3.9}$$

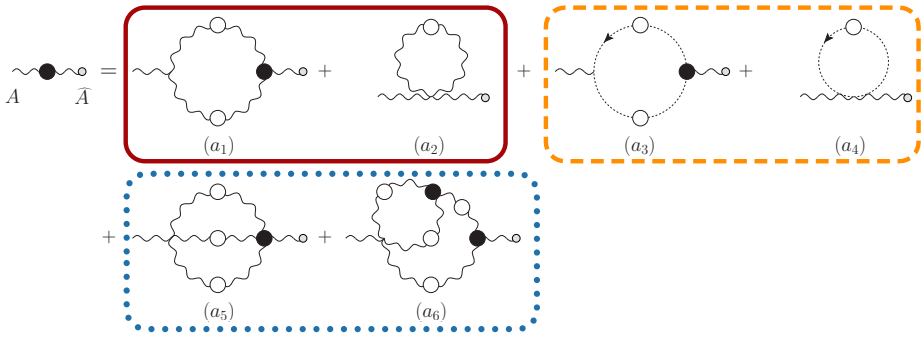

Fig. 3.2: SDE obeyed by the gluon self-energy with one quantum and one background gluons entering. The symmetry factors of the diagrams are $S(a_1, a_2, a_6) = 1/2$, $S(a_3, a_4) = -1$, $S(a_5) = 1/6$. Each box encloses a set of diagrams forming a transverse subgroup. The small gray circles appearing on the external legs (entering from the right, only!) are used to indicate background gluons.

In addition, the new vertices appearing in these SDE no longer satisfy the typical STIs, like for example that of the conventional three-gluon vertex with three quantum gluon legs (Q^3), given by [53]

$$\begin{aligned} q^\alpha \Gamma_{\alpha\mu\nu}(q,r,p) &= F(q^2)[\Delta^{-1}(p^2)P^\alpha_\nu(p)H_{\alpha\mu}(p,q,r) \\ &- \Delta^{-1}(r^2)P^\alpha_\mu(r)H_{\alpha\nu}(r,q,p)], \end{aligned} \tag{3.10}$$

where $F(q^2)$ corresponds to the ghost dressing function defined below and H is an auxiliary function containing the conventional gluon-ghost kernel shown in Fig. 3.4. Instead of these complicated identities, they will satisfy the following Abelian-like WIs when are contracted respect to the momentum of the background gluon leg:

- Vertex BQ^2 (one background and two quantum gluons),

$$q_1^\alpha \widetilde{\Gamma}^{amn}_{\alpha\mu\nu}(q_1,q_2,q_3) = g f^{amn}[\Delta^{-1}_{\mu\nu}(q_2) - \Delta^{-1}_{\mu\nu}(q_3)]. \tag{3.11}$$

- Vertex $B\bar{c}c$ (one background gluon, one anti-ghost and one ghost),

$$q_1^\alpha \widetilde{\Gamma}^{amn}_{\alpha}(q_2,q_1,q_3) = g f^{anm}[D^{-1}(q_2) - D^{-1}(q_3)]. \tag{3.12}$$

- Vertex BQ^3 (one background and three quantum gluons),

$$\begin{aligned} q_1^\alpha \widetilde{\Gamma}^{amnr}_{\alpha\mu\nu\rho}(q_1,q_2,q_3,q_4) &= ig[f^{amx}\Gamma^{nrx}_{\nu\rho\mu}(q_3,q_4,q_1+q_2) \\ &+ f^{anx}\Gamma^{rmx}_{\rho\mu\nu}(q_4,q_2,q_1+q_3) \\ &+ f^{arx}\Gamma^{mnx}_{\mu\nu\rho}(q_2,q_3,q_1+q_4)]. \end{aligned} \tag{3.13}$$

- Vertex $BQ\bar{c}c$ (one background and one quantum gluons, one anti-ghost and one ghost),

$$\begin{aligned} q_1^\alpha \widetilde{\Gamma}^{amnr}_{\alpha\mu}(q_1,q_2,q_3,q_4) &= -ig[f^{amx}\Gamma^{rxn}_{\mu}(q_4,q_1+q_2,q_3) \\ &+ f^{anx}\Gamma^{rmx}_{\mu}(q_4,q_2,q_1+q_3) \\ &+ f^{arx}\Gamma^{xmn}_{\mu}(q_1+q_4,q_2,q_3)]. \end{aligned} \tag{3.14}$$

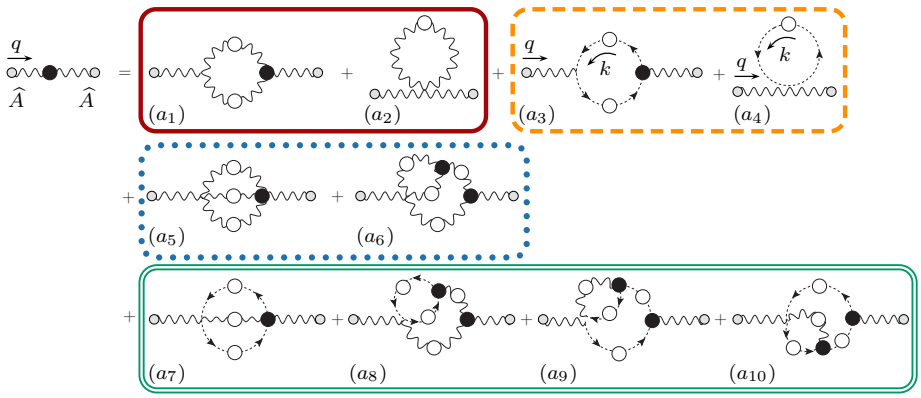

Fig. 3.3: SDE obeyed by the gluon self-energy with two background gluons entering. The symmetry factors are in this case $S(a_1,a_2,a_6) = 1/2$, $S(a_5) = 1/6$, and all the remaining diagrams have $S = -1$. The graphs inside each box form a gauge invariant subgroup, furnishing and individually transverse contribution. External background legs are indicated by the small gray circles.

Using these WIs one may show after some elementary operations that the transversality of the SDE Eq. (3.9) is realized "blockwise" [42], following

the pattern shown in Fig. 3.3, i.e.,

$$q^\mu[(a_1)+(a_2)]_{\mu\nu}=0 \quad ; \quad q^\mu[(a_3)+(a_4)]_{\mu\nu}=0$$
$$q^\mu[(a_5)+(a_6)]_{\mu\nu}=0 \quad ; \quad q^\mu[(a_7)+(a_8)+(a_9)+(a_{10})]_{\mu\nu}=0. \quad (3.15)$$

Therefore, this new SD series has a very special structure which allows us to separate the diagrams on the r.h.s of Eq. (3.9) into four obvious categories: one-loop (dressed) gluonic contributions $[(a_1)+(a_2)]$, one-loop ghost contributions $[(a_3)+(a_4)]$, two-loop gluonic contributions $[(a_5)+(a_6)]$ and two-loop ghost contributions $[(a_7)+(a_8)+(a_9)+(a_{10})]$. Furthermore, by virtue of the all-order WIs satisfied by the new fully-dressed vertices, the contribution of each one of the four subgroups will be individually transverse. In a similar fashion, the transversality of the SDE Eq. (3.8) is realized according to the pattern highlighted by the boxes of Fig. 3.2, namely,

$$q^\mu[(a_1)+(a_2)]_{\mu\nu}=0; \quad q^\mu[(a_3)+(a_4)]_{\mu\nu}=0; \quad q^\mu[(a_5)+(a_6)]_{\mu\nu}=0. \quad (3.16)$$

Thus we observe that within the PT-BFM scheme three types of gluon propagator make their appearance in a natural way:

- The conventional gluon propagator (two quantum gluons entering, QQ), denoted by $\Delta(q^2)$.
- The background gluon propagator (two background gluons entering, BB), denoted by $\widehat{\Delta}(q^2)$.
- The mixed quantum-background propagator (one quantum and one background gluons entering, BQ), denoted by $\widetilde{\Delta}(q^2)$.

These three propagators are related among each other by a set of powerful relations, known as Background-Quantum identities (BQIs) [54, 55], obtained within the Batalin-Vilkovisky formalism [56, 57]. Specifically,

$$\Delta(q^2)=[1+G(q^2)]\widetilde{\Delta}(q^2)=[1+G(q^2)]^2\widehat{\Delta}(q^2). \quad (3.17)$$

The function $G(q^2)$, whose role in enforcing these crucial relations is instrumental, is defined as the $g_{\mu\nu}$ form factor of a special two-point function, given by (see Fig. 3.4)

$$\begin{aligned}\Lambda_{\mu\nu}(q) &= -ig^2C_A\int_k \Delta^\sigma_\mu(k)D(q-k)H_{\nu\sigma}(-q,q-k,k)\\ &= g_{\mu\nu}G(q^2)+\frac{q_\mu q_\nu}{q^2}L(q^2), \quad (3.18)\end{aligned}$$

where C_A represents the Casimir eigenvalue of the adjoint representation (N for $SU(N)$), $d = 4 - \epsilon$ is the space-time dimension, and we have introduced the integral measure

$$\int_k \equiv \frac{\mu^\epsilon}{(2\pi)^d} \int d^d k, \tag{3.19}$$

with μ the 't Hooft mass. In addition, $D^{ab}(q^2) = \delta^{ab} D(q^2)$ is the ghost propagator, and $H_{\nu\sigma}$ is the gluon-ghost kernel (see Fig. 3.4). The dressed loop expansion of Λ and H is shown in Fig. 3.4. Notice finally that, in the Landau gauge, an important all-order relation exists, which links the form factors $G(q^2)$ and $L(q^2)$ to the ghost dressing function,

$$F(q^2) = q^2 D(q^2), \tag{3.20}$$

namely [39, 58–60]

$$F^{-1}(q^2) = 1 + G(q^2) + L(q^2). \tag{3.21}$$

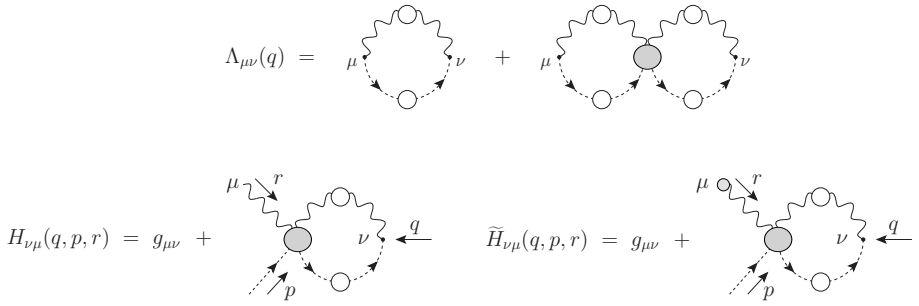

Fig. 3.4: Diagrammatic representation of the auxiliary functions Λ, H and, for later convenience, $\widetilde{H}$. Gray blobs denote 1PI (with respect to vertical cuts) Schwinger-Dyson kernels.

All of these results and special properties have far-reaching practical consequences for the treatment of the SD series. For example, keeping only the one-loop dressed gluonic contributions to Eq. (3.7), we obtain the following truncated SDE for the gluon propagator

$$\widehat{\Delta}^{-1}(q^2) P_{\mu\nu}(q) = q^2 P_{\mu\nu}(q) + i[(a_1) + (a_2)]_{\mu\nu}, \tag{3.22}$$

and from the first equation of Eq. (3.15) we now that this block of diagrams is transverse, i.e.,

$$[(a_1)+(a_2)]_{\mu\nu} = \frac{[(a_1)+(a_2)]^{\alpha}_{\alpha}}{d-1} P_{\mu\nu}(q). \tag{3.23}$$

Thus, the transverse projector $P_{\mu\nu}(q)$ appears exactly on both sides of Eq. (3.22); one may subsequently isolate the scalar cofactors on both sides obtaining a scalar equation of the form

$$\widehat{\Delta}^{-1}(q^2) = q^2 + i[(a_1)+(a_2)]^{\alpha}_{\alpha}. \tag{3.24}$$

Finally, the BQI Eq. (3.17) is used to relate $\widehat{\Delta}(q^2)$ with the conventional gluon propagator $\Delta(q^2)$. Of course, a truncated equation similar to Eq. (3.22) may be written for any other of the four groups, or for sums of these groups, without compromising the transversality of the answer.

4. THE SCHWINGER MECHANISM: PRELIMINARIES.

In this chapter we take an introductory look at the so called Schwinger mechanism, using two Abelian toy models. The first is the famous (and exactly solvable) Schwinger model [8], namely QED_2 with massless fermions. The second is the Jackiw-Johnson model [61], where the Schwinger mechanism is triggered when the chiral symmetry of a four-dimensional Abelian gauge theory is dynamically broken. Even though the non Abelian realization of the Schwinger mechanism is far more complex, these simple examples capture the basic concepts involved, and can help us fix the underlying ideas.

4.1 The basic statement of the Schwinger mechanism.

As Schwinger pointed out long time ago [8,9], the gauge invariance of a vector field does not necessarily imply zero mass for the associated particle, if the current vector coupling is sufficiently strong. Schwinger's fundamental observation was that if (for some reason) the vacuum polarization $\Pi(q^2)$ acquires a pole at zero momentum transfer, the vector meson becomes massive, even if the gauge symmetry forbids a mass at the level of the fundamental Lagrangian. The way in which the Schwinger mechanism generates a mass for the gauge boson can be seen most directly at the level of its inverse propagator

$$\Delta^{-1}(q^2) = q^2[1 + i\mathbf{\Pi}(q^2)], \tag{4.1}$$

where $\mathbf{\Pi}(q^2) = \Pi(q^2)/q^2$ is the dimensionless vacuum polarization. It is clear that if $\mathbf{\Pi}(q^2)$ develops a pole at zero momentum transfer ($q^2 = 0$) with positive residue μ^2, then the vector meson acquires a mass. Indeed, if $\mathbf{\Pi}(q^2) = m^2/q^2$, then (in Euclidean space) $\Delta^{-1}(q^2) = q^2 + m^2$, and so the vector meson becomes massive, $\Delta^{-1}(0) = m^2$, even though it is massless in the absence of interactions ($g = 0$, $\mathbf{\Pi} = 0$) [61, 62].

There is no physical principle which would preclude $\mathbf{\Pi}(q^2)$ from acquiring a pole. Since bound states are expected to exist in most physical

systems one may suppose that, for sufficiently strong binding, the mass of such bound state will be reduced to zero, thus generating a mass for the vector meson without interfering with gauge invariance. In general, the appearance of the required pole may happen for purely dynamical reasons and, in particular, without the need to introduce fundamental scalar fields in the Lagrangian. In fact, the standard Higgs mechanism can be viewed as just a very special realization of the Schwinger mechanism, where the residue of the pole is saturated by v^2, being v the vacuum expectation value of a canonical scalar field coupled to the vector meson.

4.2 Schwinger model.

The simplest situation where the triggering of the Schwinger mechanism can be analyzed is that of two-dimensional QED with massless electrons, known as the Schwinger model. The Lagrangian of this model is

$$\mathcal{L} = -\frac{1}{4}F_{\mu\nu}F^{\mu\nu} + \bar{\psi}i\gamma^{\mu}D_{\mu}\psi, \tag{4.2}$$

with $\mu, \nu = 0, 1$. As usual, the covariant derivative is defined as

$$D_{\mu} = \partial_{\mu} - ieA_{\mu}, \tag{4.3}$$

with e the (electromagnetic) coupling constant, and the field strength tensor is given by

$$F_{\mu\nu} = \partial_{\mu}A_{\nu} - \partial_{\nu}A_{\mu} = \frac{i}{e}[D_{\mu}, D_{\nu}]. \tag{4.4}$$

In addition, the Dirac matrices must be chosen to satisfy the Clifford algebra

$$\{\gamma^{\mu}, \gamma^{\nu}\} = 2g^{\mu\nu}. \tag{4.5}$$

In two dimensions the fermion spinors are two-component fields and we only have two Dirac matrices, γ^0 and γ^1. Using them, one can define the product anticommuting with each of the γ^{μ}, as $\gamma^5 = \gamma^0\gamma^1$. A representation for the gamma matrices in two dimensions is given by the Pauli matrices,

$$\gamma^0 = \sigma^3; \quad \gamma^1 = i\sigma^1; \quad \gamma^5 = -\sigma^2. \tag{4.6}$$

The Lagrangian is gauge invariant under local $U(1)$ transformations,

$$U(1) = \{\mathcal{U}(\theta) = e^{i\theta(x)} \quad : \quad \mathcal{U}^{\dagger}\mathcal{U} = \mathcal{U}\mathcal{U}^{\dagger} = 1\}, \tag{4.7}$$

and therefore, at the level of the fundamental Lagrangian, the gauge symmetry forbids the appearance of a mass term for the photon of the type $m^2 A_\mu^2$. However, in dimension $d = 2$, one can prove that the photon vacuum polarization acquires a pole, thus endowing the photon with an effective mass without interfering with the gauge invariance. The crucial point is that in this model one can evaluate this quantity exactly. This happens because all quantum corrections to the photon vacuum polarization vanish in $d = 2$, as a consequence of the trace properties for the Dirac matrices. Only the one-loop correction to the photon self-energy $\Pi_{\mu\nu}$, shown in Fig. 4.1, gives a non-zero contribution,

$$\Pi_{\mu\nu}(q) = -e^2 \int_k \frac{Tr\{\gamma_\mu(\not{k} + \not{q})\gamma_\nu \not{k}\}}{(k+q)^2 k^2}. \tag{4.8}$$

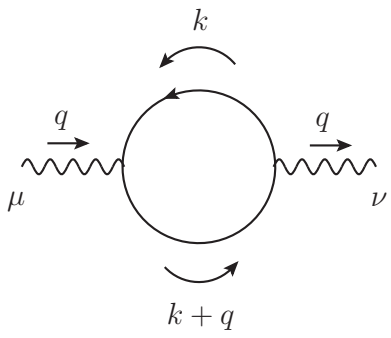

Fig. 4.1: Feynman diagram for the one-loop contribution to the photon vacuum polarization.

First of all, notice that using the elementary WI for the tree-level photon-electron vertex,

$$q^\mu \gamma_\mu = (\not{q} + \not{k}) - \not{k}, \tag{4.9}$$

it is straightforward to check that the photon self-energy satisfies the WI

$$q^\mu \Pi_{\mu\nu}(q) = 0. \tag{4.10}$$

This result affirms the transversality of the photon self-energy, as a direct consequence of the underlying gauge symmetry, and forces the vacuum

polarization to assume its characteristic form

$$\Pi_{\mu\nu}(q) = P_{\mu\nu}(q)\Pi(q^2), \tag{4.11}$$

with $P_{\mu\nu}(q)$ the usual dimensionless transverse projector. Then, taking the trace of Eq. (4.11) and using Eq. (4.8), we obtain the following expression for the photon vacuum polarization

$$\Pi(q^2) = \frac{1}{d-1} g^{\mu\nu}\Pi_{\mu\nu}(q) = -\frac{e^2}{d-1}\int_k \frac{Tr\{\gamma_\mu(\not{k}+\not{q})\gamma^\mu \not{k}\}}{(k+q)^2 k^2}. \tag{4.12}$$

Now, introducing the Feynman parameters, evaluating the trace of the Dirac matrices, and using the dimensional regularization integrals, Eq. (4.12) provides the result ($d = 2$)

$$\Pi(q^2) = i\frac{e^2}{\pi} \tag{4.13}$$

Thus, one observes that in $d = 2$ the photon vacuum polarization acquires a non-zero value in the limit of zero momentum transfer, $q^2 = 0$. Note that in $d = 2$ the coupling constant is dimensionful, $[e] = [m]$. So, when this value is inserted in Eq. (4.1), the photon propagator becomes (in Euclidean space) massive-like,

$$\Delta^{-1}(q^2) = q^2 + \frac{e^2}{\pi}, \tag{4.14}$$

with an effective mass $m_\gamma^2 = \Delta^{-1}(0) = e^2/\pi$.

Evidently, even though the $U(1)$ gauge symmetry prevents the appearance of a tree-level mass term $m^2 A_\mu^2$ at the level of the fundamental QED_2 Lagrangian, the inclusion of one-loop corrections gives a finite contribution to $\Pi(q^2)$, which can be interpreted as an effective mass term in the photon propagator. Most notably, this effective mass does not compromise the gauge invariance of the theory, as captured by the WI Eq. (4.10).

4.3 Jackiw-Johnson model.

The Jackiw-Johnson model constitutes a more elaborate example where the Schwinger mechanism is used to describe the possibility that masses of fermions and vector mesons can arise dynamically, without the presence of canonical scalar fields in the Lagrangian (Higgs mechanism). In this model we consider a theory with a massless fermion field ψ and an Abelian

gauge field (photon) A_μ interacting through an axial vector current $J_5^\mu = \bar{\psi} i\gamma^\mu\gamma_5\psi$, described by the Lagrangian

$$\mathcal{L} = i\bar{\psi}\gamma^\mu\partial_\mu\psi - \frac{1}{4}F_{\mu\nu}F^{\mu\nu} + g\bar{\psi}i\gamma^\mu\gamma_5\psi A_\mu, \tag{4.15}$$

where the Abelian field strength tensor is given by Eq. (4.4).

Next, we introduce the various nonperturbative ingredients that we are going to study. The all-order photon propagator reads in the Landau gauge ($\xi = 0$)

$$\Delta_{\mu\nu}(q) = -iP_{\mu\nu}(q)\Delta(q^2), \tag{4.16}$$

with $P_{\mu\nu}(q)$ the transverse projector. The scalar form factor $\Delta(q^2)$ appearing above is related to the all-order photon self-energy[1],

$$\Pi_{\mu\nu}(q) = iP_{\mu\nu}(q)q^2\Pi(q^2), \tag{4.17}$$

through the expression

$$\Delta^{-1}(q^2) = q^2[1 - \Pi(q^2)]. \tag{4.18}$$

The SDE satisfied by the photon self-energy, shown in Fig. 4.2, can be written as follows

$$\Pi^{\mu\nu}(q) = -g^2 Tr \int_k \Gamma_5^{\mu(0)} S(k) S(k+q) \Gamma_5^\nu(-q, k+q, -k), \tag{4.19}$$

where the extra minus sign and the trace comes from the fermionic loop. In this SDE, the quantity $\Gamma_5^{\mu(0)} = i\gamma^\mu\gamma_5$, corresponds to the tree-level value of the proper fermion-photon interaction vertex, whose all-order Feynman rule can be seen in Fig. 4.2.

At this point, one observes that the theory described by the Lagrangian Eq. (4.15) is chirally invariant, and this invariance is captured by the following all-order WI satisfied by the fermion-photon vertex,

$$q_\mu\Gamma_5^\mu(q, k, -k-q) = \gamma_5 S^{-1}(k) + S^{-1}(k+q)\gamma_5. \tag{4.20}$$

Finally, $S(q)$ represents the fully-dressed fermion propagator, which can be written in the form

$$S^{-1}(q) = -i\gamma^\mu q_\mu + i\Sigma(q), \tag{4.21}$$

[1] There is an additional factor iq^2 with respect to the usual definition Eq. (3.6) in order to follow the original conventions used in [61].

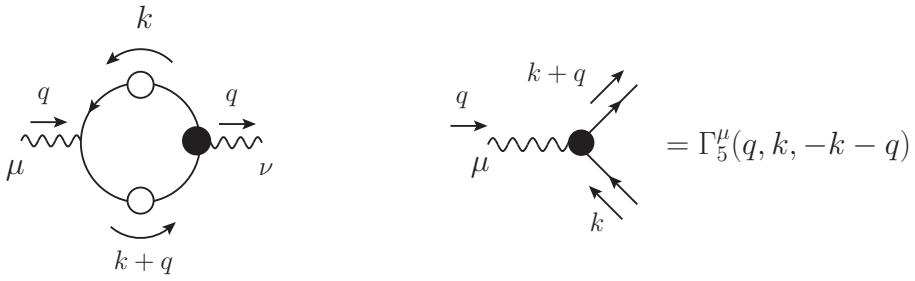

Fig. 4.2: Schwinger-Dyson equation satisfied by the photon self-energy and Feynman rule for the all-order fermion-photon proper vertex.

where $\Sigma(q)$ corresponds to the fermion self-energy, satisfying the SDE

$$\Sigma(q) = g^2 \int_k \Gamma_5^{\mu(0)} \Delta_{\mu\nu}(q) S(k+q) \Gamma_5^{\nu}(-k, k+q, -q), \tag{4.22}$$

whose diagrammatic representation is given in Fig. 4.3.

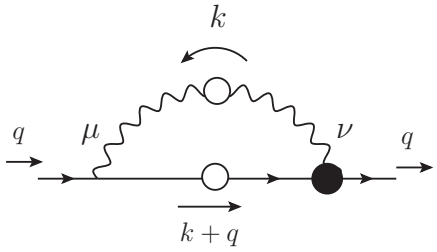

Fig. 4.3: Schwinger-Dyson equation for the fermion self-energy.

Let us next investigate under what conditions a dynamical gauge boson mass may arise in this theory. The starting point is to observe that, if the chiral symmetry of the theory is exact, the WI Eq. (4.20) ensures the finiteness of the fermion-photon vertex at zero momentum transfer, $q^2 = 0$, through the condition

$$\lim_{q\to 0} q_\mu \Gamma_5^{\mu}(q, k, -k-q) = i\{\gamma_5, \Sigma(k)\} = 0, \tag{4.23}$$

which, in turn, gives a constraint for the solutions of the SDE Eq. (4.22) that preserve chiral symmetry. Now, we assume that a chiral symmetry

breaking solution for Eq. (4.22) exists, such that $\{\gamma_5, \Sigma(k)\} \neq 0$. Note that this symmetry breaking is not due to a vacuum expectation value of a canonical scalar field in the Lagrangian; rather, it is assumed to be a consequence of a symmetry-breaking solution to the integral equations of the theory. The actual existence of such solutions must be established through a detailed Bethe-Salpeter (BS) analysis.

In fact, it is well known that this situation can occur if there is a massless, bound-state excitation in the fermion-antifermion channel. Furthermore, this bound-state must be interpreted as the massless Goldstone boson that appears when the chiral symmetry of the Lagrangian Eq. (4.15) is broken, and will be described by a propagator of the type i/q^2, as shown in Fig. 4.4. Also, the fact that this bound-state appears in the fermion-antifermion channel implies that we need to introduce a new (nonperturbative) vertex in the theory to describe the interaction between the massless bound-state and the fermion fields. The Feynman rule for this vertex, to be denoted $P(q, r, p)$, is also shown in Fig. 4.4.

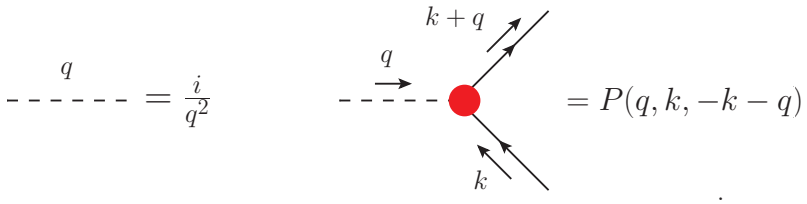

Fig. 4.4: Feynman rules for the massless propagator of the bound-state and for the effective vertex P which couples the massless excitation to the fermion fields.

Under these circumstances, the immediate consequence for the fermion-photon vertex is that the condition Eq. (4.23) is no longer valid, and the WI acquires a non-zero value in the kinematical limit $q^2 \to 0$ given by

$$\lim_{q\to 0} q_\mu \Gamma_5^\mu(q, k, -k-q) = i\{\gamma_5, \Sigma(k)\} \neq 0, \tag{4.24}$$

signaling that the chiral symmetry of the theory has been broken by the presence of the massless excitation. So, Eq. (4.24) implies that the vertex Γ_5^μ has a pole at $q^2 = 0$, with residue $i\{\gamma_5, \Sigma(k)\}$. Using then the massless propagator and the effective vertex P, we can make the nonperturbative pole manifest, and cast the pole part of the fermion-photon vertex in the

form of Fig. 4.5, by setting

$$\Gamma_5^\mu(q,p,-p-q)\big|_{pole} = I^\mu(q)\left(\frac{i}{q^2}\right)P(q,p,-p-q), \tag{4.25}$$

where we have defined the following integral

$$I^\mu(q) = -Tr\int_k \Gamma_5^{\mu(0)} S(k)S(k+q)P(-q,k+q,-k), \tag{4.26}$$

with the minus sign and the trace coming from the fermionic loop.

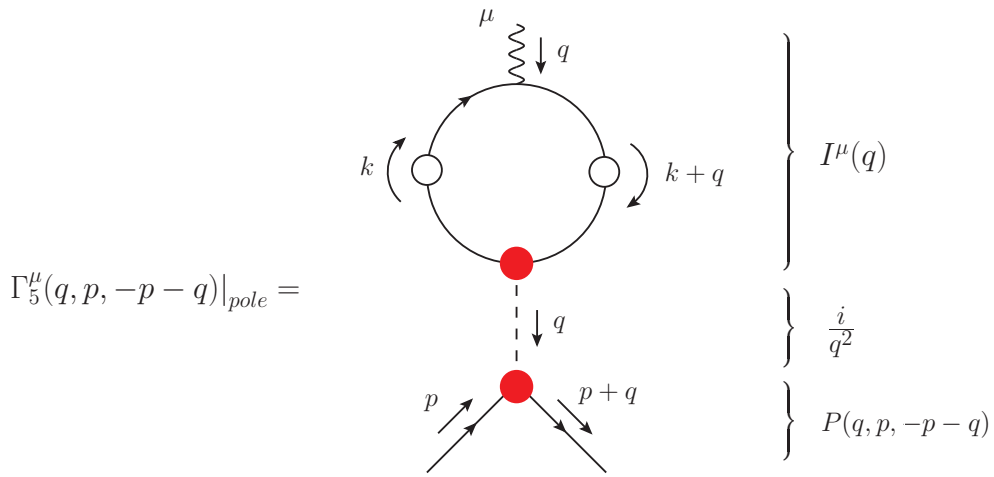

Fig. 4.5: Structure of the pole contribution to the fermion-photon vertex Γ_5^μ.

Evidently, by Lorentz invariance, we can write the integral Eq. (4.26) as $I^\mu(q) = q^\mu I(q^2)$. Using this property, and assuming that $I(0)$ is finite, one may combine expressions Eq. (4.24) and Eq. (4.25) to get the relation

$$\{\gamma_5, \Sigma(k)\} = I(0)P(0,p,-p), \tag{4.27}$$

which establishes the explicit connection between the massless excitation and the chiral symmetry breaking solutions of Eq. (4.22). It is clear at this point that $P(0,-p,p)$ must be non vanishing, or else the entire construction collapses.

Now we are in position to examine what is the effect of introducing this pole vertex into the photon self-energy. Inserting the singular part of Eq.

(4.25) into the SDE Eq. (4.19) one obtains

$$\begin{aligned}\Pi^{\mu\nu}_{pole}(q) &= -g^2 Tr\int_k \Gamma^{\mu(0)}_5 S(k)S(k+q)\Gamma^{\nu}_5(-q,k+q,-k)\Big|_{pole}\\ &= g^2\Big\{-Tr\int_k \Gamma^{\mu(0)}_5 S(k)S(k+q)P(-q,k+q,-k)\Big\}\left(\frac{i}{q^2}\right)I^{\nu}(-q)\\ &= g^2 I^{\mu}(q)\left(\frac{i}{q^2}\right)I^{\nu}(-q), \qquad (4.28)\end{aligned}$$

whose diagrammatic interpretation is shown in Fig. 4.6. So, using the fact

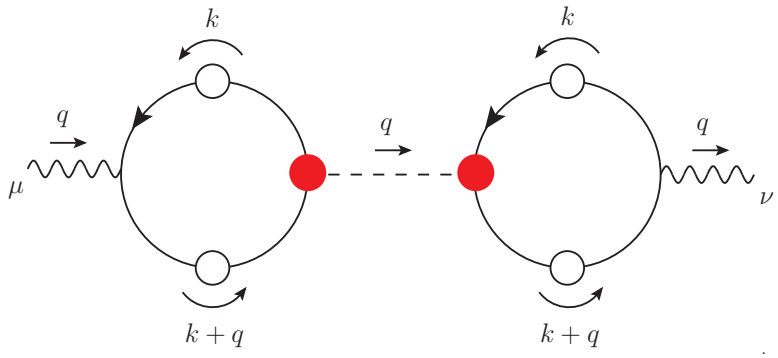

Fig. 4.6: Pole contribution to the photon self-energy.

that $I^{\nu}(-q) = -I^{\nu}(q)$, we obtain the following result

$$\Pi^{\mu\nu}_{pole}(q) = -i\frac{q^{\mu}q^{\nu}}{q^2}g^2 I^2(q^2). \qquad (4.29)$$

Therefore, Eq. (4.29) shows that $\Pi(q^2)$, defined in Eq. (4.17), has the pole

$$\Pi_{pole}(q^2) = g^2\frac{I^2(q^2)}{q^2}. \qquad (4.30)$$

This indicates that the above pole triggers the Schwinger mechanism and the photon propagator Eq. (4.18) becomes massive, acquiring an effective mass whose value at zero momentum transfer $q^2 = 0$ is given by (Euclidean space)

$$m^2(0) = \Delta^{-1}(0) = g^2 I^2(0). \qquad (4.31)$$

5. THE SCHWINGER MECHANISM IN PURE YANG-MILLS THEORIES.

The gauge-invariant generation of an effective gauge boson (gluon) mass proceeds through the well-known Schwinger mechanism, whose key dynamical ingredient is the nonperturbative formation of longitudinally coupled massless bound-state excitations. These excitations introduce poles in the vertices of the theory giving a non-vanishing contribution in the limit of zero momentum transfer ($q^2 = 0$) to the SDE of the boson self-energy and therefore endowing the gauge boson propagator with an effective mass term, as was explained in detail in the previous chapter for the simpler Schwinger model and the Abelian Jackiw-Johnson model. The principal assumption when invoking the Schwinger mechanism in Yang-Mills theories, such as QCD, is that the required poles may be produced due to purely dynamical reasons; specifically, one assumes that, for sufficiently strong binding, the mass of the appropriate bound state may be reduced to zero [15, 16, 61–63]. In addition, to triggering the Schwinger mechanism, these massless composite excitations are crucial for preserving gauge invariance. Specifically, the presence of massless poles in the off-shell interaction vertices guarantees that the Ward identities (WIs) and Slavnov-Taylor identities (STIs) of the theory maintain exactly the same form before and after mass generation (i.e., when the massless propagators appearing in them are replaced by massive ones) [7, 22]. Thus, these excitations act like dynamical Nambu-Goldstone scalars, displaying, in fact, all their typical characteristics, such as masslessness, compositeness, and longitudinal coupling; note however, that they differ from Nambu-Goldstone bosons as far as their origin is concerned, since they are not associated with the spontaneous breaking of any global symmetry [7]. Finally, every such Goldstone-like scalar, "absorbed" by a gluon in order to acquire a mass, is expected to actually cancel out of the S-matrix against other massless poles or due to current conserva-

tion [15, 16, 61–63] [1].

The main purpose of the present chapter is to scrutinize the central assumption of the dynamical scenario outlined above, namely, the possibility of actual formation of such massless excitations. The question we want to address is whether the nonperturbative Yang-Mills dynamics are indeed compatible with the generation of such a special bound-state. In particular, if we work within the PT-BFM scheme and we restrict ourselves to the one-loop dressed gluonic block shown in Fig. 5.1, the entire mechanism of

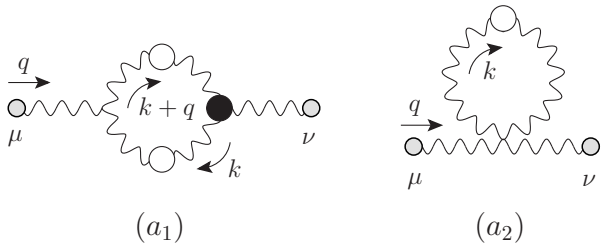

Fig. 5.1: The one-loop dressed gluon contribution to the PT-BFM gluon self-energy. White (black) circles denote fully dressed propagators (vertices); a gray circle attached to the external legs indicates that they are background gluons. Within the PT-BFM scheme these two diagrams constitute a transverse subset of the full gluon SDE.

gluon mass generation hinges on the appearance of massless poles inside the nonperturbative BQ^2 three-gluon vertex, which enters in the SDE governing the gluon propagator. These poles correspond to the propagator of the scalar massless excitation, and interact with a pair of gluons through a very characteristic proper vertex, which, of course, must be non-vanishing, or else the entire construction collapses. The way to establish the existence of this latter vertex is through the study of the homogeneous Bethe-Salpeter equation (BSE) that it satisfies, and look for non-trivial solutions, subject to the numerous stringent constraints imposed by gauge invariance.

This particular methodology has been adopted in various early contributions on this subject [15, 16, 61–63]; however, only asymptotic solutions to the corresponding equations have been considered. The detailed numerical study presented here demonstrates that, under certain simplifying assumptions for the structure of its kernel, the aforementioned integral

[1] These massless bound states should not be confused with physical excitations, such as glueballs, that may appear in the spectrum of the theory.

equation has indeed nontrivial solutions, valid for the entire range of physical momenta [64]. This result, although approximate and not fully conclusive, furnishes additional support in favor of the concrete mass generation mechanism described earlier.

The chapter is organized as follows. In Section 5.1 we outline how the vertices of the theory must be modified, through the inclusion of longitudinally coupled massless poles, in order to maintain the WIs and the STIs of the theory intact. In Section 5.2 we take a detailed look into the structure of the nonperturbative vertex that contains the required massless poles, and study its main dynamical building blocks. Specifically, the transition amplitude between a gluon and a massless excitation, and the proper vertex function (bound-state wave function), controlling the interaction of the massless excitation with two gluons. In Section 5.3 we derive an exact relation between these two quantities and the first derivative of the (momentum dependent) gluon mass. Then we derive a simple formula that, at zero momentum transfer, relates the aforementioned transition amplitude to the gluon mass. In Section 5.4 we derive the BSE that the proper vertex function satisfies, and implement a number of simplifying assumptions and in Section 5.5 we demonstrate through a detailed numerical study that the resulting homogeneous integral equation indeed admits nontrivial solutions, thus corroborating the existence of the required bound-state excitations. In Section 5.6 we demonstrate with a specific example the general mechanism that leads to the decoupling of all massless poles from the physical (on-shell) amplitude. Finally, in Section 5.7 we discuss the limitations of our results.

5.1 Gauge-invariant generation of a gluon mass.

In this section we set up the general theoretical framework related to the gauge invariant generation of a gluon mass explaining why the dynamical generation of a mass is inextricably connected to the presence of a special vertex, which exactly compensates for the appearance of massive instead of massless propagators in the corresponding WIs and STIs. If we focus our attention on the one-loop dressed gluon contributions to the PT-BFM gluon self-energy (see Fig. 5.1), the relevant Green's function to consider is the fully-dressed vertex BQ^2 shown in Fig. 5.2, connecting a background gluon with two quantum gluons, to be denoted by $\widetilde{\Gamma}_{\alpha\mu\nu}(q,r,p)$. A general Ansatz for this vertex has been obtained in [65] by applying the so called

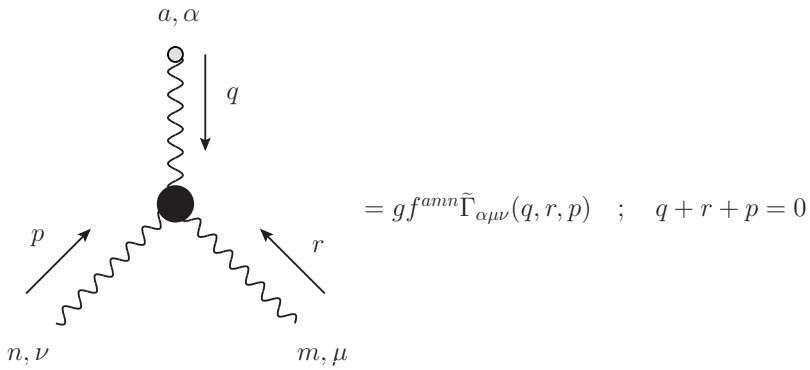

Fig. 5.2: The conventions for the momenta, color and Lorentz indices of the BQ^2 vertex connecting one background gluon with two quantum gluons.

"gauge technique", extensively used in the context of QED [66–71]. It satisfies a WI when contracted with the momentum q_α of the background gluon leg, and two STIs when contracted with the momentum r_μ or p_ν of the quantum gluon legs, namely

$$\begin{aligned} q^\alpha \widetilde{\Gamma}_{\alpha\mu\nu}(q,r,p) &= p^2 J(p^2) P_{\mu\nu}(p) - r^2 J(r^2) P_{\mu\nu}(r), \\ r^\mu \widetilde{\Gamma}_{\alpha\mu\nu}(q,r,p) &= F(r^2)[q^2 \widetilde{J}(q^2) P^\mu_\alpha(q) H_{\mu\nu}(q,r,p) - p^2 J(p^2) P^\mu_\nu(p) \widetilde{H}_{\mu\alpha}(p,r,q)], \\ p^\nu \widetilde{\Gamma}_{\alpha\mu\nu}(q,r,p) &= F(p^2)[r^2 J(r^2) P^\nu_\mu(r) \widetilde{H}_{\nu\alpha}(r,p,q) - q^2 \widetilde{J}(q^2) P^\nu_\alpha(q) H_{\nu\mu}(q,p,r)]. \end{aligned} \tag{5.1}$$

In these identities the ghost-gluon kernel $\widetilde{H}_{\mu\nu}$ is obtained from the conventional $H_{\mu\nu}$ by replacing the external quantum gluon by a background gluon, as shown in Fig. 3.4. Also, the function $\widetilde{J}(q^2)$ corresponds to the inverse dressing function of the mixed QB gluon propagator and is related to the conventional $J(q^2)$ defined in Eq. (3.5) through the BQI Eq. (3.17), i.e.,

$$\widetilde{J}(q^2) = [1 + G(q^2)] J(q^2). \tag{5.2}$$

The implementation of the Schwinger mechanism at this level requires the existence of a very special type of nonperturbative vertex, referred as the BQ^2 pole vertex and denoted by $\widetilde{V}_{\alpha\mu\nu}(q,r,p)$, which, when added to the conventional $\widetilde{\Gamma}_{\alpha\mu\nu}(q,r,p)$ has a triple effect:

- The addition of this vertex makes possible that the SDE of the gluon propagator yields $\Delta^{-1}(0) \neq 0$.

- It guarantees that the WIs and the STIs of the theory remain intact, i.e., this vertex ensures that these identities remain exactly the same before and after mass generation.
- This vertex decouples from on-shell amplitudes.

These three properties become possible because the BQ^2 pole vertex:

- Contains massless poles.
- It is completely longitudinally coupled, i.e., it satisfies the following condition

$$P^{\alpha\beta}(q)P^{\mu\rho}(r)P^{\nu\sigma}(p)\widetilde{V}_{\beta\rho\sigma}(q,r,p)=0. \tag{5.3}$$

The role of the vertex $\widetilde{V}_{\alpha\mu\nu}(q,r,p)$ is indispensable for maintaining gauge invariance, given that the massless poles that it must contain in order to trigger the Schwinger mechanism, act, at the same time, as composite, longitudinally coupled Nambu-Goldstone bosons. Specifically, in order to preserve the gauge invariance of the theory in the presence of masses, the vertex $\widetilde{V}_{\alpha\mu\nu}(q,r,p)$ must be added to the conventional $\widetilde{\Gamma}_{\alpha\mu\nu}(q,r,p)$ vertex, giving raise to the new full vertex $\widetilde{\Gamma}'_{\alpha\mu\nu}(q,r,p)$, defined as

$$\widetilde{\Gamma}'_{\alpha\mu\nu}(q,r,p)=[\widetilde{\Gamma}_m(q,r,p)+\widetilde{V}(q,r,p)]_{\alpha\mu\nu}, \tag{5.4}$$

where the subscript "m" indicates that the vertex $\widetilde{\Gamma}_m$ is given by the same graphs as Γ before but now with gluon propagators replaced by massive ones. Thus, if we describe the transition from a massless to a massive gluon propagator by carrying out the replacement (in Minkowski space)

$$\Delta^{-1}(q^2)=q^2J(q^2) \quad \longrightarrow \quad \Delta_m^{-1}(q^2)=q^2J_m(q^2)-m^2(q^2), \tag{5.5}$$

where $m^2(q^2)$ is the (momentum dependent) dynamically generated mass, gauge invariance requires that this replacement be accompanied by the simultaneous replacement

$$\widetilde{\Gamma} \quad \longrightarrow \quad \widetilde{\Gamma}'=\widetilde{\Gamma}_m+\widetilde{V}, \tag{5.6}$$

and $\widetilde{V}$ must be such that the new vertex $\widetilde{\Gamma}'$ satisfies formally the same WIs (or STIs) as $\widetilde{\Gamma}$ before. To see how this works with an explicit example consider the WI Eq. (5.1) satisfied by the vertex $\widetilde{\Gamma}$ with the Schwinger mechanism "turned off". Then, gauge invariance requires that

$$q^{\alpha}\widetilde{V}_{\alpha\mu\nu}(q,r,p)=m^2(r^2)P_{\mu\nu}(r)-m^2(p^2)P_{\mu\nu}(p), \tag{5.7}$$

so that, after turning the Schwinger mechanism on, the corresponding WI satisfied by $\widetilde{\Gamma}'$ would read

$$\begin{aligned} q^\alpha \widetilde{\Gamma}'_{\alpha\mu\nu}(q,r,p) &= q^\alpha [\widetilde{\Gamma}_m(q,r,p) + \widetilde{V}(q,r,p)]_{\alpha\mu\nu} \\ &= [p^2 J_m(p^2) - m^2(p^2)] P_{\mu\nu}(p) - [r^2 J_m(r^2) - m^2(r^2)] P_{\mu\nu}(r) \\ &= \Delta_m^{-1}(p^2) P_{\mu\nu}(p) - \Delta_m^{-1}(r^2) P_{\mu\nu}(r), \end{aligned} \tag{5.8}$$

which is indeed the identity in Eq. (5.1), with the aforementioned replacement $\Delta^{-1} \to \Delta_m^{-1}$ enforced. The remaining STIs, triggered when contracting $\widetilde{\Gamma}'$ with respect to the other two legs are realized in exactly the same fashion if we demand that the pole vertex $\widetilde{V}$ satisfies the following STIs

$$\begin{aligned} r^\mu \widetilde{V}_{\alpha\mu\nu}(q,r,p) &= F(r^2)[m^2(p^2) P^\mu_\nu(p) \widetilde{H}_{\mu\alpha}(p,r,q) - \widetilde{m}^2(q^2) P^\mu_\alpha(q) H_{\mu\nu}(q,r,p)], \\ p^\nu \widetilde{V}_{\alpha\mu\nu}(q,r,p) &= F(p^2)[\widetilde{m}^2(q^2) P^\nu_\alpha(q) H_{\nu\mu}(q,p,r) - m^2(r^2) P^\nu_\mu(r) \widetilde{H}_{\nu\alpha}(r,p,q)]. \end{aligned} \tag{5.9}$$

It must be clear at this point that the longitudinal nature of $\widetilde{V}$, combined with the WI and STIs that it must satisfy, lead inevitably to the appearance of a massless pole, as required by the Schwinger mechanism. For example, focusing only on the q-channel, the simplest toy Ansatz for the vertex is [see also Eq. (1.6)]

$$\widetilde{V}_{\alpha\mu\nu}(q,r,p) = \frac{q_\alpha}{q^2}[m^2(r^2) P_{\mu\nu}(r) - m^2(p^2) P_{\mu\nu}(p)], \tag{5.10}$$

which has a pole in q^2 and satisfies Eq. (5.7). Of course, poles associated to the other channels (r and p) will also appear, given that $\widetilde{V}$ must also satisfy the corresponding STIs with respect to r^μ and p^ν.

5.2 The BQ^2 pole vertex: Structure and properties.

As has been pointed out in the previous section, the main characteristic of the vertex $\widetilde{V}$, which sharply differentiates it from ordinary vertex contributions, is that it contain massless poles, originating from the contributions of bound-state excitations. Specifically, all terms of the vertex $\widetilde{V}$ are proportional to $1/q^2$, $1/r^2$, $1/p^2$, and products thereof as can be seen in expression Eq. (5.10). Of course, such dynamically generated poles, whose origin is purely non-perturbative, are to be clearly distinguished from poles related to ordinary massless propagators, associated with elementary fields in the original Lagrangian.

In this section we take a detailed look at the structure of the BQ^2 pole vertex $\widetilde{V}$. In particular, we identify the diagrammatic origin and field-theoretic nature of the various quantities contributing to it, and specify the way it enters into the SDE of the full vertex $\widetilde{\Gamma}'$, defined in Eq. (5.4). When doing this, new objects will emerge in a natural way. Namely the transition amplitude $\widetilde{I}_\alpha(q)$ connecting a background gluon with the massless excitation, and a series of effective vertices B mixing the massless excitation with gluons or ghosts. Also, the general features of these quantities will be established.

5.2.1 General structure of the vertex $\tilde{V}$.

In general, when setting up the usual SDE for any vertex, a particular field (leg) is singled out and is connected to the various multiparticle kernels through all elementary vertices of the theory involving this field (leg). The remaining legs enter into the various diagrams through the aforementioned multiparticle kernels, or, in terms of the standard skeleton expansions, through fully dressed vertices (instead of tree-level ones). For the case of the BQ^2 vertex $\widetilde{\Gamma}_{\alpha\mu\nu}(q,r,p)$ that we consider here, whose SDE is shown in Fig. 5.3, it is convenient (but not obligatory) to identify as the

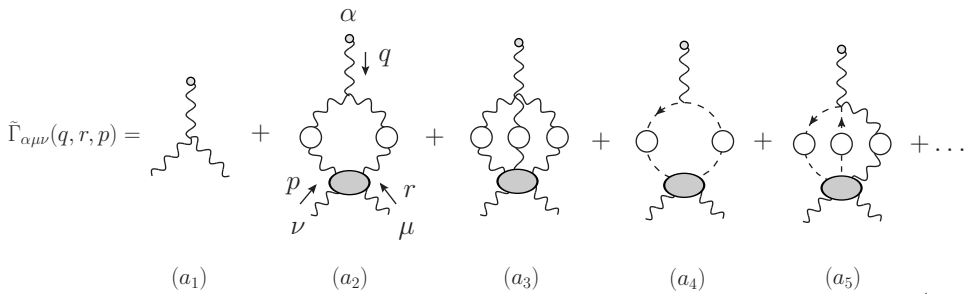

Fig. 5.3: The SDE for the BQ^2 vertex $\widetilde{\Gamma}_{\alpha\mu\nu}$ which connects a background gluon with two quantum gluons. Gray blobs denote the conventional 1PI (with respect to vertical cuts) Schwinger-Dyson kernels.

special leg the background gluon, carrying momentum q. Now, with the Schwinger mechanism turned off, the various multiparticle kernels appearing in the SDE for the BQ^2 vertex have a complicated skeleton expansion, see [23, 52], but their common characteristic is that they are one-particle irreducible with respect to cuts in the direction of the momentum q. Thus

a diagram such as the (a) of Fig. 5.4 is explicitly excluded from the (gray) four-gluon kernel, and the same is true for all other kernels.

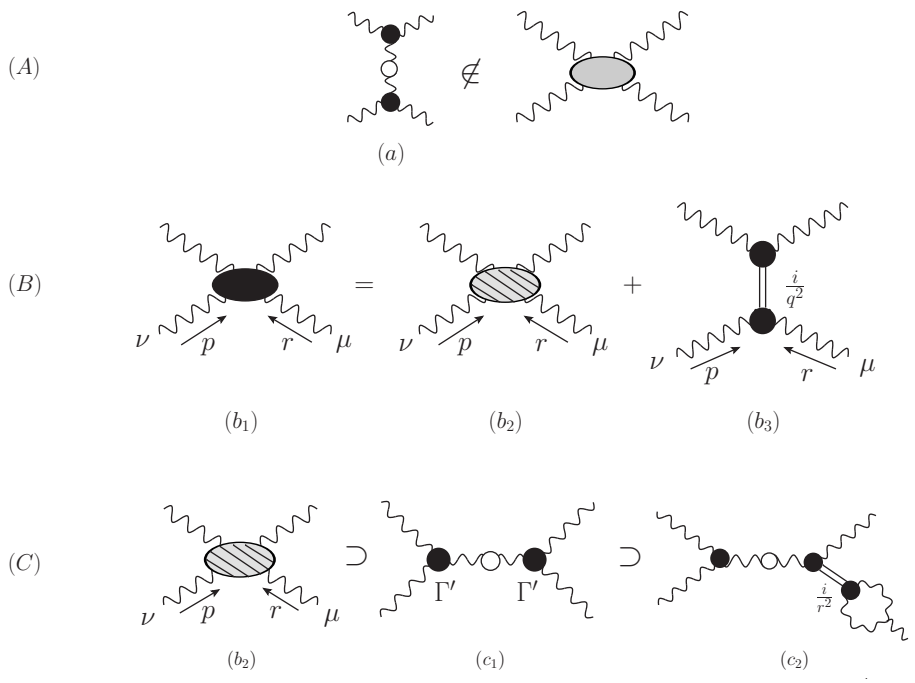

Fig. 5.4: (A) A diagram that does not belong to the standard four-gluon kernel. (B) The black kernel is the resulting four-gluon kernel when the Schwinger mechanism is turned on. It contains the lined gray kernel corresponding to the regular part with respect to q, and the composite massless excitation in the q-channel. (C) The lined gray kernel is made of the original gray kernel but with massive gluon propagators, and the $\widetilde{R}$ part of the BQ^2 pole vertex $\widetilde{V}$.

When the Schwinger mechanism is turned on, the structure of the kernels is modified by the presence of composite massless excitations, described by a propagator of the type i/q^2. For example, as shown in Fig. 5.4, the gray four-gluon kernel becomes a black kernel, diagram (b_1), which is the sum of two parts:

- The term (b_2) which corresponds to a "regular" kernel (lined gray) with respect to the direction of the momentum q.
- The term (b_3) which describes the exchange of the composite massless

excitation between two gluons in the q-channel.

This modifications define in a natural way two parts inside the BQ^2 pole vertex $\widetilde{V}$. The sum of the dynamical generated terms coming from all the multiparticle kernels, like diagram (b_3) in Fig. 5.4, will constitute a characteristic part of the vertex $\widetilde{V}$, to be denoted by $\widetilde{\mathcal{U}}$, namely the part that contains at least a massless propagator i/q^2. The remaining parts of the vertex $\widetilde{V}$, to be denoted by $\widetilde{R}$, contain massless excitations in the other two channels, namely $1/r^2$ and $1/p^2$ (but not $1/q^2$), and originate from graphs such as (c_2) of Fig. 5.4. Indeed, note that the kernel (b_2) is composed of an infinite number of diagrams, such as (c_1), containing the full vertex $\widetilde{\Gamma}'$; these graphs, in turn, will furnish terms proportional to $1/r^2$ and $1/p^2$. An explicit diagrammatic example about how these two parts of the vertex $\widetilde{V}$ emerge when the Schwinger mechanism is turned on can be seen in Fig. 5.5.

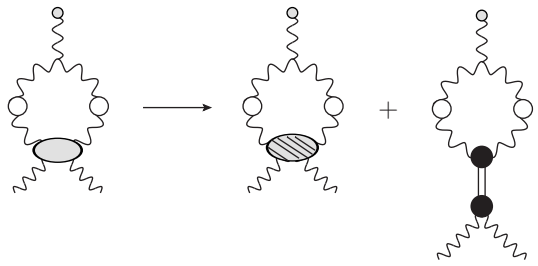

Fig. 5.5: Modification of diagram (a_2) in Fig. 5.3 when the Schwinger mechanism is triggered by the vertex $\widetilde{V}$. The first diagram is assigned to the $\widetilde{R}$ part while the second diagram is one of the contributions to the $\widetilde{\mathcal{U}}$ part of the vertex $\widetilde{V}$.

In order to study further the structure and properties of the vertex $\widetilde{V}$, let us first define the full vertex $\widetilde{\mathcal{V}}^{amn}_{\alpha\mu\nu}(q,r,p)$, given by

$$\widetilde{\mathcal{V}}^{amn}_{\alpha\mu\nu}(q,r,p) = gf^{amn}\widetilde{V}_{\alpha\mu\nu}(q,r,p), \tag{5.11}$$

with $\widetilde{V}_{\alpha\mu\nu}(q,r,p)$ satisfying Eq. (5.3), the WI Eq. (5.7) and the STIs Eq. (5.9). Using a general Lorentz basis this vertex can be expanded in terms of scalar form factors as follows

$$\begin{aligned}\widetilde{V}_{\alpha\mu\nu}(q,r,p) &= \widetilde{V}_1 q_\alpha g_{\mu\nu} + \widetilde{V}_2 q_\alpha q_\mu q_\nu + \widetilde{V}_3 q_\alpha p_\mu p_\nu + \widetilde{V}_4 q_\alpha r_\mu q_\nu + \widetilde{V}_5 q_\alpha r_\mu p_\nu \\ &+ \widetilde{V}_6 r_\mu g_{\alpha\nu} + \widetilde{V}_7 r_\alpha r_\mu r_\nu + \widetilde{V}_8 r_\alpha r_\mu p_\nu + \widetilde{V}_9 p_\nu g_{\alpha\mu} + \widetilde{V}_{10} p_\alpha p_\mu p_\nu.\end{aligned} \tag{5.12}$$

According to the arguments presented above, $\widetilde{V}$ may be decomposed into two parts

$$\widetilde{V}_{\alpha\mu\nu}(q,r,p) = \widetilde{\mathcal{U}}_{\alpha\mu\nu}(q,r,p) + \widetilde{R}_{\alpha\mu\nu}(q,r,p), \tag{5.13}$$

with

$$\widetilde{\mathcal{U}}_{\alpha\mu\nu}(q,r,p) = q_\alpha(\widetilde{V}_1 g_{\mu\nu} + \widetilde{V}_2 q_\mu q_\nu + \widetilde{V}_3 p_\mu p_\nu + \widetilde{V}_4 r_\mu q_\nu + \widetilde{V}_5 r_\mu p_\nu), \tag{5.14}$$

and

$$\begin{aligned} \widetilde{R}_{\alpha\mu\nu}(q,r,p) &= \left(\widetilde{V}_6 g_{\alpha\nu} + \widetilde{V}_7 r_\alpha r_\nu + \frac{\widetilde{V}_8}{2} r_\alpha p_\nu\right) r_\mu \\ &+ \left(\frac{\widetilde{V}_8}{2} r_\alpha r_\mu + \widetilde{V}_9 g_{\alpha\mu} + \widetilde{V}_{10} p_\alpha p_\mu\right) p_\nu. \end{aligned} \tag{5.15}$$

All form factors of $\widetilde{\mathcal{U}}$ (namely $\widetilde{V}_1$ - $\widetilde{V}_5$) must contain a pole $1/q^2$, while some of them may contain, in addition, $1/r^2$ and $1/p^2$ poles. On the other hand, none of the form factors of $\widetilde{R}$ (namely $\widetilde{V}_6$ - $\widetilde{V}_{10}$) contains $1/q^2$ poles, but only $1/r^2$ and $1/p^2$ poles.

In what follows we will focus on $\widetilde{\mathcal{U}}_{\alpha\mu\nu}(q,r,p)$, which contains the explicit q-channel massless excitation, since this is the relevant channel in the SDE of the gluon propagator, where $\widetilde{V}_{\alpha\mu\nu}(q,r,p)$ will be eventually inserted [graph (a_1) in Fig. 5.1]. In fact, with the two internal gluons of diagram (a_1) in the Landau gauge, we have that

$$\begin{aligned} P^{\mu\rho}(r)P^{\nu\sigma}(p)\widetilde{V}_{\alpha\rho\sigma}(q,r,p) &= P^{\mu\rho}(r)P^{\nu\sigma}(p)\widetilde{\mathcal{U}}_{\alpha\rho\sigma}(q,r,p) \\ &= P^{\mu\rho}(r)P^{\nu\sigma}(p)q_\alpha(\widetilde{V}_1 g_{\rho\sigma} + \widetilde{V}_2 q_\rho q_\sigma), \end{aligned} \tag{5.16}$$

so that the only relevant form factors are $\widetilde{V}_1$ and $\widetilde{V}_2$.

5.2.2 The transition amplitude $\tilde{I}_\alpha(q)$ and the effective vertices B.

The previous discussion suggest that one may cast the $\widetilde{\mathcal{U}}$ part of the pole vertex $\widetilde{V}$, see Fig. 5.6, in such form that the nonperturbative pole becomes manifest, namely

$$\widetilde{\mathcal{U}}^{amn}_{\alpha\mu\nu}(q,r,p) = \widetilde{\mathcal{I}}^{ab}_\alpha(q)\left(\frac{i}{q^2}\delta^{bc}\right)\mathcal{B}^{cmn}_{\mu\nu}(q,r,p). \tag{5.17}$$

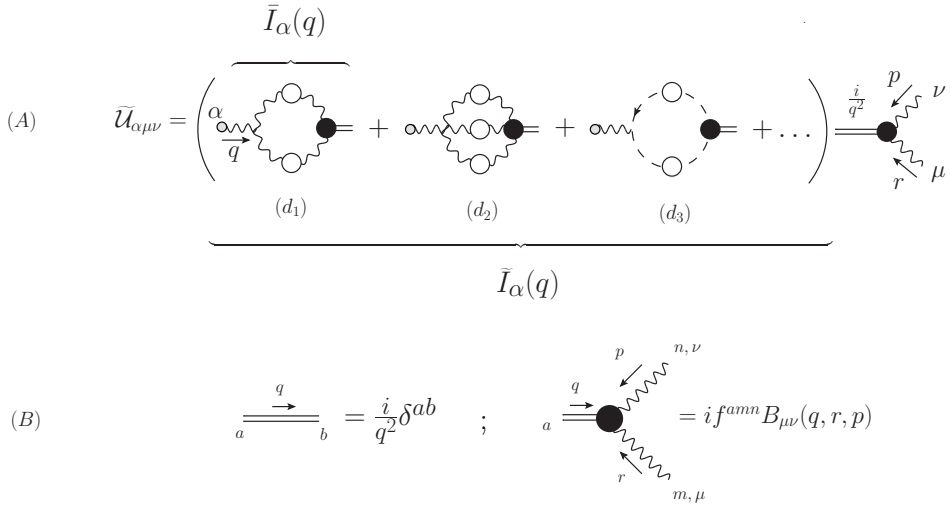

Fig. 5.6: (*A*) The vertex $\widetilde{\mathcal{U}}_{\alpha\mu\nu}$ is composed of three main ingredients: the transition amplitude $\widetilde{I}_\alpha$, which mixes the (background) gluon with a massless excitation, the propagator of the massless excitation, and the effective vertex $B_{\mu\nu}$ which couples the massless excitation with two gluons. (*B*) The Feynman rules (with color factors included) for (i) the propagator of the massless excitation and (ii) the effective vertex $B_{\mu\nu}$.

In this expression the nonperturbative quantity

$$\mathcal{B}^{cmn}_{\mu\nu}(q,r,p) = if^{cmn}B_{\mu\nu}(q,r,p), \tag{5.18}$$

which can be expanded in form factors using a Lorentz basis as follows

$$B_{\mu\nu}(q,r,p) = B_1 g_{\mu\nu} + B_2 q_\mu q_\nu + B_3 p_\mu p_\nu + B_4 r_\mu q_\nu + B_5 r_\mu p_\nu, \tag{5.19}$$

is the effective vertex (or "proper vertex function" [62]) describing the interaction between the massless excitation and two gluons. In the standard language used in bound state physics, $B_{\mu\nu}(q,r,p)$ represents the "bound-state wave function" (or "Bethe-Salpeter wave function") of the two-gluon bound state shown in (b_3) of Fig. 5.5. Indeed, as can be seen in the latter figure, $B_{\mu\nu}$ enters quadratically in the amplitude mediated by the massless excitation and its behavior must be described through a (homogeneous) BSE, as we will see in more detail in Section 5.4. In addition, i/q^2 is the propagator of the scalar massless excitation. Finally,

$$\widetilde{\mathcal{I}}^{ab}_\alpha(q) = g\delta^{ab}\widetilde{I}_\alpha(q), \tag{5.20}$$

is the (nonperturbative) transition amplitude introduced in Fig. 5.6, allowing the mixing between a background gluon and the massless excitation. Evidently, by Lorentz invariance,

$$\widetilde{I}_\alpha(q) = q_\alpha \widetilde{I}(q^2), \tag{5.21}$$

and the scalar cofactor, to be referred as the "transition function", is simply given by

$$\widetilde{I}(q^2) = \frac{q^\alpha}{q^2}\widetilde{I}_\alpha(q). \tag{5.22}$$

Thus, using all of these ingredients we can write Eq. (5.17) as

$$\widetilde{\mathcal{U}}_{\alpha\mu\nu}(q,r,p) = -\frac{1}{q^2}\widetilde{I}_\alpha(q) B_{\mu\nu}(q,r,p) = -\frac{q_\alpha}{q^2}\widetilde{I}(q^2) B_{\mu\nu}(q,r,p), \tag{5.23}$$

so that the Lorentz expansions Eq. (5.14) and Eq. (5.19) allow us to write the form factors of the $\widetilde{\mathcal{U}}$ part in terms of the transition function and the form factors of the effective vertex $B_{\mu\nu}$ in the following form,

$$\widetilde{V}_j(q,r,p) = -\frac{1}{q^2}\widetilde{I}(q^2) B_j(q,r,p); \quad j = 1,\ldots,5. \tag{5.24}$$

Note that, due to the Bose symmetry (already at the level of $\widetilde{V}$) with respect to the interchange $\mu \leftrightarrow \nu$ and $p \leftrightarrow r$, we must have

$$B_{1,2}(q,r,p) = -B_{1,2}(q,p,r), \tag{5.25}$$

which implies that, in the limit $q \to 0$, these form factors are zero by antisymmetry

$$B_{1,2}(0,-p,p) = 0. \tag{5.26}$$

Finally, in principle, all other elementary vertices of the theory may also develop pole parts, which will play a role completely analogous to that of $\widetilde{V}_{\alpha\mu\nu}$ in maintaining the corresponding STIs in the presence of a gluon mass. Specifically, in the absence of quarks, the remaining vertices are the $B\bar{c}c$ vertex, $\widetilde{\Gamma}_\alpha$, the BQ^3 vertex, $\widetilde{\Gamma}_{\alpha\mu\nu\rho}$, and the $BQ\bar{c}c$ vertex, $\widetilde{\Gamma}_{\alpha\mu}$, which is particular of the PT-BFM formulation. The parts of their pole vertices containing the i/q^2 massless excitation, denoted by $\widetilde{\mathcal{U}}_\alpha$, $\widetilde{\mathcal{U}}_{\alpha\mu\nu\rho}$ and $\widetilde{\mathcal{U}}_{\alpha\mu}$, respectively, will assume (color indices suppressed) the common form

$$\widetilde{\mathcal{U}}_{\alpha\{\ldots\}}(q,\ldots) = \widetilde{\mathcal{I}}_\alpha(q)\left(\frac{i}{q^2}\right)\mathcal{B}_{\{\ldots\}}(q,\ldots), \tag{5.27}$$

where the various $\mathcal{B}_{\{\ldots\}}$ are shown in Fig. 5.7. As a final remark, it is important to recognize that the transition amplitude $\widetilde{I}_\alpha(q)$ is universal, in the sense that it enters not only in the pole part $\widetilde{V}$ associated with the three-gluon vertex, but rather in all possible such pole parts associated with all other vertices. Indeed, looking at Eq. (5.27), one observes that the pole parts of the interaction vertices share the transition amplitude and, what really characterizes them, is the effective vertex joined to the transition amplitude through the propagator of the massless excitation.

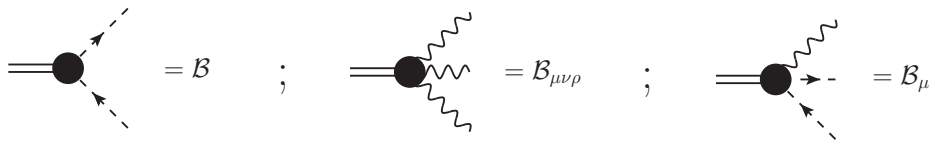

Fig. 5.7: The various effective vertices appearing in Eq. (5.27) describing the interaction between the massless excitation and gluons or ghosts.

5.2.3 *One-loop dressed approximation for the transition function.*

We will next approximate the transition amplitude $\widetilde{I}_\alpha(q)$, connecting the gluon with the massless excitation, by considering only diagram (d_1) in Fig. 5.6, corresponding to the gluonic one-loop dressed approximation; we will denote the resulting expression by $\bar{I}_\alpha(q)$.

Still in a general R_ξ gauge, we can write down (see Fig. 5.8) the following expression for the one-loop dressed gluonic approximation of the transition amplitude,

$$\bar{I}_\alpha(q) = \frac{i}{2} C_A \int_k \widetilde{\Gamma}^{(0)}_{\alpha\mu\nu}(q, -k-q, k) \Delta^{\mu\sigma}(k+q) \Delta^{\nu\rho}(k) B_{\rho\sigma}(-q, -k, k+q). \tag{5.28}$$

In this expression $\widetilde{\Gamma}^{(0)}_{\alpha\mu\nu}$ is the tree-level value of the three-gluon vertex in the BFM, which contains a dependence ξ^{-1} in the gauge fixing parameter, and therefore the projection to the Landau gauge is a subtle exercise because one cannot set directly $\xi = 0$. This projection is achieved [26] by first isolating from the tree-level vertex $\widetilde{\Gamma}^{(0)}_{\alpha\mu\nu}$ the pinch part according to the decomposition

$$\widetilde{\Gamma}^{(0)}_{\alpha\mu\nu}(q, -k-q, k) = \Gamma^{(0)}_{\alpha\mu\nu}(q, -k-q, k) - \frac{1}{\xi} \Gamma^{P}_{\alpha\mu\nu}(q, -k-q, k), \tag{5.29}$$

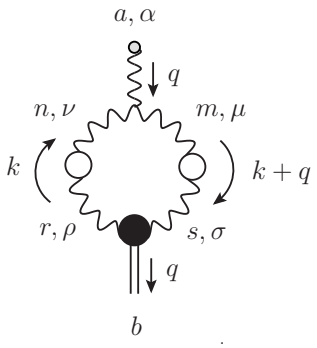

Fig. 5.8: Contribution to the one-loop dressed approximation for the transition amplitude. The diagram has a symmetry factor 1/2 and the color and Lorentz indices, as well as the momentum routing used in the calculation, are explicitly specified.

where $\Gamma^{(0)}_{\alpha\mu\nu}$ is the standard three-gluon vertex at tree-level,

$$\Gamma^{(0)}_{\alpha\mu\nu}(q,-k-q,k) = -(2k+q)_\alpha g_{\mu\nu} + (k-q)_\mu g_{\nu\alpha} + (2q+k)_\nu g_{\alpha\mu}, \quad (5.30)$$

and $\Gamma^{P}_{\alpha\mu\nu}$ is the pinch part of the three-gluon vertex given by

$$\Gamma^{P}_{\alpha\mu\nu}(q,-k-q,k) = g_{\alpha\mu}k_\nu + g_{\alpha\nu}(k+q)_\mu. \quad (5.31)$$

Then, using the following identity triggered by the longitudinal momenta of the pinch part

$$\frac{1}{\xi}k_\nu \Delta^{\nu\rho}(k) = \frac{k^\rho}{k^2}, \quad (5.32)$$

one gets rid of the ξ^{-1} dependence, allowing the projection to the Landau gauge. So, according to this procedure, and after the appropriate shifts in the momentum as well as using the property of Eq. (5.25) in order to interchange the arguments of $B_{\rho\sigma}$, one obtains from Eq. (5.28) the result

$$\begin{aligned} \bar{I}_\alpha(q) &= \frac{i}{2}C_A \int_k \Gamma^{(0)}_{\alpha\mu\nu}(q,-k-q,k)\Delta^{\mu\sigma}(k+q)\Delta^{\nu\rho}(k)B_{\rho\sigma}(-q,-k,k+q) \\ &- iC_A \int_k \frac{k^\rho}{k^2}\Delta^{\sigma}_{\alpha}(k+q)B_{\rho\sigma}(-q,-k,k+q), \end{aligned} \quad (5.33)$$

where, from now on it will be understood that the gluon propagators are written in the Landau gauge, i.e, they assume the totally transverse form

$\Delta_{\mu\nu}(q) = \Delta(q^2)P_{\mu\nu}(q)$ [notice that we have factorized out the $(-i)$ factor with respect to our general definition Eq. (3.4)]. We observe then that the extra term which appears when expression Eq. (5.28) is projected to the Landau gauge contains the contraction of the effective vertex $B_{\rho\sigma}$ with respect to the momentum of one of its gluon legs. This in turn implies that, in order to evaluate this integral, the knowledge of the STI satisfied by this effective vertex is required. The details of this calculation will be given in Chapter 7 but, anticipating results, the role of this term is adding the scalar form factor $G(q^2)$ of the auxiliary function Eq. (3.18) in order to complete a BQI for the transition amplitude. However, to further simplify the discussion without compromising its essential features, we will next set $G(q^2) = 0$. Thus, at this point, there is no distinction between a background and a quantum gluon. With this simplification, Eq. (5.33) reduces to

$$\bar{I}_\alpha(q) = \frac{i}{2}C_A \int_k \Gamma^{(0)}_{\alpha\mu\nu}(q, -k-q, k)\Delta^{\mu\sigma}(k+q)\Delta^{\nu\rho}(k)B_{\rho\sigma}(-q, -k, k+q). \tag{5.34}$$

Now using Eq. (5.22) and the WI satisfied by the tree-level three-gluon vertex

$$q^\alpha \Gamma^{(0)}_{\alpha\mu\nu}(q, -k-q, k) = k^2 P_{\mu\nu}(k) - (k+q)^2 P_{\mu\nu}(k+q), \tag{5.35}$$

we derive, after the appropriate shifts in the momentum, the expression for the one-loop dressed approximation of the transition function

$$\begin{aligned} \bar{I}(q^2) &= \frac{i}{q^2}C_A \int_k k^2 \Delta^{\mu\sigma}(k+q)\Delta^\rho_\mu(k)B_{\rho\sigma}(-q, -k, k+q) \\ &= \frac{i}{q^2}C_A \int_k k^2 \Delta^{\mu\sigma}(k+q)\Delta^\rho_\mu(k)[B_1 g_{\rho\sigma} + B_2 q_\rho q_\sigma], \end{aligned} \tag{5.36}$$

where in the last step we have used Eq. (5.19) and the fact that the gluon propagators are in the Landau gauge.

Now, we are interested in obtaining the value of this quantity in the limit $q \to 0$. The reason is because in the next section we will be able to relate this particular value of the transition function with the effective gluon mass. To that end, we will carry out the Taylor expansions of the several form factors appearing in Eq. (5.36) in the limit $q \to 0$. Consider then the Taylor expansion of an arbitrary function $f(q, r, p)$ around $q = 0$ (and $r = -p$). In general we have

$$\begin{aligned} f(q, -p-q, p) &= f(-p, p) + [2(q\cdot p) + q^2]f'(-p, p) \\ &+ 2(q\cdot p)^2 f''(-p, p) + \mathcal{O}(q^3), \end{aligned} \tag{5.37}$$

where the prime denotes differentiation with respect to $(p+q)^2$ and subsequently taking the limit $q \to 0$, i.e,

$$f'(-p,p) \equiv \lim_{q\to 0}\left\{\frac{\partial f(q,-p-q,p)}{\partial (p+q)^2}\right\}. \tag{5.38}$$

So, if the function is antisymmetric under $p \leftrightarrow r$, as happens with the form factors $B_{1,2}$, then $f(-p,p)=0$. Thus, for the case of the form factors in question, the Taylor expansion is

$$\begin{aligned} B_j(q,-p-q,p) &= [2(q\cdot p)+q^2]B_j'(-p,p) \\ &+ 2(q\cdot p)^2 B_j''(-p,p)+\mathcal{O}(q^3); \quad j=1,2. \end{aligned} \tag{5.39}$$

Also, the corresponding Taylor expansion for the gluon propagator will be given by

$$\Delta(p+q)=\Delta(p)+[2(q\cdot p)+q^2]\Delta'(p)+2(q\cdot p)^2\Delta''(p)+\mathcal{O}(q^3). \tag{5.40}$$

Using these Taylor expansions, spherical coordinates to write $(q\cdot k)^2 = q^2k^2\cos^2\theta$, and the integral

$$\int_k f(k^2)\cos^2\theta = \frac{1}{d}\int_k f(k^2), \tag{5.41}$$

Eq. (5.36) becomes in the limit $q\to 0$ (in $d=4$)

$$\bar{I}(0) = -3iC_A\left\{\int_k k^2\Delta^2(k)B_1'(k)+\frac{1}{2}\int_k k^4\frac{\partial}{\partial k^2}[\Delta^2(k)B_1'(k)]\right\}. \tag{5.42}$$

Observe that we have used the property of Eq. (5.25) in order to interchange the arguments of $B_{1,2}$ in Eq. (5.36), so that the Taylor expansion of Eq. (5.39) may be applied directly; this accounts for the additional minus sign. Then, partial integration yields

$$\int_k k^4\frac{\partial}{\partial k^2}[\Delta^2(k)B_1'(k)] = -3\int_k k^2\Delta^2(k)B_1'(k), \tag{5.43}$$

and finally one arrives at (Minkowski space)

$$\bar{I}(0) = \frac{3}{2}iC_A\int_k k^2\Delta^2(k)B_1'(k), \tag{5.44}$$

which corresponds to the value at zero momentum transfer for the one-loop dressed gluonic approximation of the transition function.

The transition to the Euclidean space proceeds by using the standard formulas that allow the conversion from the physical Minkowski momentum q^2 to the Euclidean $q_E^2 = -q^2 > 0$; specifically

$$\Delta_E(q_E^2) = -\Delta(-q_E^2); \quad \partial_{q^2} = -\partial_{q_E^2}; \quad \int_k = i\int_{k_E}. \tag{5.45}$$

Then, dropping the subscript "E", we obtain the Euclidean version of Eq. (5.44),

$$\bar{I}(0) = -\frac{3}{2}C_A \int_k k^2 \Delta^2(k) B_1'(k). \tag{5.46}$$

If we define now $y \equiv k^2$ and writing the Euclidean integration measure in spherical coordinates,

$$\int \frac{d^4k_E}{(2\pi)^4} = \frac{1}{(2\pi)^3}\int_0^\infty dyy \int_0^\pi d\theta \sin^2\theta, \tag{5.47}$$

we arrive finally to the result

$$\bar{I}(0) = -\frac{3C_A}{32\pi^2}\int_0^\infty dyy^2 \Delta^2(y) B_1'(y). \tag{5.48}$$

We end this subsection with a comment on the dimensions of the various form factors that we have introduced in our calculations. The BQ^2 pole vertex $\widetilde{V}$ has mass dimensions $[m]$, and so the form factors $\widetilde{V}_1$, $\widetilde{V}_6$ and $\widetilde{V}_9$ are dimensionless, while the remaining form factors of the vertex have dimension $[m]^{-2}$. The integral $\bar{I}(q)$ has the same dimension as B_1, and as result, in order to keep $\widetilde{V}_1$ dimensionless, B_1 must have dimensions of $[m]$.

5.3 Making contact with the effective gluon mass.

Once the general structure of the BQ^2 pole vertex $\widetilde{V}$ has been established we are going to relate in this section their main dynamical constituents, namely the transition amplitude $\widetilde{I}_\alpha$ and the effective vertex $B_{\mu\nu}$, with the effective gluon mass.

5.3.1 An exact relation.

The WI of Eq. (5.7) furnishes an exact relation between the dynamical gluon mass, the transition function at zero momentum transfer, and the

form factor B_1. Specifically, contracting both sides of the WI with two transverse projectors, one obtains,

$$P^{\mu\rho}(r)P^{\nu\sigma}(p)q^{\alpha}\widetilde{V}_{\alpha\rho\sigma}(q,r,p) = [m^2(r) - m^2(p)]P^{\mu}_{\sigma}(r)P^{\sigma\nu}(p). \tag{5.49}$$

On the other hand, contracting Eq. (5.16) with the momentum of the background leg and using the relation Eq. (5.24), we get

$$q^{\alpha}P^{\mu\rho}(r)P^{\nu\sigma}(p)\widetilde{V}_{\alpha\rho\sigma}(q,r,p) = -\widetilde{I}(q)[B_1 g_{\rho\sigma} + B_2 q_{\rho}q_{\sigma}]P^{\mu\rho}(r)P^{\nu\sigma}(p). \tag{5.50}$$

Thus, equating both results, one arrives at

$$\widetilde{I}(q)B_1(q,r,p) = m^2(p) - m^2(r); \quad B_2(q,r,p) = 0. \tag{5.51}$$

The above relations, together with those of Eq. (5.24), determine exactly the from factors $\widetilde{V}_1$ and $\widetilde{V}_2$ of the BQ^2 pole vertex, namely

$$\widetilde{V}_1(q,r,p) = \frac{m^2(r) - m^2(p)}{q^2}; \quad \widetilde{V}_2(q,r,p) = 0. \tag{5.52}$$

Once determined these form factors we will take the limit $q \to 0$ of Eq. (5.51). For this, using Eq. (5.39) as well as the corresponding Taylor expansion ($r = -q - p$)

$$m^2(r) - m^2(p) = 2(q\cdot p)[m^2(p)]' + \mathcal{O}(q^2), \tag{5.53}$$

assuming that the complete transition function $\widetilde{I}(0)$ is finite, as indeed is the one-loop dressed approximation Eq. (5.44), and equating the coefficients in front of $(q\cdot p)$, we arrive at (Minkowski space)

$$[m^2(p)]' = -\widetilde{I}(0)B_1'(p). \tag{5.54}$$

We emphasize that this is an exact relation, whose derivation relies only on the WI and Bose symmetry that the BQ^2 pole vertex satisfies, as captured by Eq. (5.7) and Eq. (5.25), respectively.

5.3.2 Relating the gluon mass with the transition amplitude.

In this subsection we show how the vertex $\widetilde{V}$ gives raise to a gluon mass when inserted into the corresponding SDE. We will restrict ourselves to the one-loop dressed gluonic block shown in Fig. 5.1, and we will finally express

$m^2(0)$ exclusively in terms of $\bar{I}(0)$, which, in turn depends on the existence of $B_{\mu\nu}$ through Eq. (5.44).

In the PT-BFM scheme, after the replacements Eq. (5.5) and Eq. (5.6), the truncated SDE Eq. (3.22) of the gluon propagator corresponding to the one-loop dressed gluonic block assumes the form

$$[q^2 J_m(q^2) - m^2(q^2)]P_{\mu\nu}(q) = \frac{q^2 P_{\mu\nu}(q) + i[(a_1) + (a_2)]'_{\mu\nu}}{[1 + G(q^2)]^2}, \tag{5.55}$$

where the prime indicates that the fully dressed three-gluon vertex in diagram (a_1) must be replaced by its primed counterpart, as in Eq. (5.6), and the various dressed gluon propagators appearing inside the corresponding diagrams must be replaced by their massive version Eq. (5.5). The most straightforward way to relate the gluon mass to the transition function $\bar{I}$ is to identify, on both sides of Eq. (5.55), the cofactors of the tensorial structure $q_\mu q_\nu/q^2$ which survive the limit $q \to 0$, and then set them equal to each other. It is clear that the left-hand side (lhs) of Eq. (5.55) furnishes simply

$$lhs\big|_{q_\mu q_\nu/q^2} = m^2(q^2). \tag{5.56}$$

To obtain the right-hand side (rhs) of Eq. (5.55) one must isolate the $q_\mu q_\nu/q^2$ component of the contribution to diagram (a_1) coming from the $\widetilde{V}$ vertex. Specifically, if we denote by $(a_1^{\widetilde{V}})_{\mu\nu}$ this contribution, the starting expression is

$$(a_1^{\widetilde{V}})_{\mu\nu} = \frac{1}{2} g^2 C_A \int_k \widetilde{\Gamma}^{(0)}_{\mu\alpha\beta}(q, -k-q, k)\Delta^{\alpha\rho}(k+q)\Delta^{\beta\sigma}(k)\widetilde{V}_{\nu\sigma\rho}(-q, -k, k+q). \tag{5.57}$$

At this point, the projection to the Landau gauge cannot be done directly because of the BQ^2 tree-level vertex contains a ξ^{-1} dependence in the gauge fixing parameter. As was argued in the previous section, we can bypass this problem by setting $G(q^2) = 0$, given that the additional piece which appears when we project to the Landau gauge is proportional to this form factor. With this approximation, and the two internal gluons of diagram (a_1) written in the Landau gauge, according to Eq. (5.16), we have that

$$(a_1^{\widetilde{V}})_{\mu\nu} = \frac{1}{2} g^2 C_A \int_k \Gamma^{(0)}_{\mu\alpha\beta}(q, -k-q, k)\Delta^{\alpha\sigma}(k+q)\Delta^{\beta\rho}(k)\widetilde{\mathcal{U}}_{\nu\rho\sigma}(-q, -k, k+q). \tag{5.58}$$

So, if we use the one-loop dressed approximation for the transition amplitude ($\widetilde{I} \to \bar{I}$), applying Eq. (5.23) we obtain from Eq. (5.58) the following result

$$\begin{aligned}(a_1^{\widetilde{V}})_{\mu\nu} &= -\frac{1}{2}g^2 C_A \int_k \Gamma^{(0)}_{\mu\alpha\beta}\Delta^{\alpha\sigma}(k+q)\Delta^{\beta\rho}(k)\left[\frac{1}{q^2}\bar{I}_\nu(-q)B_{\rho\sigma}\right] \\ &= g^2\left\{\frac{i}{2}C_A \int_k \Gamma^{(0)}_{\mu\alpha\beta}\Delta^{\alpha\sigma}(k+q)\Delta^{\beta\rho}(k)B_{\rho\sigma}\right\}\left(\frac{i}{q^2}\right)\bar{I}_\nu(-q) \\ &= g^2\bar{I}_\mu(q)\left(\frac{i}{q^2}\right)\bar{I}_\nu(-q), \end{aligned} \tag{5.59}$$

where in the last equality we have used Eq. (5.34). It is now relatively

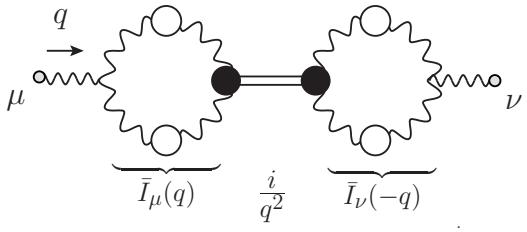

Fig. 5.9: The squared diagram.

straightforward to recognize that the contribution to the rhs comes from the "squared" diagram shown in Fig. 5.9. Finally, applying Eq. (5.21) together with the fact that $\bar{I}_\nu(-q) = -\bar{I}_\nu(q)$, we deduce the following result

$$(a_1^{\widetilde{V}})_{\mu\nu} = -ig^2\bar{I}^2(q)\frac{q_\mu q_\nu}{q^2}. \tag{5.60}$$

Therefore, the mass-related contribution coming from the rhs of Eq. (5.55) is given by a term

$$rhs\big|_{q_\mu q_\nu/q^2} = i(a_1^{\widetilde{V}})_{\mu\nu} = g^2\bar{I}^2(q). \tag{5.61}$$

Equating then the expressions Eq. (5.56) and Eq. (5.61) we obtain finally the following formula, which relates the effective gluon mass with the square of the (one-loop dressed) transition function,

$$m^2(q^2) = g^2\bar{I}^2(q). \tag{5.62}$$

We next take the limit $q \to 0$ and go to the Euclidean space using the usual rules and the result Eq. (5.48), obtaining

$$m^2(0) = g^2 \bar{I}^2(0). \tag{5.63}$$

Note that the $m^2(0)$ so obtained is positive-definite. We emphasize that this relation constitutes the one-loop dressed approximation of the complete relation; indeed, both the SDE used as starting point as well as the expression for $\bar{I}$ are precisely the corresponding one-loop dressed contributions, containing gluons (but not ghosts). Also, the formal projection to the Landau gauge has been avoided and we have set $G(q^2) = 0$.

All these deficiencies will be fixed in the next chapters. The relevant lesson to extract here is that, effectively the Schwinger mechanism is triggered by the vertex $\widetilde{V}$ at the level of the SDE, and that the mass relation obtained is positive-definite in the Euclidean space.

5.4 BSE for the bound-state wave function.

As has become clear in the previous section, the gauge boson (gluon) mass is inextricably connected to the existence of the quantity B_1'. Indeed, if B_1' were to vanish, then, by virtue of Eq. (5.48) so would $\bar{I}(0)$, and therefore, through Eq. (5.63) we would obtain a vanishing $m^2(0)$. Thus, the existence of B_1' is of paramount importance for the mass generation mechanism envisaged here; essentially, the question boils down to whether or not the dynamical formation of a massless bound-state excitation of the type postulated above is possible. As is well known, in order to establish the existence of such a bound-state one must derive the appropriate BSE for the corresponding bound-state wave function, $B_{\mu\nu}$, (or, in this case, its derivative), and find nontrivial solutions for this integral equation.

To be sure, this dynamical equation will be derived under certain simplifying assumptions, which will be further refined in order to obtain numerical solutions. We emphasize, therefore, that the analysis presented here is meant to provide preliminary quantitative evidence for the realization of the dynamical scenario considered, but cannot be regarded as a conclusive demonstration.

The starting point is the BSE, shown in Fig. 5.10, for the vertex $\widetilde{\Gamma}'_{\alpha\mu\nu}(q,r,p)$ defined in Eq. (5.4). Note that, unlike the corresponding SDE of Fig. 5.3, the vertices where the background gluon is entering (carrying momentum q) are now fully-dressed. As a consequence, the corresponding multiparticle

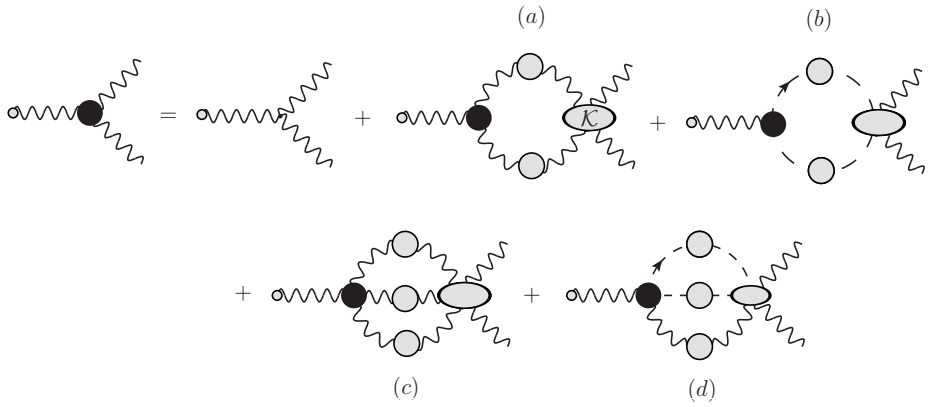

Fig. 5.10: The complete BSE for the full three-gluon vertex $\widetilde{\Gamma}'_{\alpha\mu\nu}(q,r,p)$.

kernels appearing in Fig. 5.10 are different from those of the SDE, as shown in Fig. 5.11.

The general methodology of how to isolate from the BSE shown in Fig. 5.10 the corresponding dynamical equation for the quantity $B_{\mu\nu}$ has been explained in [16, 62]. Specifically, one separates on both sides of the BSE each vertex (black circle) into two parts, a "regular" part and another containing a pole $1/q^2$; this separation is shown in Fig. 5.12. Then, the BSE for $B_{\mu\nu}(q,r,p)$ is obtained simply by equating the pole parts on both sides. Of course, for the case we consider the full implementation of this general procedure would lead to a very complicated structure, because, in principle, all fully dressed vertices appearing on the rhs of Fig. 5.10 may contain pole parts [i.e., not just the three-gluon vertex of (a) but also those in (b), (c), and (d)].Thus, one would be led to an equation, whose lhs would consist of $B_{\mu\nu}$, but whose rhs would contain the $B_{\mu\nu}$ together with all other similar vertices, denoted by $\mathcal{B}_{\{\ldots\}}$ in Eq. (5.27). Therefore, this equation must be supplemented by a set of analogous equations, obtained from the BSEs of all other vertices appearing on the rhs of Fig. 5.10 [i.e., those in (b), (c), (d)]. So, if all the vertices involved contain a pole part, one would arrive at a system of several coupled integral equations, containing complicated combinations of the numerous form factors composing these vertices (see, for example [16]).

It is clear that for practical purposes the above procedure must be simplified to something more manageable. To that end, we will consider

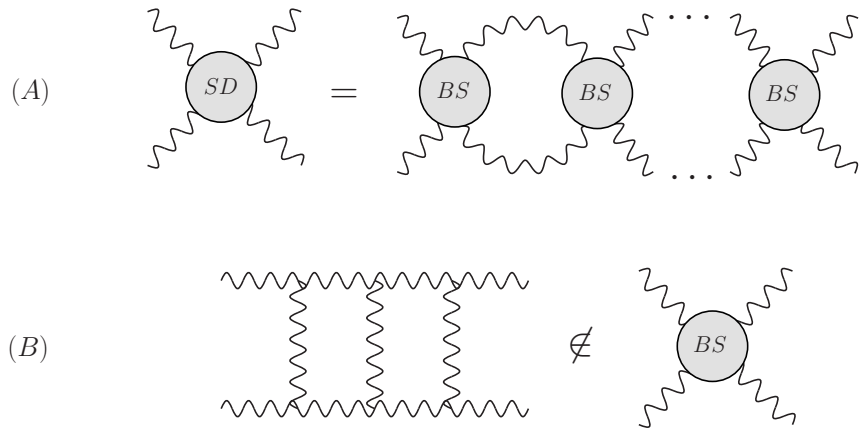

Fig. 5.11: (A) Schematic relation between the SDE and BSE kernels. (B) Example of a diagram not contained in the corresponding BSE kernel, in order to avoid overcounting.

graph (a) on the rhs of Fig. 5.10, thus reducing the problem to the treatment of a single integral equation. Specifically, the BSE we are going to study for $B_{\mu\nu}$ can be seen in Fig. 5.12 and is given by

$$\mathcal{B}^{amn}_{\mu\nu} = \int_k \mathcal{B}^{abc}_{\alpha\beta}\Delta^{\alpha\rho}_{br}(k+q)\Delta^{\beta\sigma}_{cs}(k)\mathcal{K}^{snmr}_{\sigma\nu\mu\rho}. \tag{5.64}$$

In addition, we will approximate the four-gluon BS kernel $\mathcal{K}$ by the lowest-order set of diagrams shown in Fig. 5.13, where the vertices are bare, while the internal gluon propagators are fully-dressed. To proceed further, observe that the diagram (a_1) does not contribute to the BSE, because the color structure of the tree-level four-gluon vertex vanishes when contracted with the color factor f^{abc} of the $\mathcal{B}^{abc}_{\alpha\beta}$. Diagrams (a_2) and (a_3) are equal, and are multiplied by a symmetry factor 1/2. So, in this approximation, the BS kernel is given by

$$\mathcal{K}^{snmr}_{\sigma\nu\mu\rho}(-k,p,-p-q,k+q) = -ig^2 f^{sne}f^{emr}\Gamma^{(0)}_{\sigma\gamma\nu}\Delta^{\gamma\lambda}(k-p)\Gamma^{(0)}_{\mu\lambda\rho}, \tag{5.65}$$

where (as usual) $\Gamma^{(0)}_{\alpha\mu\nu}$ is the tree-level value of the three-gluon vertex. So, using this kernel and setting the gluon propagators in the Landau gauge, the BSE becomes

$$B_{\mu\nu} = -2\pi i\alpha_S C_A \int_k B_{\alpha\beta}\Delta^{\alpha\rho}(k+q)\Delta^{\beta\sigma}(k)\Delta^{\gamma\lambda}(k-p)\Gamma^{(0)}_{\mu\lambda\rho}\Gamma^{(0)}_{\sigma\gamma\nu}, \tag{5.66}$$

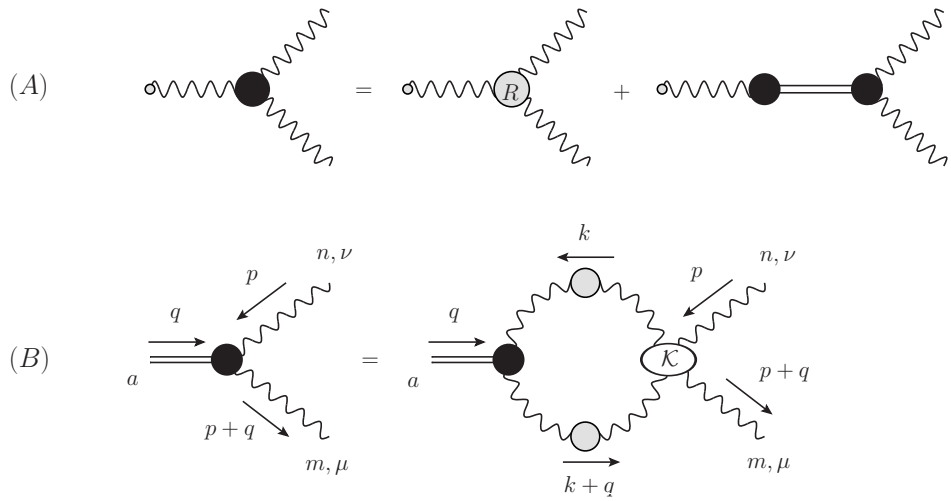

Fig. 5.12: (A) The separation of the vertex in regular and pole parts. (B) The BSE for the bound-state wave function $B_{\mu\nu}$.

where we have canceled out a color factor f^{abc} from both sides.

Let us focus on the lhs of Eq. (5.66). Using the Taylor expansion in Eq. (5.39), the fact that $B_2 = 0$ [see Eq. (5.51)], and multiplying by a transverse projector we obtain, in $d = 4$ dimensions,

$$P^{\mu\nu}(p)B_{\mu\nu} = 6(q\cdot p)B_1'(p) + \mathcal{O}(q^2). \tag{5.67}$$

Next, let us denote by $[rhs]_{\mu\nu}$ the rhs of Eq. (5.66). Inserting the bare value for the three-gluon vertices, multiplying by the transverse projector, and using the Taylor expansions in Eq. (5.39) and Eq. (5.40), after standard manipulations one obtains the result $(d = 4)$

$$P^{\mu\nu}(p)[rhs]_{\mu\nu} = -4\pi i\alpha_S C_A(q\cdot p)\int_k B_1'(k)\Delta^2(k)\Delta(k-p)\mathcal{N}(p,k) + \mathcal{O}(q^2), \tag{5.68}$$

where we have defined the kernel

$$\mathcal{N}(p,k) = \frac{4(p\cdot k)[p^2k^2-(p\cdot k)^2]}{p^4k^2(k-p)^2}[8p^2k^2 - 6(pk)(p^2+k^2) + 3(p^4+k^4) + (pk)^2]. \tag{5.69}$$

Thus, equating the lhs with the rhs, we derive the following BSE for the

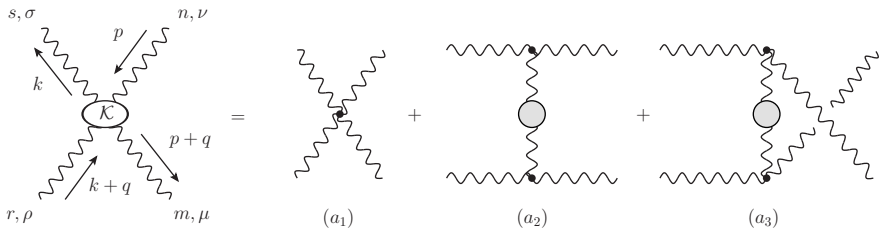

Fig. 5.13: The Feynman diagrams considered for the BS kernel. The interaction vertices are approximated by their tree-level values, while the internal gluon propagators are fully-dressed.

derivative of the form factor that appears in the mass relation Eq. (5.54)

$$B_1'(p) = -\frac{2\pi i}{3}\alpha_S C_A \int_k B_1'(k)\Delta^2(k)\Delta(k-p)\mathcal{N}(p,k). \tag{5.70}$$

Going to Euclidean space, we define

$$x \equiv p^2; \quad y \equiv k^2; \quad z \equiv (p+k)^2, \tag{5.71}$$

and the Euclidean integration measure in spherical coordinates is given by Eq. (5.47), so that the BSE becomes

$$\begin{aligned} B_1'(x) &= -\frac{\alpha_S C_A}{12\pi^2}\int_0^\infty dy y B_1'(y)\Delta^2(y)\sqrt{\frac{y}{x}}\int_0^\pi d\theta \sin^4\theta\cos\theta \\ &\times \left[z + 10(x+y) + \frac{1}{z}(x^2+y^2+10xy)\right]\Delta(z). \end{aligned} \tag{5.72}$$

Then, one may determine the value of B_1' at zero momentum transfer. In spherical coordinates we have $z = x + y + 2\sqrt{xy}\cos\theta$. So, around $x = 0$,

$$\frac{1}{z} = \frac{1}{x+y}\left[1 - 2\frac{\sqrt{xy}}{x+y}\cos\theta\right], \tag{5.73}$$

and using the Taylor expansion for the gluon propagator $\Delta(z)$, the limit $x \to 0$ can be taken in the BSE, giving the value

$$B_1'(0) = -\frac{\alpha_S C_A}{8\pi}\int_0^\infty dy y^3 B_1'(y)\Delta^2(y)\Delta'(y). \tag{5.74}$$

Let us finally implement an additional simplification to Eq. (5.72), which will allow us to carry out the angular integration exactly, thus reducing the problem to the solution of a one-dimensional integral equation. Specifically, the simplification consists in approximating the gluon propagator $\Delta(z)$ appearing in the BSE of Eq. (5.72) [but not the $\Delta^2(y)$] by its tree-level value, that is, $\Delta(z) = 1/z$. Then, with the aid of the angular integrals,

$$\sqrt{\frac{y}{x}}\int_0^\pi d\theta \frac{\sin^4\theta\cos\theta}{z} = \frac{\pi}{16x}\left[\frac{y}{x^2}(y-2x)\Theta(x-y)+\frac{x}{y^2}(x-2y)\Theta(y-x)\right],$$
$$\sqrt{\frac{y}{x}}\int_0^\pi d\theta \frac{\sin^4\theta\cos\theta}{z^2} = -\frac{\pi}{4x}\left[\frac{y}{x^2}\Theta(x-y)+\frac{x}{y^2}\Theta(y-x)\right], \qquad (5.75)$$

one brings Eq. (5.72) into the form

$$\begin{aligned} B_1'(x) &= \frac{\alpha_S C_A}{24\pi}\left\{\int_0^x dy B_1'(y)\Delta^2(y)\frac{y^2}{x}\left(3+\frac{25}{4}\frac{y}{x}-\frac{3}{4}\frac{y^2}{x^2}\right)\right. \\ &+ \left.\int_x^\infty dy B_1'(y)\Delta^2(y) y\left(3+\frac{25}{4}\frac{x}{y}-\frac{3}{4}\frac{x^2}{y^2}\right)\right\}. \end{aligned} \qquad (5.76)$$

The limit $x \to 0$ of this equation is given by (the change of variable $y = tx$ may be found useful)

$$B_1'(0) = \frac{\alpha_S C_A}{8\pi}\int_0^\infty dy y B_1'(y)\Delta^2(y). \qquad (5.77)$$

Note that this result coincides, as it should, with that obtained from Eq. (5.74) after setting $\Delta'(y) = -1/y$, namely, the derivative of the tree-level propagator.

5.5 *Numerical solutions and existence of a bound state.*

In this section we will carry out a detailed numerical analysis of the integral equation obtained in the previous section, namely, Eq. (5.76). The main objective of this study is to establish the existence of nontrivial solutions for B_1' and study their dependence on the value of the strong coupling α_S.

First of all, let us point out that, despite appearances, the integral equation Eq. (5.76) is not linear in the unknown function $B_1'(x)$. The nonlinearity enters through the propagator $\Delta(y)$, which depends on the

dynamical mass $m^2(y)$ through Eq. (5.5); as a result, and by virtue of Eq. (5.54), which, in Euclidean space reads

$$[m^2(y)]' = -\widetilde{I}(0)B_1'(y), \tag{5.78}$$

it is clear that $\Delta(y)$ depends on $B_1'(y)$ in a complicated way. Specifically, from the aforementioned equations we have

$$\Delta_m^{-1}(y) = yJ_m(y) + m^2(y), \tag{5.79}$$

$$m^2(y) = m^2(0) - \widetilde{I}(0)\int_0^y dz B_1'(z). \tag{5.80}$$

Then, Eq. (5.76) must be solved together with the two additional relations given in Eq. (5.79) and Eq. (5.80), as a nonlinear system.

For the purposes of the present analysis we will simplify somewhat the procedure described above. In particular, we will study Eq. (5.76) in isolation, using simple Ansätze for $\Delta(y)$. Specifically, in order to explore the sensitivity of the solutions on the details of $\Delta(q^2)$, we will employ three infrared-finite forms, to be denoted by $\Delta_1(q^2)$, $\Delta_2(q^2)$ and $\Delta_3(q^2)$, focusing on their differences in the intermediate and asymptotic regions of momenta.

Let us start with the simplest such propagator, namely, a tree-level massive propagator of the form

$$\Delta_1^{-1}(q^2) = q^2 + m_0^2, \tag{5.81}$$

where m_0^2 is a hard mass, that will be treated as a free parameter. On Fig. 5.14, the (blue) dotted curve represents $\Delta_1(q^2)$ for $m_0 = 376$ MeV.

The second model is an improved version of the first, where we introduce the renormalization-group logarithm next to the momentum q^2, more specifically

$$\Delta_2^{-1}(q^2) = q^2\left[1 + \frac{13C_A g^2}{96\pi^2}\ln\left(\frac{q^2+\rho m_0^2}{\mu^2}\right)\right] + m_0^2, \tag{5.82}$$

where ρ is an adjustable parameter varying in the range $\rho \in [2, 16]$. Notice that the hard mass m_0^2 appearing in the argument of the perturbative logarithm acts as an infrared cutoff; so, instead of the logarithm diverging at the Landau pole, it saturates at a finite value. The (black) dashed line in Fig. 5.14 represents the Eq. (5.82) when $\rho = 16$, $m_0 = 376$ MeV, and $\mu = 4.3$ GeV.

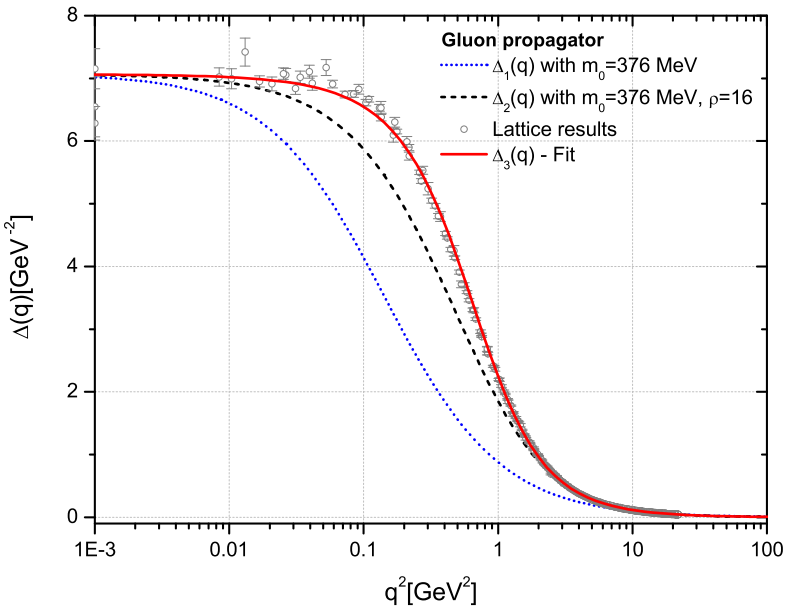

Fig. 5.14: The three models for the gluon propagator as function of the momentum q^2. The (red) continuous line is the fit for the lattice gluon propagator given by Eq. (5.83) when $m = 520$ MeV, $g_1^2 = 5.68$, $\rho_1 = 8.55$, $\rho_2 = 1.91$, and $\mu = 4.3$ GeV; the (black) dashed line is the model of Eq. (5.82) with $\rho = 16$, $\alpha_s = 0.667$ and $m_0 = 376\,\text{MeV}$, while the (blue) dotted line represents the massive propagator of Eq. (5.81) when $m_0 = 376\,\text{MeV}$.

The third model is simply a physically motivated fit for the gluon propagator determined by the large-volume lattice simulations of [32]. The lattice data presented there correspond to a $SU(3)$ quenched lattice simulation, where $\Delta(q^2)$ is renormalized at $\mu = 4.3$ GeV. This gluon propagator can be accurately fitted by the expression [see also Eq. (2.1) in Chapter 2]

$$\Delta_3^{-1}(q^2) = q^2\left[1 + \frac{13C_A g_1^2}{96\pi^2}\ln\left(\frac{q^2 + \rho_1 m_g^2(q^2)}{\mu^2}\right)\right] + m_g^2(q^2), \qquad (5.83)$$

where $m_g^2(q^2)$ is a running mass given by

$$m_g^2(q^2) = \frac{m^4}{q^2 + \rho_2 m^2}, \qquad (5.84)$$

and the values of the fitting parameters are $m = 250$ MeV, $g_1^2 = 5.68$,

$\rho_1 = 8.55$ and $\rho_2 = 1.91$. On Fig. 5.14, the (red) continuous line represents the fit for the lattice gluon propagator given by Eq. (5.83). Notice that, in all three cases, we have fixed the value of $\Delta^{-1}(0) = m_0^2 \approx 0.14$.

Our main findings may be summarized as follows:

- In Fig. 5.15 we show the solutions of Eq. (5.76) obtained using as input the three gluon propagators shown on Fig. 5.14. For the simple massive propagator of Eq. (5.81), a solution for $B_1'(q)$ is found for $\alpha_S = 1.48$; in the case of $\Delta_2(q^2)$ given by Eq. (5.82), a solution is obtained when $\alpha_S = 0.667$, while for the lattice propagator $\Delta_3(q^2)$ of Eq. (5.83) a nontrivial solution is found when $\alpha_S = 0.492$.

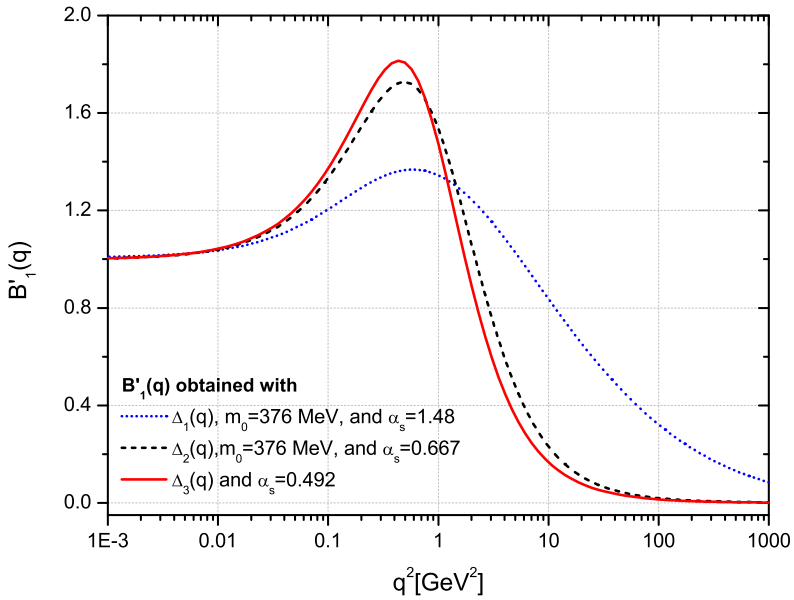

Fig. 5.15: The corresponding solutions of Eq. (5.76) obtained with the gluon propagators shown on the left panel. The solutions for $B_1'(q)$ are obtained when we fix the value of $\alpha_s = 1.48$, $\alpha_s = 0.667$, and $\alpha_s = 0.492$ for $\Delta_1(q)$, $\Delta_2(q)$, and $\Delta_3(q)$, respectively.

- Since $\Delta(y)$ at this level is treated as an "external" object, the homogeneous Eq. (5.76) becomes linear in B_1'; as a result, given one solution we obtain a family of such solutions [64], i.e., if $B_1'(q)$ is a solution then the function $cB_1'(q)$ is also a solution, for any real constant

c. Therefore, the solutions shown on Fig. 5.15 correspond to a representative case of a family of possible solutions, where the constant c was chosen such that $B_1'(0) = 1$. This arbitrariness in the value of c may be completely eliminated if one restores the nonlinearity of Eq. (5.76) considering also Eq. (5.79) and Eq. (5.80). As a consequence one should be able to obtain a single expression for $B_1'(q)$ for a unique value of α_S.

- Another interesting feature of the solutions of Eq. (5.76) is the dependence of the observed peak on the support of the gluon propagator in the intermediate region of momenta. Specifically, an increase of the support of the gluon propagator in the approximate range $(0.3 - 1)$ GeV results in a more pronounced peak in $B_1'(q)$.

- In addition, observe that due to the presence of the perturbative logarithm in the expression of $\Delta_2(q^2)$ and $\Delta_3(q^2)$, the corresponding solutions $B_1'(q)$ fall off in the ultraviolet region much faster than those obtained using the simple $\Delta_1(q^2)$ of Eq. (5.81).

5.6 Decoupling of the massless excitation.

As we have seen throughout this chapter, the interaction vertices of the theory must be modified adding a pole part, which introduces the required massless excitations in order to trigger the Schwinger mechanism. These massless excitations, in turn, modify the off-shell amplitudes appearing in the skeleton expansions of the interaction vertices by introducing poles in their structures. Nevertheless, it is true that the full on-shell amplitudes do not possess such poles and, hence, the massless excitations decouple from the theory.

In this section we give an explicit example of how the massless excitation decouples from an on-shell amplitude. Specifically, we will show how this is indeed what happens in the case of the four-gluon amplitude. To be sure, a complete proof of the decoupling of the massless excitation from all Yang-Mills amplitudes requires the treatment of kernels with an arbitrary number of incoming gluons. However, the example consider here captures the essence of the underlying decoupling mechanism.

The demonstration followed here is similar to that given in [61] for the case of an Abelian model. One starts by considering the complete four-gluon amplitude, given by graph (a) in Fig. 5.16, which consist on three

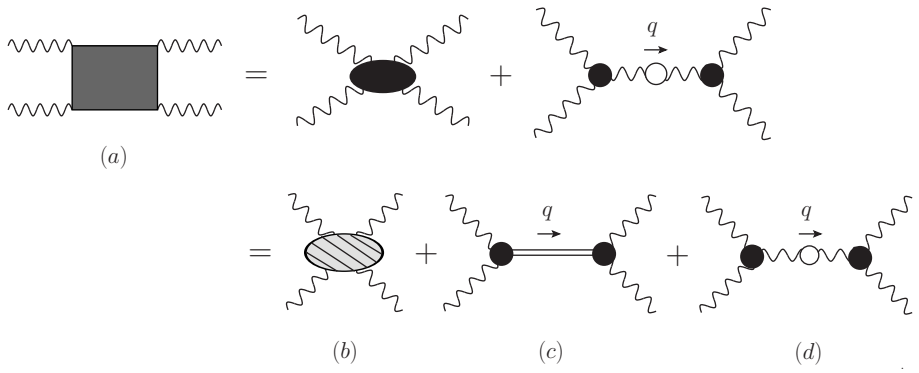

Fig. 5.16: The complete four-gluon amplitude and the various terms composing it.

distinct pieces:

- The amplitude represented by the diagram (b), which is regular as $q^2 \to 0$.
- The graph (c), which contains the massless excitation, coupled to the external gluons through the proper vertex function $B_{\mu\nu}$.
- The one-particle reducible term, denoted by (d), which is excluded from the SDE kernel in the usual skeleton expansion.

Of course, the above amplitudes are none other than (b_2), (b_3) and (a), in Fig. 5.4, respectively. Since the amplitude (b) is regular by construction, one must only demonstrate that, as $q^2 \to 0$, the divergent part of (c), whose origin is the massless excitation, cancels exactly against an analogous contribution contained in (d), leaving finally a regular result.

We start by considering the term (d). Within the PT-BFM framework that we use, the off-shell gluon (carrying momentum q) is effectively converted into a background gluon; thus, the gluon propagator appearing inside (d) is given by $\widehat{\Delta}(q^2)$, while the two three-gluon vertices are the $\widetilde{\Gamma}'$ defined in Eq. (5.4). So,

$$\begin{aligned}(d) &= -ig^2\widetilde{\Gamma}'_{\alpha\mu\nu}(-q,p_1,p_2)P^{\alpha\beta}(q)\widehat{\Delta}(q^2)\widetilde{\Gamma}'_{\beta\rho\sigma}(q,p_3,p_4)\\ &= -ig^2\widetilde{\Gamma}'_{\alpha\mu\nu}(-q,p_1,p_2)\widehat{\Delta}(q^2)\Gamma'^{\alpha}_{\rho\sigma}(q,p_3,p_4),\end{aligned} \tag{5.85}$$

where the factor $(-i)$ comes from the definition of the gluon propagator, Eq. (3.4). In the second line we have eliminated the longitudinal term

$q^\alpha q^\beta/q^2$ inside $P^{\alpha\beta}(q)$ using the "on-shellness" condition

$$q^\alpha \widetilde{\Gamma}'_{\alpha\mu\nu}(q,r,p)\big|_{o.s.} = [\Delta^{-1}(p)P_{\mu\nu}(p) - \Delta^{-1}(r)P_{\mu\nu}(r)]\big|_{o.s.} = 0, \qquad (5.86)$$

valid for both three-gluon vertices. We emphasize that the full $\widetilde{\Gamma}'$ is needed (with the $\widetilde{V}$ part included) for the on-shellness condition of Eq. (5.86) to be fulfilled. Note also that, if one had chosen a nonvanishing gauge-fixing parameter ξ for the gluon propagator (instead of the $\xi = 0$ of the Landau gauge), then the condition of Eq. (5.86) is instrumental for the cancellation of the unphysical parameter ξ from the physical amplitude.

Next, it is clear that from the vertex $\widetilde{V}$ contained in $\widetilde{\Gamma}'$ only the $\widetilde{\mathcal{U}}$ part survives, because all longitudinal momenta contained in $\widetilde{R}$ are annihilated on shell, i.e., when contracted with the appropriate polarization vectors $e_\mu(p)$, due to the validity of the relation $p^\mu e_\mu(p) = 0$. Then, we have that (suppressing indices)

$$\widetilde{\Gamma}'\widehat{\Delta}\widetilde{\Gamma}' = (\widetilde{\Gamma}_m + \widetilde{\mathcal{U}})\widehat{\Delta}(\widetilde{\Gamma}_m + \widetilde{\mathcal{U}}) = \widetilde{\Gamma}_m\widehat{\Delta}\widetilde{\Gamma}_m + \widetilde{\Gamma}'\widehat{\Delta}\widetilde{\mathcal{U}} + \widetilde{\mathcal{U}}\widehat{\Delta}\widetilde{\Gamma}' - \widetilde{\mathcal{U}}\widehat{\Delta}\widetilde{\mathcal{U}}. \quad (5.87)$$

Given that the first term in Eq. (5.87) is regular, while the second and third term vanish on-shell by virtue of Eq. (5.86) [which is triggered because $\widetilde{\mathcal{U}}$ is proportional to q_α, see Eq. (5.14)], we are led to the following expression for the pole part of (d)

$$(d)\big|_{pole} = ig^2\widetilde{\mathcal{U}}_{\alpha\mu\nu}\widehat{\Delta}(q^2)\widetilde{\mathcal{U}}^\alpha_{\rho\sigma}. \qquad (5.88)$$

Then, using Eq. (5.23), we obtain

$$(d)\big|_{pole} = -\left\{B_{\mu\nu}\left(\frac{i}{q^2}\right)B_{\rho\sigma}\right\}[g^2\widetilde{I}^2(q^2)\widehat{\Delta}(q^2)]. \qquad (5.89)$$

Now, in the limit $q^2 \to 0$, the quantity in square brackets goes to 1, precisely by virtue of Eq. (5.63) [remember, $\widehat{\Delta}^{-1}(0) = \widehat{m}^2(0)$]. Therefore,

$$\lim_{q^2\to 0}(d)\big|_{pole} = -\lim_{q^2\to 0}\left\{B_{\mu\nu}\left(\frac{i}{q^2}\right)B_{\rho\sigma}\right\}, \qquad (5.90)$$

which is precisely the contribution of the term (c) in the same kinematic limit, but with the opposite sign. Therefore, the on-shell four-gluon amplitude is free from poles at $q^2 = 0$, as announced.

5.7 Discussion.

Some comments about the limitations of the results obtained here must be added. First of all, the formal projection to the Landau gauge of some of the equations we have derived in this chapter requires the knowledge of the STI satisfied by the effective vertex $B_{\mu\nu}$. We will see that this STI gives raise to terms proportional to the form factor $G(q^2)$ of the auxiliary function Eq. (3.18) and this is the reason for setting $G(q^2) = 0$. This approximation do not interfere with the essence and the ideas presented here. Nevertheless, a self-consistent description of the Schwinger mechanism must take into account this aspect.

Another limitation of our results is that both, the expression Eq. (5.48) for the transition amplitude and the formula Eq. (5.63) for the gluon mass, have been obtained in the one-loop dressed approximation. In principle, the analysis presented above may be extended to include the rest of the graphs contributing to the transition amplitude and the gluon SDE, invoking the corresponding pole parts of the remaining vertices. This task will be achieved in the subsequent chapters.

In fact the extension of this analysis beyond the one-loop dressed approximation is absolutely essential to obtain a consistent description of the effective gluon mass. To explain how one reaches the above conclusion, consider again Eq. (5.78) relating the derivative of the effective gluon mass with the value at $q^2 = 0$ of the full transition amplitude,

$$[m^2(y)]' = -\widetilde{I}(0)B_1'(y).$$

The numerical results for the BSE which describes the behavior of B_1', shown in Fig. 5.15, reveal that this quantity is positive definite in the entire range of physical momenta, i.e., $B_1'(y) > 0$. So, if one wants to find monotonically decreasing solutions for the effective gluon mass, the value $\widetilde{I}(0)$ must be positive. When this happens, the derivative of the effective gluon mass is negative and provides the desired kind of solutions. However, the one-loop dressed approximation for the transition amplitude Eq. (5.48) gives a negative value $\bar{I}(0) < 0$. As a consequence, the derivative of the effective gluon mass in this approximation is positive, $[m^2(y)]' > 0$, and one arrives to the conclusion that monotonically decreasing solutions are not compatible with these constraints. So, it is clear that something is missing in the one-loop dressed approximation. Thus, one expects that the addition of higher order contributions be able to reverse the sign of the value $\bar{I}(0)$, providing the right sign for the derivative of the effective gluon

mass. For this reason, the next chapters will be dedicated to obtaining the full description (and not only the one-loop dressed approximation) of the dynamical gluon mass generation mechanism.

6. THE ALL-ORDER EQUATION OF THE EFFECTIVE GLUON MASS.

At the level of the SDE for the gluon propagator, the analysis of the mass generation mechanism finally boils down to the derivation of an integral equation that determines the evolution of the dynamical gluon mass, $m^2(q^2)$, as a function of the momentum q^2. The main purpose of this chapter is to present the general derivation of the complete gluon mass equation [72], employing the full SDE of the gluon propagator, and show that this equation supports solutions giving raise to an infrared-finite gluon propagator, i.e., $\Delta^{-1}(0) = m^2(0)$.

In order to address this difficult question, we consider the set of modified SDEs obtained within the framework of the PT-BFM scheme. In particular, one gains a considerable advantage by considering the version of the identity Eq. (3.17) connecting the QQ with the QB propagators. The resulting SDE (to be denoted as the "QB version") displays the powerful block-wise transversality property known from the BB case and has two additional important features: it contains fewer graphs, and the limiting procedure necessary for projecting the result to the Landau gauge is significantly less involved.

Even within this improved framework, one still faces the fundamental question of how to disentangle from the SDE of the entire gluon propagator the part that controls the evolution of the mass from the part that controls the evolution of the "kinetic" term. In this chapter we present a new unambiguous way for implementing this separation, which exploits to the fullest the characteristic structure of the pole vertices V introduced in the previous chapter.

It turns out that the very special nature of these vertices furnishes a solid guiding principle for implementing the aforementioned separation between mass and kinetic terms. In particular, their longitudinal structure, coupled to the fact that we work in the Landau gauge, completely determines the $q_\mu q_\nu$ component of the mass equation; this is tantamount to knowing the

full mass equation, given that the answer is transverse (so, the $g_{\mu\nu}$ part is automatically fixed from its $q_\mu q_\nu$ counterpart).

As already mentioned, in the present chapter we include all fully dressed graphs (one and two loops) comprising the corresponding full SDE of the QB propagator. Going beyond the "one-loop" dressed analysis is highly nontrivial, because it requires the introduction of a new V-type vertex, never considered before. Specifically, in addition to the Vs related to the three-gluon vertices, known from the one-loop case, the V vertex associated with the fully-dressed four gluon vertex BQ^3 must be included in the corresponding "two-loop dressed" diagram. As happens in the one-loop case with the three-gluon V, this new four-gluon V vertex must satisfy a very concrete Abelian-like WI, in order to ensure the transversality of the "two-loop dressed" part of the calculation. Interestingly enough, and again as a consequence of their longitudinal nature and the Landau gauge, the WIs (and in some case the STI) satisfied by all V-type vertices involved in this problem is all that one needs for calculating their effects exactly. This fact clearly constitutes an important simplification and bypasses the need to actually construct explicitly the corresponding vertices.

As a consequence of the novel aspects introduced to our approach, the "one-loop" calculation presented in the first part of our derivation (Section 6.2) proceeds in a far more concise way compared to the corresponding analysis carried out in [22], rectifying, in fact, the form of the resulting mass equation. The two-loop contribution is considerably more cumbersome to obtain, and is expressed in terms of a kernel that, in addition to full gluon propagators, involves also the conventional, fully dressed, three gluon vertex (Q^3). The two-loop part of the mass equation is subsequently simplified by choosing tree-level values for a judicious combinations of its ingredients, a fact that allows us to carry out explicitly one of the two integrations over virtual momenta. In order to gain insight on the numerical subtleties associated with this equation, we first consider its limit at vanishing physical momenta, thus converting it into a nonlinear constraint. Already at this level, the contribution from the two-loop part appears to be of paramount importance, having far-reaching consequences for the behavior of the resulting solutions. The detailed numerical solution of the full equation (for arbitrary values of the physical momentum) confirms this impression, revealing the existence of positive-definite and monotonically decreasing solutions.

The chapter is organized as follows. In Section 6.1 we outline in detail

the methodology that allows one to extract from the corresponding SDE two separate equations, one for the mass and one for the kinetic term, and explain the advantage of selecting out the $q_\mu q_\nu$ component. Section 6.2 is dedicated to the concise derivation of the one-loop version of the mass equation. In addition, a brief discussion about the ghost sector (only "one-loop" in this new SDE version) is included, explaining why the ghost graphs do not affect the mass equation. In Section 6.3 we present the full two-loop calculation, organizing the corresponding technical aspects into various self-contained subsections. In Section 6.4 we present the final form of the integral equation that governs the dynamical mass, and discuss some of its general properties. In addition, we calculate an approximate expression for the new contribution to the kernel of this integral equation, to be used in the ensuing numerical analysis. In Section 6.5 we solve numerically the integral equation, we determine a family of positive-definite and monotonically decreasing solutions, and study their dependence on the value of the strong coupling constant.

6.1 Deriving the mass equation: General methodology

The starting point to derive the mass equation will be the SDE satisfied by the QB gluon propagator $\widetilde{\Delta}(q^2)$ [see Eq. (3.8)] and the second relation in Eq. (3.17). Then, the corresponding version of the SDE for the conventional gluon propagator (in the Landau gauge) reads

$$\Delta^{-1}(q^2)P_{\mu\nu}(q) = \frac{q^2 P_{\mu\nu}(q) + i\sum_{i=1}^{6}(a_i)_{\mu\nu}}{1+G(q^2)}, \tag{6.1}$$

where the diagrams (a_i) are shown in Fig. 3.2. The crucial points to recognize are:

- One has a reduced set of Feynman diagrams (six instead of ten) compared to those appearing in the formulation in terms of $\widehat{\Delta}(q^2)$, see Fig. 3.3.

- The quantum leg enterig from the left in diagram (a_1) contains the tree-level conventional three-gluon vertex $\Gamma^{(0)}_{\alpha\mu\nu}$ instead of the tree-level BQ^2 vertex $\widetilde{\Gamma}^{(0)}_{\alpha\mu\nu}$. This fact will allow the projection to the Landau gauge directly in the part of the calculation related to the masses without the necessity of applying the decomposition Eq. (5.29) and the identity Eq. (5.32).

- The most important feature of the PT-BFM formalism for our purposes, namely the block-wise transversality imposed at the level of the SDE for the gluon self-energy, is still present. In particular, the transversality of the gluon self-energy is realized according to the pattern highlighted by the boxes of Fig. 3.2 and shown in Eq. (3.16).

As explained in the previous chapter, see Section 4.1, the special vertices $\widetilde{V}$ (and V) enforce the transversality of the rhs of Eq. (6.1) in the presence of gluon masses. Specifically, writing the $\Delta_m^{-1}(q^2)$ on the lhs of Eq. (6.1) in the form given in Eq. (5.5) , one has that

$$[q^2 J_m(q^2) - m^2(q^2)]P_{\mu\nu}(q) = \frac{q^2 P_{\mu\nu}(q) + i\sum_{i=1}^{6}(a_i')_{\mu\nu}}{1+G(q^2)}, \qquad (6.2)$$

where the "primes" indicates that (in general) the various fully dressed vertices appearing inside the corresponding diagrams must be replaced by their primed counterparts, as in Eq. (5.6). Thus, in graph (a_1) the BQ^2 vertex will be substituted by $\widetilde{\Gamma}'$, while in graph (a_6) both the BQ^2 and the Q^3 type of vertices must contain the corresponding $\widetilde{V}$ and V components, respectively. In addition, in diagram (a_5) the primed version of the vertex BQ^3 will make its appearance. These modifications have an important effect: the blockwise transversality property of Eq. (3.16) holds also for the "primed" graphs, *i.e.*, when $(a_i) \to (a_i')$.

The lhs of Eq. (6.2) involves two unknown quantities, $J_m(q^2)$ and $m^2(q^2)$, which will eventually satisfy two separate, but coupled, integral equations. of the generic type

$$\begin{aligned} J_m(q^2) &= 1 + \int_k \mathcal{K}_1(q^2, m^2, \Delta_m), \\ m^2(q^2) &= \int_k \mathcal{K}_2(q^2, m^2, \Delta_m). \end{aligned} \qquad (6.3)$$

such that $q^2\mathcal{K}_1(q^2, m^2, \Delta_m) \to 0$, as $q^2 \to 0$, whereas $\mathcal{K}_2(q^2, m^2, \Delta_m) \neq 0$ in the same limit, precisely because it includes the $1/q^2$ terms contained inside the various V and $\widetilde{V}$ terms.

In this chapter we will focus on the derivation of the closed form of the integral equation governing $m^2(q^2)$. To that end, we must identify all mass related contributions contained in the Feynman graphs that comprise the rhs of Eq. (6.2). Now, with the transversality of both sides of Eq. (6.2) guaranteed, it turns out that it is far more economical to derive the mass

equation by isolating the appropriate cofactors of $q_\mu q_\nu/q^2$ on both sides, instead of the $g_{\mu\nu}$, or instead of taking the trace. In particular, to obtain the rhs of the mass equation, one must

- Consider the graphs that contain a vertex $\widetilde{V}$.
- Isolate the $q_\mu q_\nu/q^2$ component of the contributions coming from the $\widetilde{V}$ vertices.

To explain how one reaches the above conclusion, let us point out that, clearly, were it not for the $\widetilde{V}$ and V terms that contain the massless poles, no gluon mass could be generated. However, as we will see in detail in what follows, the longitudinal nature of the vertices $\widetilde{V}$ [*viz.* Eq. (5.3)], coupled to the fact that we work in the Landau gauge, force the corresponding contribution to be proportional to q_ν [see Eqs. (6.24) and (6.42)]. The only exception to this rule is the V that appears inside graph (a_6), as part of the Q^3 vertex Γ'; however, the corresponding contribution is shown to vanish identically in the Landau gauge (see Sec. 6.3). Thus, if we denote by $(a_i^{\tilde{V}})_{\mu\nu}$ the $\widetilde{V}$-related contributions of the corresponding diagrams, these latter terms are proportional to $q_\mu q_\nu/q^2$ only, namely

$$(a_i^{\tilde{V}})_{\mu\nu} = \frac{q_\mu q_\nu}{q^2} a_i^{\tilde{V}}(q^2) \tag{6.4}$$

so that

$$m^2(q^2) = \frac{i\sum_{i=1} a_i^{\tilde{V}}(q^2)}{1+G(q^2)}\,, \tag{6.5}$$

where the sum includes only the graphs $i = 1, 5, 6$.

Similarly, the equation for $J_m(q^2)$ may be obtained from the $q_\mu q_\nu/q^2$ component of the parts of the graphs that do not contain V components. These graphs are identical to the original set $(a_1)-(a_6)$, but now $\widetilde{\Gamma} \to \widetilde{\Gamma}_m$, $\Delta \to \Delta_m$, etc. To avoid notational clutter we will use the same letter as before, and the aforementioned changes are understood. These contributions may be separated in $g_{\mu\nu}$ and $q_\mu q_\nu/q^2$ components,

$$(a_i)_{\mu\nu} = g_{\mu\nu}\, A_i(q^2) + \frac{q_\mu q_\nu}{q^2} B_i(q^2) \tag{6.6}$$

Note that graphs (a_2) and (a_4) are proportional to $g_{\mu\nu}$ only; so, in the notation introduced above, $B_2(q^2) = B_4(q^2) = 0$. Then, the corresponding equation for $J_m(q^2)$ reads

$$-q^2 J_m(q^2) = \frac{-q^2 + i\sum_{i=1} B_i(q^2)}{1+G(q^2)}, \tag{6.7}$$

with $i = 1, 3, 5, 6$.

We hasten to emphasize that the fact that we focus on the $q_\mu q_\nu/q^2$ terms, instead of the $g_{\mu\nu}$, in no way indicates a potential clash with the transversality of the gluon self-energy, which is manifestly preserved throughout. In fact, it is precisely the validity of Eq. (3.6) that allows one to choose freely between the two tensorial structures. The point is that the transversality of Eq. (6.2) should not be interpreted to mean that the algebraic origin of the terms proportional to $g_{\mu\nu}$ is the same as that of the terms proportional to $q_\mu q_\nu/q^2$. In particular, the $q_\mu q_\nu/q^2$ of $J_m(q^2)$ and $m^2(q^2)$ are easily separable, as the Eqs. (6.5) and (6.7) indicate, whereas their $g_{\mu\nu}$ parts are entangled, and their separation is significantly more delicate.

As a particular example of how the $g_{\mu\nu}$ part requires an elaborate treatment, while the $q_\mu q_\nu/q^2$ does not, let us consider the basic cancellation taking place at the "one-loop dressed" level, enforced by the so-called "seagull identity": the (quadratic) divergence of the "seagull" diagram (a_2) is annihilated exactly by a very particular contribution coming from graph (a_1), by virtue of the identity (valid in dimensional regularization) [43]

$$\int_k k^2 \frac{\mathrm{d}\Delta_m(k^2)}{\mathrm{d}k^2} + \frac{d}{2}\int_k \Delta_m(k^2) = 0. \tag{6.8}$$

The point is that, all terms involved in this cancellation are proportional to $g_{\mu\nu}$, and it is only after they are properly combined that their total contribution vanishes (as $q^2 \to 0$), by virtue of Eq. (6.8); instead, their $q_\mu q_\nu/q^2$ counterparts vanish *individually*, in the same limit.

In order to appreciate this last point, consider the expression

$$I_{\mu\nu}(q) \equiv \int_k k_\mu k_\nu f(k,q) \tag{6.9}$$

where $f(k,q)$ is an arbitrary function that remains finite in the limit $q^2 \to 0$. Clearly,

$$I_{\mu\nu}(q) = g_{\mu\nu} A(q^2) + \frac{q_\mu q_\nu}{q^2} B(q^2)\,, \tag{6.10}$$

and the form factors $A(q^2)$ and $B(q^2)$ are given by

$$\begin{aligned} A(q^2) &= \frac{1}{d-1}\int_k \left[k^2 - \frac{(k\cdot q)^2}{q^2}\right] f(k,q), \\ B(q^2) &= -\frac{1}{d-1}\int_k \left[k^2 - d\frac{(k\cdot q)^2}{q^2}\right] f(k,q) \end{aligned} \tag{6.11}$$

Then, setting $(q \cdot k)^2 = q^2 k^2 \cos^2\theta$, and using the angular integral Eq. (5.41), we obtain from Eq. (6.11) that, as $q^2 \to 0$,

$$A(0) = \frac{1}{d}\int_k k^2\, f(k); \qquad B(0) = 0. \tag{6.12}$$

Evidently, the function f may be such that the integral defining $A(0)$ diverges, while, for the same function, $B(0)$ vanishes.

Now, in the context of the "one-loop" dressed calculation, the term $I_{\mu\nu}(q)$ originates from graph (a_1), with the replacement $\widetilde{\Gamma} \to \widetilde{\Gamma}_m$, $\Delta \to \Delta_m$, as mentioned above. The WI satisfied by $\widetilde{\Gamma}_m$ is that of Eq. (5.1) with $J \to J_m$, and similar but more complicated STIs hold when contracting with respect to the other momenta. Note that what appears in the WI and STIs is J_m and *not* Δ_m. Then, as has been shown in [65], the longitudinal part of $\widetilde{\Gamma}_m$ may be expressed in terms of J_m (and other Green's functions), and as a result, the function $f(k)$ (at $q^2 = 0$) is given by

$$f(k^2) = -\Delta_m^2(k^2)\frac{\mathrm{d}\left(k^2 J_m(k^2)\right)}{\mathrm{d}k^2} \tag{6.13}$$

Now, the point is that, in order to trigger Eq. (6.8), $f(k^2)$ should be instead

$$f(k^2) = -\Delta_m^2(k^2)\frac{\mathrm{d}\Delta^{-1}(k^2)}{\mathrm{d}k^2} = \frac{\mathrm{d}\Delta_m(k^2)}{\mathrm{d}k^2}. \tag{6.14}$$

To accomplish this, one adds and subtracts $m^2(k^2)$ to the $f(k)$ of the $A(0)$ given in Eq. (6.12), thus obtaining

$$A(0) = \frac{1}{d}\left[\int_k k^2 \frac{\mathrm{d}\Delta_m(k^2)}{\mathrm{d}k^2} - \int_k k^2 \frac{\mathrm{d}m^2(k^2)}{\mathrm{d}k^2}\right]. \tag{6.15}$$

At that point, the first term on the rhs of Eq. (6.15) goes to the $g_{\mu\nu}$ part of the equation of $J_m(q^2)$; when added to the term (a_2), which is also assigned (in its entirety) to the $g_{\mu\nu}$ part of that same equation, it finally gives rise, by virtue of Eq. (6.8), to a contribution that is free of quadratic divergences and vanishes in the $q^2 = 0$ limit, as it should. On the other hand, the second term on the rhs of Eq. (6.15) is allotted to the mass equation. Thus, unlike $B(q^2)$, which unambiguously contributes to the $q_\mu q_\nu/q^2$ part of the equation for $J_m(q^2)$ [and satisfies automatically $B(0) = 0$], the $A(q^2)$ contributes to the $g_{\mu\nu}$ component of *both* equations.

Let us finally point out that the purely longitudinal nature of the vertices $\widetilde{V}$ (and V) expressed through conditions such as Eq. (5.3), combined

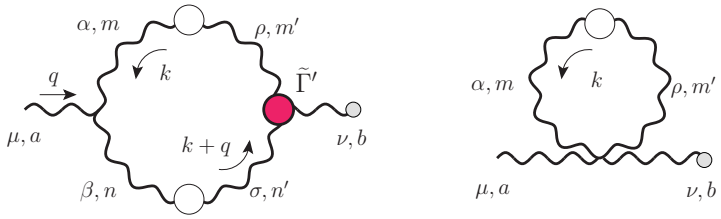

Fig. 6.1: The "one-loop dressed" part of the SDE that contains only gluons. Thick lines represent gluon propagators endowed with a momentum-dependent mass. The fully dressed "primed" vertex, $\widetilde{\Gamma}'$, enforces gauge invariance in the presence of such a mass. The symmetry factors are 1/2 and 1 respectively; we also show for the reader's convenience (in this and the next figures) the color and Lorentz indices, as well as the momentum routing used in our calculations.

with the fact that we work in the Landau gauge, allows one to obtain all relevant contributions simply from the knowledge of the WI (or STI) that these vertices satisfy, without the need to construct them *explicitly*. This is particularly important in the case of the vertex $\widetilde{V}_{\nu\rho\sigma\tau}$, appearing in graph (a_5); indeed, constructing this vertex explicitly would constitute an arduous task, given the complicated STIs that it satisfies when contracted by the momentum of any of its three quantum legs.

6.2 The "one-loop dressed" mass equation: Concise derivation

According to the methodology outlined in the previous section, the one-loop dressed contribution to the gluon mass equation stems solely from the $\widetilde{V}$-part of graph $(a_1')_{\mu\nu}$, to be denoted by $(a_1^{\widetilde{V}})_{\mu\nu}$.

The first simplification stemming from the use of the SDE for the QB propagator (as opposed to the BB employed in [22]) is that the Landau gauge limit $\xi = 0$ may be taken directly, in the part of the calculation related to the masses. Indeed, the only source of terms proportional to ξ^{-1} (which require special care) is the tree-level part of the BQ^2 vertex, which only affect the equation for $J(q^2)$ (and can be easily dealt with, following the procedure explained in [26]). Then (see Fig. 6.1 for the Lorentz and color

indices as well as the momenta routing used in the following calculation)

$$(a_1^{\tilde{V}})_{\mu\nu} = \frac{1}{2}\, g^2 C_A \int_k \Gamma^{(0)}_{\mu\alpha\beta}(q,k,-k-q)\Delta^{\alpha\rho}(k)\Delta^{\beta\sigma}(k+q)\widetilde{V}_{\nu\rho\sigma}(q,k,-k-q)\,, \tag{6.16}$$

where $\Gamma^{(0)}_{\mu\alpha\beta}$ is the *conventional* three-gluon vertex of the linear covariant gauges,

$$\Gamma^{(0)}_{\mu\alpha\beta}(q,k,-k-q) = (q-k)_\beta\, g_{\mu\alpha} + (2k+q)_\mu\, g_{\alpha\beta} - (2q+k)_\alpha\, g_{\beta\mu}, \tag{6.17}$$

and $\Delta_{\alpha\beta}(k)$ is the totally transverse Landau gauge propagator, namely

$$\Delta_{\alpha\beta}(k) = P_{\alpha\beta}(k)\Delta(k^2), \tag{6.18}$$

[notice the minus sign difference with respect to our general definition Eq. (3.1)]. Finally, the trivial color factor δ^{ab} has been factored out.

As explained in detail in Section 4.1 of the previous chapter, gauge invariance requires that, when contracted by the momentum of the background leg, the vertex $\widetilde{V}_{\nu\rho\sigma}(q,k,-k-q)$ satisfies the WI of Eq. (5.7) with $r=k$ and $p=-(k+q)$, namely

$$q^\nu \widetilde{V}_{\nu\rho\sigma}(q,k,-k-q) = m^2(k)P_{\rho\sigma}(k) - m^2(k+q)P_{\rho\sigma}(k+q). \tag{6.19}$$

Now, it is relatively straightforward to recognize that $(a_i^{\tilde{V}})_{\mu\nu}$ is proportional to $q_\mu q_\nu/q^2$ only. Indeed, the condition of complete longitudinality of $\widetilde{V}$, given in Eq. (5.3), becomes

$$P^{\nu\nu'}(q)P^{\alpha\rho}(k)P^{\beta\sigma}(k+q)\widetilde{V}_{\nu'\rho\sigma}(q,k,-k-q) = 0, \tag{6.20}$$

from which follows immediately that

$$P^{\alpha\rho}(k)P^{\beta\sigma}(k+q)\widetilde{V}^{\nu}_{\rho\sigma}(q,k,-k-q) = \frac{q^\nu}{q^2}\big(q^{\nu'}\widetilde{V}_{\nu'\rho\sigma}\big)P^{\alpha\rho}(k)P^{\beta\sigma}(k+q). \tag{6.21}$$

Thus, interestingly enough, the rhs of Eq. (6.21) is completely determined from the WI of Eq. (5.7); specifically, using (6.19), we get

$$P^{\alpha\rho}(k)P^{\beta\sigma}(k+q)\widetilde{V}^{\nu}_{\rho\sigma}(q,k,-k-q) = \frac{q^\nu}{q^2}\left[m^2(k) - m^2(k+q)\right] P^{\alpha\rho}(k)P^{\beta}_{\rho}(k+q). \tag{6.22}$$

Then, using the elementary tree-level WI

$$q^\mu \Gamma^{(0)}_{\mu\alpha\beta}(q,k,-k-q) = (k+q)^2 P_{\alpha\beta}(k+q) - k^2 P_{\alpha\beta}(k), \tag{6.23}$$

one can show, after appropriate shifts of the integration variables [*i.e.*, $(k+q) \to k$], that indeed

$$(a_1^{\tilde{V}})_{\mu\nu} = \frac{q_\mu q_\nu}{q^2} \frac{g^2 C_A}{q^2} \int_k m^2(k^2) \left[(k+q)^2 - k^2\right] \Delta^{\alpha\rho}(k) \Delta_{\alpha\rho}(k+q), \quad (6.24)$$

yielding

$$a_1^{\tilde{V}}(q^2) = \frac{g^2 C_A}{q^2} \int_k m^2(k^2) \left[(k+q)^2 - k^2\right] \Delta^{\alpha\rho}(k) \Delta_{\alpha\rho}(k+q). \quad (6.25)$$

Thus, the "one-loop dressed" mass equation becomes

$$\begin{aligned} m^2(q^2) &= \frac{ig^2 C_A}{1+G(q^2)} a_1^{\tilde{V}}(q^2) \\ &= \frac{ig^2 C_A}{1+G(q^2)} \frac{1}{q^2} \int_k m^2(k^2) \left[(k+q)^2 - k^2\right] \Delta^{\alpha\rho}(k) \Delta_{\alpha\rho}(k+q). \end{aligned} \quad (6.26)$$

Notice that at the one-loop dressed level the ghost diagrams (a_3) and (a_4) of Fig. 3.2 should also be considered. However, their analysis can be simplified by appealing to some basic properties of the ghost propagator in the Landau gauge, established through detailed large-volume lattice simulations, as well as a variety of analytic studies [73–75]. Specifically, we will take for granted that the ghost propagator D in the Landau gauge remains massless, $D^{-1}(0) = 0$, while its dressing function F is infrared finite, $F(0) = c > 0$.

The main implications of these properties for the case at hand is that the corresponding fully dressed ghost vertex appearing in graph (a_3) does *not* need to be modified by the presence of V-type of vertices. Specifically, in the absence of a gluon mass the vertex $B\bar{c}c$ appearing in (a_3) satisfies

$$\begin{aligned} q^\mu \Gamma_\mu &= iD^{-1}(k+q) - iD^{-1}(k) \\ &= (k+q)^2 F^{-1}(k+q) - k^2 F^{-1}(k). \end{aligned} \quad (6.27)$$

If $D(q)$ remains massless, as we assume, the only effect of the gluon mass is to make the dressing function infrared finite, *i.e.*, implement in (6.27) the replacement $F(q) \to F_m(q)$. Thus, for instance, if $F(q) \sim \ln q^2$, the gluon mass induces the qualitative change of the type $F_m(q) \sim \ln(q^2 + m^2)$, accounting for the aforementioned infrared finiteness of the ghost dressing

function. The point to realize is that this proceeds without the need to modify $\widetilde{\Gamma}_\mu$ explicitly, by adding to it a V-type of vertex; $\widetilde{\Gamma}_\mu$ will change only through its implicit dependence of the gluon propagators (as well as all other vertices), contained inside the diagrams defining its own SDE, which have now become "massive". Given these considerations, the result given in Eq. (6.26) exhausts the "one-loop dressed" case.

After these comments about the one-loop dressed diagrams containing the ghost loops, let us return to Eq. (6.26). The transition to the Euclidean space proceeds by using the standard formulas that allow the conversion of the various Green's functions from the physical Minkowski momentum q^2 to the Euclidean $q_{\rm E}^2 = -q^2 > 0$; specifically

$$\Delta_{\rm E}(q_{\rm E}^2) = -\Delta(-q_{\rm E}^2); \quad m_{\rm E}^2(q_{\rm E}^2) = m^2(-q_{\rm E}^2); \quad G_{\rm E}(q_{\rm E}^2) = G(-q_{\rm E}^2); \quad \int_k = i\int_{k_{\rm E}}. \tag{6.28}$$

Then dropping the subscript "E", we arrive at the final result

$$m^2(q^2) = -\frac{g^2 C_A}{1+G(q^2)}\frac{1}{q^2}\int_k m^2(k^2)\Delta^{\alpha\rho}(k)\Delta_{\alpha\rho}(k+q)\left[(k+q)^2 - k^2\right]. \tag{6.29}$$

Consider finally the $q^2 \to 0$ limit of the above equation. Using the general Taylor expansion [with $y = k^2$ and $w = (k+q)^2$]

$$f(w) = f(y) + (w-y)f'(y) + \mathcal{O}(q^2), \tag{6.30}$$

together with Eqs. (3.21) and (5.41) as well as the fact that in $d = 4$ one has $L(0) = 0$ [60], we find

$$m^2(0) = \frac{3}{2}g^2 C_A F(0)\int_k k^2\Delta^2(k^2)[m^2(k^2)]'. \tag{6.31}$$

Note that the result obtained for this limiting case coincides with the one found in [22].

6.3 The "two-loop dressed" contributions

In this section we will study in detail the "two-loop dressed" diagrams (a_5) and (a_6), and their respective contribution to the mass equation (see Fig. 6.2 for the color and Lorentz indices as well as for the momentum routing). Note that, in the alternative QB version of the SDE equation for

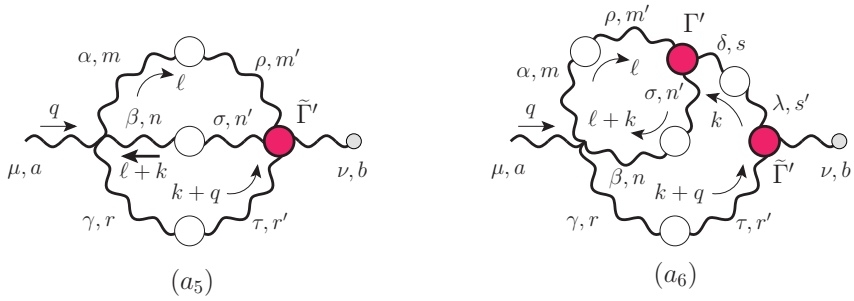

Fig. 6.2: The "two-loop dressed" diagrams. The symmetry factors are 1/6 and 1/2 respectively.

the gluon propagator that we consider here, there are no additional "two-loop dressed" diagrams. In particular, there are no diagrams involving the fully dressed $BQ\bar{c}c$ vertices (the fourths subset in the usual BB version of the SDE), simply because these vertices cannot be joined in any way with the conventional tree-level vertices appearing on the other side of the (would be) diagram, where the Q-type gluon enters.

6.3.1 General considerations regarding the graph (a_5)

Before switching the Schwinger mechanism on, the graph (a_5), for a general values of the gauge-fixing parameter ξ, is given by

$$(a_5)^{ab}_{\mu\nu} = -\frac{i}{6}\Gamma^{(0)amnr}_{\mu\alpha\beta\gamma}\int_k\int_\ell \Delta^{\alpha\rho}(\ell)\Delta^{\beta\sigma}(\ell+k)\Delta^{\gamma\tau}(k+q)\widetilde{\Gamma}^{brnm}_{\nu\tau\sigma\rho}(-q,k+q,-\ell-k,\ell), \tag{6.32}$$

where the tree-level value of the conventional (Q^4) four-gluon vertex is given by

$$\begin{aligned}\Gamma^{(0)amnr}_{\mu\alpha\beta\gamma} &= -ig^2[f^{arx}f^{xnm}(g_{\mu\beta}g_{\alpha\gamma}-g_{\mu\alpha}g_{\beta\gamma}) + f^{amx}f^{xrn}(g_{\mu\gamma}g_{\alpha\beta}-g_{\mu\beta}g_{\alpha\gamma})\\ &+ f^{anx}f^{xrm}(g_{\mu\gamma}g_{\alpha\beta}-g_{\mu\alpha}g_{\beta\gamma})].\end{aligned} \tag{6.33}$$

The fully dressed vertex BQ^3 satisfies WI given in Eq. (3.13), where it should be emphasized that on the rhs appear the conventional (and not the BFM) trilinear vertices, which satisfy STIs with respect to all their legs, like that of Eq. (3.10) and cyclic permutations.

Let us next switch the Schwinger mechanism on. Then, both sides of the WI of Eq. (3.13) must be replaced by "primed" vertices. Now,

the "primed" three-gluon vertices appearing on the rhs are of the type Q^3, namely $\Gamma'_{\alpha\mu\nu}(q,r,p) = \Gamma_{m\alpha\mu\nu}(q,r,p) + V_{\alpha\mu\nu}(q,r,p)$, where Γ_m satisfies (3.10) with $J \to J_m$ (and $H \to H_m$, which however we refrain from indicating), while V must satisfy, correspondingly,

$$q^\alpha V_{\alpha\mu\nu}(q,r,p) = F(q)[m^2(r^2)P^\alpha_\mu(r)H_{\alpha\nu}(r,q,p) - m^2(p^2)P^\alpha_\nu(p)H_{\alpha\mu}(p,q,r)], \tag{6.34}$$

and cyclic permutations. Note the difference between Eq. (6.34) and the corresponding relation satisfied by $\widetilde{V}$, given in Eq. (5.7): the latter is an Abelian WI with no reference to the ghost sector, while the former is an STI, depending explicitly contains the ghost-related quantities F and H.

Then, the only possibility for maintaining the original WI of Eq. (3.13) intact is if the quadrilinear vertex on its lhs gets also modified into a vertex satisfying the identity

$$\begin{aligned} q^\alpha \widetilde{\Gamma}'^{abcd}_{\alpha\mu\nu\rho}(q,r,p,t) &= q^\alpha \left[\widetilde{\Gamma}^{abcd}_{m\,\alpha\mu\nu\rho}(q,r,p,t) + \widetilde{V}^{abcd}_{\alpha\mu\nu\rho}(q,r,p,t)\right] \\ &= ig^2 \Big[f^{abx}f^{xcd}\Gamma'_{\nu\rho\mu}(p,t,q+r) + f^{acx}f^{xdb}\Gamma'_{\rho\mu\nu}(t,r,q+p) \\ &+ f^{adx}f^{xbc}\Gamma'_{\mu\nu\rho}(r,p,q+t)\Big], \end{aligned} \tag{6.35}$$

where $\widetilde{\Gamma}_m$ and $\widetilde{V}$ satisfy separately the no-pole (Γ_m) and pole (V) part of the trilinear Q^3 vertex, respectively. In particular, the $\widetilde{V}$ part, which we will be of central importance in what follows, satisfies

$$\begin{aligned} q^\alpha \widetilde{V}^{abcd}_{\alpha\mu\nu\rho}(q,r,p,t) &= ig^2 \Big[f^{abx}f^{xcd}V_{\nu\rho\mu}(p,t,q+r) + f^{acx}f^{xdb}V_{\rho\mu\nu}(t,r,q+p) \\ &+ f^{adx}f^{xbc}V_{\mu\nu\rho}(r,p,q+t)\Big]. \end{aligned} \tag{6.36}$$

6.3.2 The contribution $a_5^{\widetilde{V}}(q^2)$.

Let us now focus on the part of the diagram (a_5) that contains the pole component $\widetilde{V}$ of the fully-dressed BQ^3 vertex $\widetilde{\Gamma}'$, to be denoted by ($a_5^{\widetilde{V}}$). The projection to the Landau gauge is straightforward, since there are no ξ^{-1} terms anywhere in this diagram, and one obtains

$$(a_5^{\widetilde{V}})^{ab}_{\mu\nu} = \frac{i}{6}\Gamma^{(0)amnr}_{\mu\alpha\beta\gamma}\int_k\int_\ell \Delta^{\alpha\rho}(\ell)\Delta^{\beta\sigma}(\ell+k)\Delta^{\gamma\tau}(k+q)\widetilde{V}^{brnm}_{\nu\tau\sigma\rho}(-q,k+q,-\ell-k,\ell), \tag{6.37}$$

where all gluon propagators assume the transverse form of Eq. (6.18).

We can apply the totally longitudinally coupled condition satisfied by $\widetilde{V}_{\lambda\tau\sigma\rho}$,

$$P^{\lambda}_{\nu}(q)P^{\gamma\tau}(k+q)P^{\beta\sigma}(\ell+k)P^{\alpha\rho}(l)\widetilde{V}_{\lambda\tau\sigma\rho}(-q,k+q,-\ell-k,\ell)=0, \quad (6.38)$$

to write (6.37), after splitting $P^{\lambda}_{\nu}(q)$, as follows

$$\begin{aligned}(a_5^{\widetilde{V}})^{ab}_{\mu\nu} &= \frac{i}{6}\Gamma^{(0)amnr}_{\mu\alpha\beta\gamma}\frac{q_\nu}{q^2}\int_k\int_\ell \Delta^{\alpha\rho}(\ell)\Delta^{\beta\sigma}(\ell+k)\Delta^{\gamma\tau}(k+q)\\ &\times\ q^{\lambda}\widetilde{V}^{brnm}_{\lambda\tau\sigma\rho}(-q,k+q,-\ell-k,\ell). \end{aligned} \quad (6.39)$$

Using then the WI Eq. (3.13) adapted to the present kinematics, as well as the results

$$\begin{aligned} f^{brx}f^{xnm}\Gamma^{(0)amnr}_{\mu\alpha\beta\gamma} &= i\frac{3}{2}g^2C_A^2\delta^{ab}(g_{\mu\alpha}g_{\beta\gamma}-g_{\mu\beta}g_{\alpha\gamma});\\ f^{bnx}f^{xmr}\Gamma^{(0)amnr}_{\mu\alpha\beta\gamma} &= i\frac{3}{2}g^2C_A^2\delta^{ab}(g_{\mu\gamma}g_{\alpha\beta}-g_{\mu\alpha}g_{\beta\gamma});\\ f^{bmx}f^{xrn}\Gamma^{(0)amnr}_{\mu\alpha\beta\gamma} &= i\frac{3}{2}g^2C_A^2\delta^{ab}(g_{\mu\beta}g_{\alpha\gamma}-g_{\mu\gamma}g_{\alpha\beta}); \end{aligned} \quad (6.40)$$

one finds that each one of the terms of the WI gives rise to an integral of the form

$$t^{\mu}_j(q)=t_j(q^2)q^{\mu}; \quad j=1,2,3 \quad (6.41)$$

so that Eq. (6.39) can be written as

$$(a_5^{\widetilde{V}})^{ab}_{\mu\nu}=\frac{i}{4}g^4C_A^2\delta^{ab}\frac{q_\mu q_\nu}{q^2}\sum_{j=1}^{3}t_j(q^2), \quad (6.42)$$

with

$$\begin{aligned} t_1(q^2) &= \frac{1}{q^2}(q_\beta g_{\alpha\gamma}-q_\alpha g_{\beta\gamma})\\ &\times \int_k\int_\ell \Delta^{\alpha\rho}(\ell)\Delta^{\beta\sigma}(\ell+k)\Delta^{\gamma\tau}(k+q)V_{\sigma\rho\tau}(-\ell-k,\ell,k);\\ t_2(q^2) &= \frac{1}{q^2}(q_\alpha g_{\beta\gamma}-q_\gamma g_{\alpha\beta})\\ &\times \int_k\int_\ell \Delta^{\alpha\rho}(\ell)\Delta^{\beta\sigma}(\ell+k)\Delta^{\gamma\tau}(k+q)V_{\rho\tau\sigma}(\ell,k+q,-q-\ell-k);\\ t_3(q^2) &= \frac{1}{q^2}(q_\gamma g_{\alpha\beta}-q_\beta g_{\alpha\gamma})\\ &\times \int_k\int_\ell \Delta^{\alpha\rho}(\ell)\Delta^{\beta\sigma}(\ell+k)\Delta^{\gamma\tau}(k+q)V_{\tau\sigma\rho}(k+q,-\ell-k,-q+\ell). \end{aligned} \quad (6.43)$$

Now it turns out that, after the appropriate shifts in the momenta, relabeling the Lorentz dummy indices, and applying the Bose symmetry of $V_{\alpha\beta\gamma}$, the three terms are actually equal. Then, using the totally longitudinally coupled condition for the vertex V, and the fact that, in the Landau gauge, $k_\tau \Delta^{\gamma\tau}(k+q) = -q_\tau \Delta^{\gamma\tau}(k+q)$, we get

$$\begin{aligned} t(q^2) &= \sum_{j=1}^{3} t_j(q^2) \\ &= 3\frac{q_\tau}{q^2}(q_\alpha g_{\beta\gamma} - q_\beta g_{\alpha\gamma}) \int_k \Delta^{\gamma\tau}(k+q) \int_\ell \Delta^{\alpha\rho}(\ell)\Delta^{\beta\sigma}(\ell+k) \\ &\times \frac{k^\lambda}{k^2} V_{\sigma\rho\lambda}(-\ell-k,\ell,k). \end{aligned} \tag{6.44}$$

Then, the integral over ℓ is a function of k (but not of q), and has two free Lorentz indices, α and β, so that

$$\int_\ell \Delta^{\alpha\rho}(\ell)\Delta^{\beta\sigma}(\ell+k)\frac{k^\lambda}{k^2}V_{\sigma\rho\lambda}(-\ell-k,\ell,k) = A(k^2)g^{\alpha\beta} + B(k^2)k^\alpha k^\beta. \tag{6.45}$$

Therefore,

$$t(q^2) = 3\frac{q_\tau}{q^2}(q_\alpha g_{\beta\gamma} - q_\beta g_{\alpha\gamma}) \int_k \Delta^{\gamma\tau}(k+q)\,[A(k^2)g^{\alpha\beta} + B(k^2)k^\alpha k^\beta]. \tag{6.46}$$

But this term vanishes, regardless of the closed form of $A(k^2)$ and $B(k^2)$, because the prefactor is antisymmetric under the exchange $\alpha \leftrightarrow \beta$ whereas the integral is symmetric.

Thus, one finally arrives at the important result

$$a_5^{\widetilde{V}}(q^2) = 0, \tag{6.47}$$

namely that the graph (a_5) makes no contribution to the gluon mass equation.

6.3.3 The contributions from graph (a_6)

Let us now consider the graph (a_6), for a general value of the gauge-fixing parameter ξ. This graph contains the BQ^2 and Q^3 fully-dressed three-gluon vertices, namely $\widetilde{\Gamma}$ and Γ. We proceed directly to the massive situation,

where these two vertices have been replaced by their "primed" counterparts, namely

$$\begin{aligned}(a_6)^{ab}_{\mu\nu} &= \frac{3}{4} i g^4 C_A^2 \delta^{ab} \left(g_{\mu\alpha} g_{\beta\gamma} - g_{\mu\beta} g_{\alpha\gamma}\right) \int_k \Delta^{\gamma\tau}(k+q) \Delta^{\delta\lambda}(k) \\ &\times \widetilde{\Gamma}'_{\nu\tau\lambda}(-q, k+q, -k) \int_\ell \Delta^{\alpha\rho}(\ell) \Delta^{\beta\sigma}(\ell+k) \Gamma'_{\sigma\rho\delta}(-\ell-k, \ell, k).\end{aligned} \tag{6.48}$$

Evidently, $\widetilde{\Gamma}'$ and Γ' contain the pole parts $\widetilde{V}$ and V, respectively, satisfying the general properties mentioned earlier. We will next isolate the terms proportional to $\widetilde{V}$ and V, since it is these terms that determine the corresponding contribution of the entire graph (a_6) to the gluon mass equation. This amounts to writing the product $\widetilde{\Gamma}'\Gamma'$ as

$$\begin{aligned}\widetilde{\Gamma}'\Gamma' &= (\widetilde{\Gamma}_m + \widetilde{V})(\Gamma_m + V) \\ &= \widetilde{\Gamma}_m \Gamma_m + \widetilde{V}\Gamma_m + \widetilde{\Gamma}_m V + \widetilde{V} V,\end{aligned} \tag{6.49}$$

and considering only the last three terms.

Vanishing of the terms proportional to V

To proceed with the demonstration, note that if we were in the Landau gauge, *i.e.*, if the gluon propagators in Eq. (6.48) had the fully transverse form of Eq. (6.18), then V would vanish identically, due to its property of complete longitudinality, given that it is an internal vertex (Q^3-type). The limit $\xi = 0$ may be taken directly in the part of the graph involving the term $\widetilde{V}V$, and therefore this term vanishes immediately. As for the combination $\widetilde{\Gamma}_m V$, one can take directly the limit $\xi = 0$ everywhere, thus making it vanish, except for the term that contains the tree-level part of $\widetilde{\Gamma}_m$ that is proportional to ξ^{-1}. Specifically, the tree-level part of the BQ^2 vertex is given by

$$\widetilde{\Gamma}^{(0)}_{\nu\tau\lambda}(-q, k+q, -k) = \Gamma^{(0)}_{\nu\tau\lambda}(-q, k+q, -k) - \xi^{-1} \Gamma^{\rm P}_{\nu\tau\lambda}(-q, k+q, -k), \tag{6.50}$$

where the purely longitudinal "pinch part" $\Gamma^{\rm P}$ is given by

$$\Gamma^{\rm P}_{\nu\tau\lambda}(-q, k+q, -k) = -g_{\nu\lambda}(k+q)_\tau - g_{\tau\nu} k_\lambda. \tag{6.51}$$

The contraction of this term with the propagators $\Delta^{\gamma\tau}(k+q)\Delta^{\delta\lambda}(k)$ (with ξ still general) yields

$$\xi^{-1}\Gamma^{\rm P}_{\nu\tau\lambda}(-q,k+q,-k)\Delta^{\gamma\tau}(k+q)\Delta^{\delta\lambda}(k) = \frac{k^\delta}{k^2}\Delta^\gamma_\nu(k+q) + \frac{(k+q)^\gamma}{(k+q)^2}\Delta^\delta_\nu(k). \tag{6.52}$$

In this way, the ξ^{-1} term cancels, making the limit $\xi \to 0$ smooth. So, after setting $\xi = 0$, the second term in Eq. (6.52) vanishes, because V will be contracted by three transverse projectors; on the other hand, the first term survives, since V is contracted only by two. However, as we will see now, this last term finally also vanishes, due to a different reason. Specifically, denoting this contribution by $(a_6^V)_{\mu\nu}$ (thus factoring out the trivial color structure δ^{ab}), we have

$$\begin{aligned}(a_6^V)_{\mu\nu} &= \frac{3}{4}ig^4C_A^2\,(g_{\mu\alpha}g_{\beta\gamma} - g_{\mu\beta}g_{\alpha\gamma})\int_k \Delta^\gamma_\nu(k+q) \\ &\times \int_\ell \Delta^{\alpha\rho}(\ell)\Delta^{\beta\sigma}(\ell+k)\frac{k^\delta}{k^2}V_{\sigma\rho\delta}(-\ell-k,\ell,k).\end{aligned} \tag{6.53}$$

Now, the integral $\int_\ell$ contains k but no q, and has two free Lorentz indices, α and β; therefore, it can only be proportional to $A(k^2)g_{\alpha\beta}$ and $B(k^2)k_\alpha k_\beta$. But, since both these terms are symmetric under $\alpha \leftrightarrow \beta$, while the prefactor is antisymmetric, this term vanishes.

The term $a_6^{\widetilde{V}}(q^2)$

Let us finally consider the term $\widetilde{V}\Gamma_m$ in Eq. (6.49), to be denoted by $(a_6^{\widetilde{V}})_{\mu\nu}$. It is convenient to define the quantity

$$Y^{\alpha\beta}_\delta(k) = \int_\ell \Delta^{\alpha\rho}(\ell)\Delta^{\beta\sigma}(\ell+k)\Gamma_{\sigma\rho\delta}(-\ell-k,\ell,k), \tag{6.54}$$

corresponding to the subdiagram on the upper left corner of (a_6). Then, $(a_6^{\widetilde{V}})_{\mu\nu}$ is given by

$$\begin{aligned}(a_6^{\widetilde{V}})_{\mu\nu} &= \frac{3}{4}ig^4C_A^2\,(g_{\mu\alpha}g_{\beta\gamma} - g_{\mu\beta}g_{\alpha\gamma}) \\ &\times \int_k Y^{\alpha\beta}_\delta(k)\Delta^{\gamma\tau}(k+q)\Delta^{\delta\lambda}(k)\widetilde{V}_{\nu\tau\lambda}(-q,k+q,-k)\end{aligned} \tag{6.55}$$

Then, using once again Eqs. (5.3), (5.7) and (6.21), we obtain

$$\begin{aligned}(a_6^{\widetilde{V}})_{\mu\nu} &= \frac{3}{4} i g^4 C_A^2 \left(g_{\mu\alpha} g_{\beta\gamma} - g_{\mu\beta} g_{\alpha\gamma}\right) \\ &\times \frac{q^\nu}{q^2} \int_k \left[m^2(k) - m^2(k+q)\right] \Delta^\delta_\lambda(k) \Delta^{\gamma\lambda}(k+q) Y_\delta^{\alpha\beta}(k) \\ &= \frac{q_\mu q_\nu}{q^2} a_6^{\widetilde{V}}(q^2)\,, \end{aligned} \tag{6.56}$$

and so

$$\begin{aligned} a_6^{\widetilde{V}}(q^2) &= \frac{3}{4} i g^4 C_A^2 \left(q_\alpha g_{\beta\gamma} - q_\beta g_{\alpha\gamma}\right) \\ &\times \frac{1}{q^2} \int_k \left[m^2(k) - m^2(k+q)\right] \Delta^\delta_\lambda(k) \Delta^{\gamma\lambda}(k+q) Y_\delta^{\alpha\beta}(k). \end{aligned} \tag{6.57}$$

At this point it is easy to show that the integral Y is antisymmetric under the $\alpha \leftrightarrow \beta$ exchange; thus, given also the antisymmetry of the $a_6^{\widetilde{V}}$ prefactor under the same exchange, one can write

$$Y_\delta^{\alpha\beta}(k) = (k^\alpha g_\delta^\beta - k^\beta g_\delta^\alpha) Y(k^2); \qquad Y(k^2) = \frac{1}{d-1} \frac{1}{k^2}\, k_\alpha g_\beta^\delta Y_\delta^{\alpha\beta}(k)\,, \tag{6.58}$$

which gives us the final result

$$\begin{aligned} a_6^{\widetilde{V}}(q^2) &= \frac{3}{4} i \frac{g^4 C_A^2}{q^2} \int_k m^2(k^2) [(k+q)^2 - k^2] [Y(k+q) + Y(k)] \Delta^\delta_\lambda(k) \Delta^\lambda_\delta(k+q) \\ &+ \frac{3}{4} i \frac{g^4 C_A^2}{q^2} (q^2 g_{\delta\gamma} - 2 q_\delta q_\gamma) \int_k m^2(k^2) [Y(k+q) - Y(k)] \Delta^\delta_\lambda(k) \Delta^{\gamma\lambda}(k+q). \end{aligned} \tag{6.59}$$

6.3.4 Explicit check of the two-loop dressed "blockwise" transversality

The vanishing of the term $a_5^{\widetilde{V}}$ may appear somewhat surprising, since, in the PT-BFM framework that we employ, it is exactly the V and $\widetilde{V}$ type of vertices that allow for the appearance of a dynamically generated gluon mass in a gauge-invariant way. Thus, one might wonder whether the result (6.47) is in any way at odds with the characteristic property of the "blockwise" transversality, mentioned earlier.

To show that this is not the case, let us contract diagram (a_5) with the physical momentum q; after carrying out the usual splitting of the BQ^3

full vertex $\widetilde{\Gamma} \to \widetilde{\Gamma}_m + \widetilde{V}$, using the result (6.47) and applying the WI Eq. (3.13) to the remaining term, we get

$$\begin{aligned} q^\nu (a_5^{\widetilde{\Gamma}'})^{ab}_{\mu\nu} &= q^\nu (a_5^{\widetilde{\Gamma}_m})^{ab}_{\mu\nu} \\ &= \frac{3}{4} i g^4 C_A^2 \delta^{ab} (g_{\mu\beta} g_{\alpha\gamma} - g_{\mu\alpha} g_{\beta\gamma}) \\ &\times \int_k \int_\ell \Delta^\alpha_\rho(\ell) \Delta^\beta_\sigma(\ell + k) \Delta^\gamma_\tau(k+q) \Gamma_m^{\sigma\rho\tau}(-\ell - k, \ell, k). \end{aligned} \tag{6.60}$$

As far as the contribution of diagram (a_6) is concerned, we know that it cannot be projected directly to the Landau gauge, because the tree-level part of the fully-dressed BQ^2 vertex contains terms proportional to $1/\xi$. However, proceeding as in subsection 6.3.3, one writes

$$\widetilde{\Gamma}'_{\nu\tau\epsilon}(-q, k+q, -k) = \widetilde{\Gamma}'^{\,\mathrm{reg}}_{\nu\tau\epsilon}(-q, k+q, -k) - \xi^{-1} \Gamma^{\mathrm{P}}_{\nu\tau\epsilon}(-q, k+q, -k), \tag{6.61}$$

where evidently the regular part $\widetilde{\Gamma}'^{\,\mathrm{reg}}$ differs from the usual $\widetilde{\Gamma}'$ by a tree-level term. For the regular term, after using the identity

$$q^\nu \widetilde{\Gamma}'^{\,\mathrm{reg}}_{\nu\tau\epsilon}(-q, k+q, -k) = \Delta^{-1}(k) P_{\tau\epsilon}(k) - \Delta^{-1}(k+q) P_{\tau\epsilon}(k+q), \tag{6.62}$$

one gets

$$\begin{aligned} q^\nu (a_6^{\widetilde{\Gamma}'^{\,\mathrm{reg}}})^{ab}_{\mu\nu} &= \frac{3}{4} i g^4 C_A^2 \delta^{ab} (g_{\mu\alpha} g_{\beta\gamma} - g_{\mu\beta} g_{\alpha\gamma}) \int_k \int_\ell [\Delta(k+q) - \Delta(k)] \\ &\times P_{\tau\delta}(k) P^{\gamma\tau}(k+q) \Delta^\alpha_\rho(\ell) \Delta^\beta_\sigma(\ell+k) \Gamma_m^{\sigma\rho\delta}(-\ell - k, \ell, k). \end{aligned} \tag{6.63}$$

For the pinch part, after using Eq. (6.52) to cancel the ξ^{-1} dependence, one obtains (now in the Landau gauge)

$$\begin{aligned} (a_6^{\Gamma^{\mathrm{P}}})^{ab}_{\mu\nu} &= \frac{3}{4} i g^4 C_A^2 \delta^{ab} (g_{\mu\beta} g_{\alpha\gamma} - g_{\mu\alpha} g_{\beta\gamma}) \int_k \left[\frac{k^\delta}{k^2} \Delta^\gamma_\nu(k+q) + \frac{(k+q)^\gamma}{(k+q)^2} \Delta^\delta_\nu(k) \right] \\ &\times \int_\ell \Delta^{\alpha\rho}(\ell) \Delta^{\beta\sigma}(\ell + k) \Gamma'_{\sigma\rho\delta}(-\ell - k, \ell, k). \end{aligned} \tag{6.64}$$

On the other hand, observing that

$$\begin{aligned} q^\nu \left[\frac{k^\delta}{k^2} \Delta^\gamma_\nu(k+q) + \frac{(k+q)^\gamma}{(k+q)^2} \Delta^\delta_\nu(k) \right] &= \Delta^{\gamma\delta}(k) - \Delta^{\gamma\delta}(k+q) \\ &+ [\Delta(k+q) - \Delta(k)] P^{\delta\nu}(k) P^\gamma_\nu(k+q), \end{aligned} \tag{6.65}$$

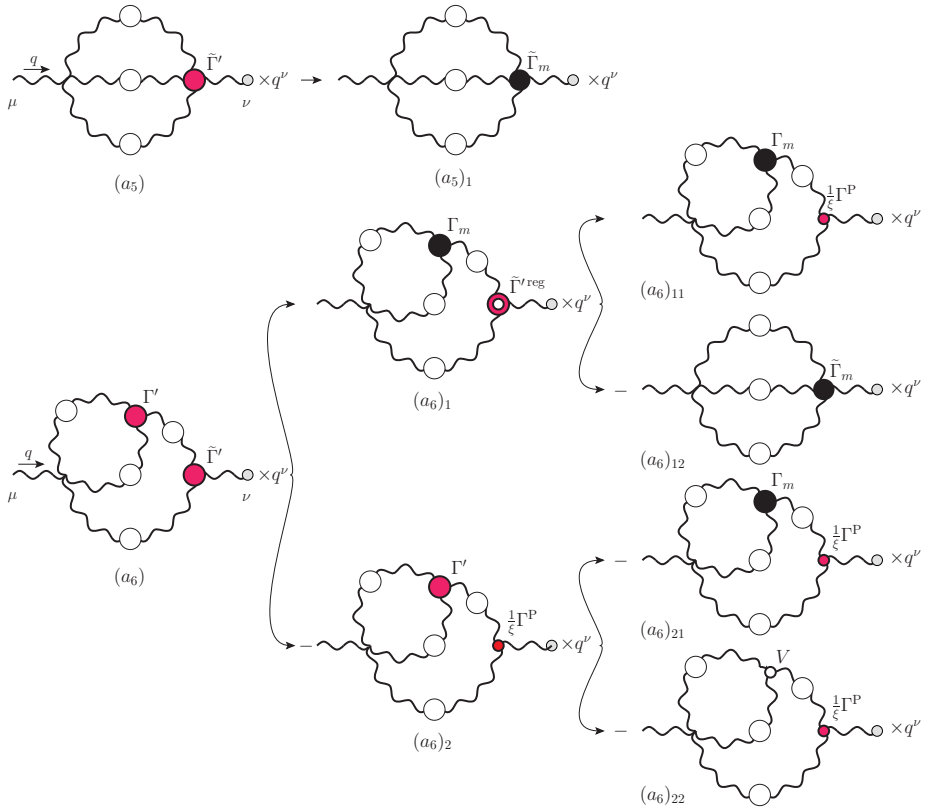

Fig. 6.3: Diagrammatic realization of the WI for the two-loop dressed diagrams in the Landau gauge. One has the cancellations $(a_5)_1 + (a_6)_{12} = 0$ and $(a_6)_{11} + (a_6)_{21} = 0$, while the term $(a_6)_{22}$ vanishes.

Eq. (6.64) becomes

$$\begin{aligned} q^\nu (a_6^{\Gamma^P})^{ab}_{\mu\nu} &= \frac{3}{4} i g^4 C_A^2 \delta^{ab} (g_{\mu\beta} g_{\alpha\gamma} - g_{\mu\alpha} g_{\beta\gamma}) \\ &\times \left\{ \int_k \int_\ell \Delta^\gamma_\delta(k) \Delta^\alpha_\rho(\ell) \Delta^\beta_\sigma(\ell+k) \Gamma^{\sigma\rho\delta}_m(-\ell-k,\ell,k) \right. \\ &- \int_k \int_\ell \Delta^{\gamma\delta}(k+q) \Delta^{\alpha\rho}(\ell) \Delta^{\beta\sigma}(\ell+k) \Gamma'_{\sigma\rho\delta}(-\ell-k,\ell,k) \\ &+ \int_k \int_l [\Delta(k+q) - \Delta(k)] P^\nu_\delta(k) P^\gamma_\nu(k+q) \Delta^\alpha_\rho(l) \Delta^\beta_\sigma(l+k) \\ &\times \left. \Gamma^{\sigma\rho\delta}_m(-l-k,l,k) \right\}. \end{aligned} \tag{6.66}$$

Clearly the first term integrates to zero, since, being independent of q, it cannot saturate its free index μ, while the third term cancels exactly against (6.63). As far as the second term is concerned, notice that it still contains a pole part, since the total longitudinality condition of Eq. (5.3) cannot be triggered in this case. However, after splitting the full vertex Γ' one finds that the Γ_m part cancels with the term (6.60), while it is easy to show that the pole part V vanishes along the same lines described when dealing with graph $a_5^{\widetilde{V}}$.

The realization of the two-loop dressed "blockwise" transversality in the Landau gauge is shown diagrammatically in Fig. 6.3.

6.4 The full mass equation

After these rather technical considerations, we are now in position to write down the all-order mass equation. Using Eq. (6.5), together with the results (6.25) and (6.59), one finds

$$\begin{aligned} m^2(q^2) &= \frac{i}{1+G(q^2)} \left[a_1^{\widetilde{V}}(q^2) + a_6^{\widetilde{V}}(q^2) \right] \\ &= \frac{i g^2 C_A}{1+G(q^2)} \frac{1}{q^2} \int_k m^2(k^2) [(k+q)^2 - k^2] \Delta^{\alpha\rho}(k) \Delta_{\alpha\rho}(k+q) \\ &\times \left\{ 1 + \frac{3}{4} i g^2 C_A [Y(k+q) + Y(k)] \right\} - \frac{3}{4} \frac{g^4 C_A^2}{1+G(q^2)} \frac{1}{q^2} (q^2 g_{\delta\gamma} - 2 q_\delta q_\gamma) \\ &\times \int_k m^2(k^2) [Y(k+q) - Y(k)] \Delta^\delta_\epsilon(k) \Delta^{\gamma\epsilon}(k+q). \end{aligned} \tag{6.67}$$

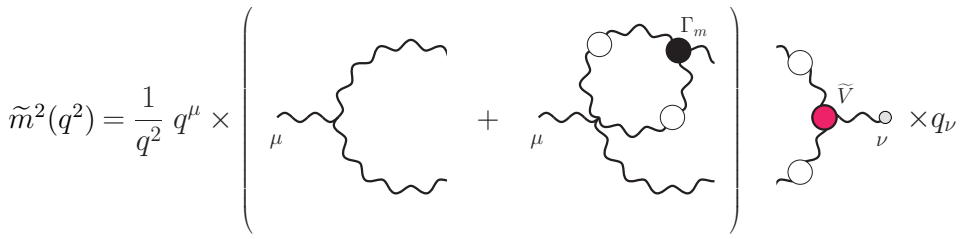

Fig. 6.4: Diagrammatic representation of the condensed operations leading to the all order gluon mass equation, where we have introduced the shorthand notation $\widetilde{m}^2(q^2) = m^2(q^2)[1+G(q^2)]$. All internal propagators are in the Landau gauge.

The transition to the Euclidean momenta can be performed by using the standard formulas (6.28) supplemented with the relation $Y_E(q_E^2) = -iY(-q_E^2)$; then one obtains (suppressing the "E" subscript as usual)

$$\begin{aligned} m^2(q^2) &= -\frac{g^2 C_A}{1+G(q^2)}\frac{1}{q^2}\int_k m^2(k^2)[(k+q)^2-k^2]\Delta^{\alpha\rho}(k)\Delta_{\alpha\rho}(k+q) \\ &\times \left\{1 - \frac{3}{4}g^2 C_A[Y(k+q)+Y(k)]\right\} + \frac{3}{4}\frac{g^4 C_A^2}{1+G(q^2)}\frac{1}{q^2}(q^2 g_{\delta\gamma} - 2q_\delta q_\gamma) \\ &\times \int_k m^2(k^2)[Y(k+q)-Y(k)]\Delta^\delta_\epsilon(k)\Delta^{\gamma\epsilon}(k+q). \end{aligned} \tag{6.68}$$

Interestingly enough, the full diagrammatic analysis presented in sections 6.2 and 6.3, in conjunction with the methodology developed in section 6.1, may be pictorially summarized, in a rather concise way, as shown in Fig 6.4.

Note that the quantities entering in Eq. (6.68) are bare, and must eventually undergo renormalization. The renormalized version of Eq. (6.68) will involve some of the cutoff-dependent renormalization constants Z_i introduced during the renormalization procedure, in a way analogous to what happens in the case of the integral equation for the dynamical quark mass (see, *e.g.*, [40,76]); however, for the purposes of the present work, we will ignore these constants (replacing them, effectively, by unity, *i.e.*, $Z_i \to 1$), and will simply consider Eq. (6.68), assuming that the quantities appearing there are now the renormalized ones.

As has been explained in section 6.1, the mass equation derived in Eq. (6.68) constitutes one of the two coupled integral equations that govern simultaneously the dynamics of $m^2(q^2)$ and $J(q^2)$ [see, for example,

Eq. (6.3)]. If the corresponding all order integral equation for $J(q^2)$ were known, then one could attempt to solve the coupled system, after carrying out the additional substitution $\Delta(k^2) = [k^2 J(k^2) + m^2(k^2)]^{-1}$ [*viz.* Eq. (5.5)] to all gluon propagators appearing inside the various kernels. It turns out that the derivation of the all order integral equation for $J(q^2)$ is technically far more difficult, mainly due to the presence of the fully-dressed four gluon vertex BQ^3 [see graph (a_5) in Fig. 3.2], which is a largely unexplored quantity, with a complicated Lorentz and color structure, and a vast proliferation of form factors. In fact, unlike what happens in the case of the three-gluon vertex BQ^2 [65], no gauge-technique Ansatz exist for this four gluon vertex. Thus, for the rest of this analysis [see next section] we will study Eq. (6.68) in isolation, treating all full propagators appearing in it as external quantities, whose form will be determined by resorting to information beyond the SDEs, such as the large-volume lattice simulations. Therefore, Eq. (6.68) is effectively converted into a homogeneous *linear* integral equation for the unknown function $m^2(q^2)$.

Evidently, the quantity $Y_\delta^{\alpha\beta}(k)$ introduced in Eq. (6.54) accounts for the bulk of the two-loop contribution, and depends explicitly on the fully dressed three gluon vertex Γ (of the type Q^3), in the Landau gauge. This Bose-symmetric vertex satisfies the well-known STI Eq. (3.10) and its cyclic permutations, which allow, in turn, for the reconstruction of the longitudinal form factors of Γ in terms of J, F, and the various form factors of the ghost-gluon kernel H [48]. Clearly, the inclusion of the (ten) longitudinal vertex form factors into $Y_\delta^{\alpha\beta}(k)$, and through it into Eq. (6.68), will give rise to rather complicated expressions, whose numerical treatment lies beyond the scope of this work.

In what follows we will simplify this preliminary analysis by considering simply the lowest order perturbative expression for Y, obtained by substituting tree-level values for all quantities appearing in Eq. (6.54), and using (6.58). It turns out that even so, the resulting expression for Y has sufficient structure to effectively reverse the overall sign of the equation, and give rise to physically meaningful solutions for $m^2(q^2)$. In particular,

one has

$$\begin{aligned} Y(k^2) &= \frac{1}{d-1}\frac{k_\alpha}{k^2}\int_\ell \frac{1}{\ell^2(\ell+k)^2} P^{\alpha\rho}(\ell)P^{\beta\sigma}(\ell+k)\Gamma^{(0)}_{\sigma\rho\beta}(-\ell-k,\ell,k) \\ &= \frac{1}{d-1}\frac{k_\alpha}{k^2}(2g_{\beta\sigma}k_\rho + g_{\sigma\rho}k_\beta - 2g_{\beta\rho}k_\sigma) \\ &\times \int_l \frac{1}{l^2(l+k)^2}\left[g^{\alpha\rho}g^{\beta\sigma} - \frac{1}{l^2}(l^\alpha l^\rho g^{\beta\sigma} + l^\beta l^\sigma g^{\alpha\rho})\right. \\ &+ \left.\frac{1}{l^2(l+k)^2} l^\alpha l^\rho (l+k)^\beta (l+k)^\sigma\right], \end{aligned} \tag{6.69}$$

and a straightforward calculation yields (in dimensional regularization, Euclidean space)

$$Y(k^2) = \frac{1}{3(4\pi)^2}\left[\frac{15}{4}\left(\frac{2}{\epsilon}\right) - \frac{15}{4}\left(\gamma_{\rm E} - \log 4\pi + \log\frac{k^2}{\mu^2}\right) + \frac{63}{12}\right], \tag{6.70}$$

where μ is the 't Hooft mass introduced at Eq. (3.19). $Y(k^2)$ may be renormalized within the MOM scheme, by simply subtracting its value at $k^2 = \bar{\mu}^2$, yielding

$$Y_{\rm R}(k^2) = -\frac{1}{(4\pi)^2}\frac{5}{4}\log\frac{k^2}{\bar{\mu}^2}. \tag{6.71}$$

6.5 Numerical analysis

In this section we carry out a rather thorough numerical analysis of the mass equation derived in the previous sections.

To begin with, let us rewrite the equation (for the $d = 4$ case) in a form that will be suited for the ensuing numerical treatment. After setting $x = q^2$, observing that $(k+q)^2 = x+y+2\sqrt{xy}\cos\theta$, and using the measure

$$\int_k = \frac{1}{(2\pi)^3}\int_0^\pi {\rm d}\theta\ \sin^2\theta \int_0^\infty {\rm d}y\ y, \tag{6.72}$$

we obtain

$$\begin{aligned} m^2(x) &= -\lambda\frac{F(x)}{x}\int_0^\pi {\rm d}\theta\ \sin^2\theta\int_0^\infty {\rm d}y\ y\, m^2(y)\Delta(y)\Delta(x+y+2\sqrt{xy}\cos\theta) \\ &\times \{A(x,y,\theta)B(x,y,\theta)\left[1 - C\left(Y(x+y+2\sqrt{xy}\cos\theta) + Y(y)\right)\right] \\ &- CE(x,y,\theta)\left(Y(x+y+2\sqrt{xy}\cos\theta) - Y(y)\right)\}, \end{aligned} \tag{6.73}$$

where we have used the approximation [60] $1 + G(x) \approx F^{-1}(x)$, and set

$$\begin{aligned} A(x,y,\theta) &= 3 - \frac{x\sin^2\theta}{x+y+2\sqrt{xy}\cos\theta}; \\ B(x,y,\theta) &= x + 2\sqrt{xy}\cos\theta; \\ E(x,y,\theta) &= \frac{xy + x\cos^2\theta(x+2\sqrt{xy}\cos\theta) + 2(x+\sqrt{xy}\cos\theta)^2}{x+y+2\sqrt{xy}\cos\theta}. \end{aligned} \tag{6.74}$$

and we have defined ($\alpha_s = g^2/4\pi$)

$$\lambda = \frac{\alpha_s C_A}{2\pi^2}, \tag{6.75}$$

In addition, we have introduced the constant C, multiplying the contribution to the mass equation that is of pure two-loop origin. Of course, the value of C corresponding to the approximate expression Eq. (6.71) that we employ is fixed, namely

$$C = 3\pi C_A \alpha_s; \tag{6.76}$$

however, during a significant part of the ensuing analysis we will treat C as a free parameter. Thus, essentially one disentangles C from the value of α_s, and studies what happens to the gluon mass equation when one varies independently α_s and C. The reason for doing this is twofold: (*i*) one has the ability to switch off completely the two-loop corrections (by setting $C = 0$), and (*ii*) by varying the value of C one may study, in some additional detail, the quantitative impact of the two-loop contribution. Specifically, the philosophy underlying point (*ii*) is that, whereas the expression in Eq. (6.71) furnishes a concrete form for the two-loop correction, by no means does it exhaust it; thus, by varying C we basically model, in a rather heuristic way, further correction that may be added to the "skeleton" provided by the $Y(k^2)$ of Eq. (6.71) (for a fixed value of α_s). Of course, the case where C admits the actual value of Eq. (6.76) will emerge as a special case of this general two-parameter study. In view of the ensuing analysis it is convenient to measure C in units of $3\pi C_A$; to this end, we introduce the reduced parameter $C_r = C/3\pi C_A$, and drop the suffix "r" in what follows.

The integral equation to solve is a homogenous Fredholm equation of the second kind, and can be rewritten schematically as

$$m^2(x) = -\lambda \int_0^\pi \mathrm{d}\theta \int_0^b \mathrm{d}y \; \mathcal{K}(x,y,\theta)\, m^2(y), \tag{6.77}$$

where $b = \infty$, but in practice we will choose $b \gg 1$ but finite. A possible way of solving this equation is to expand the unknown function in terms of a suitable function basis, and subsequently determine the coefficients of this expansion. In particular [77, 78], using the Chebishev polynomials of the first kind T_k, one can write

$$m^2(x) = \frac{c_0}{2} + \sum_{k=1}^{n} c_k T_k(x). \tag{6.78}$$

In order to determine the $n+1$ coefficients characterizing the expansion, one discretizes $x \in [0, b]$ choosing the x_j values that corresponds to the extrema of the n^{th} Chebishev polynomial in that interval, *i.e.*,

$$x_j = \frac{b}{2} \cos\left(\frac{\pi}{n}(n-j)\right) + \frac{b}{2}, \qquad j = 0, \ldots, n. \tag{6.79}$$

The problem is then reduced to finding the values of λ for which the matrix $A + \lambda B$ is singular, where

$$A_{ij} = \delta T_i\left(\frac{2x_j - b}{b}\right); \qquad B_{ij} = \delta \int_0^{\pi} \mathrm{d}\theta \int_0^{b} \mathrm{d}y \; \mathcal{K}(x_j, y, \theta)\, T_i\left(\frac{2x_j - b}{b}\right), \tag{6.80}$$

and $\delta = 1$, unless $i = 0$, in which case it is $1/2$. Specifically one is looking for the smallest positive root λ_s of the generalized characteristic polynomial of the matrices A and $-B$. Provided that λ_s exists, one can next determine all the expansion coefficients c_k by simply assigning to c_0 a predetermined value (we choose $c_0 = 1$) and then solving the resulting reduced system; the corresponding value of the coupling constant can then be obtained through Eq. (6.75). The solution can be finally rescaled by an arbitrary (positive) constant, due to the freedom allowed by the linearity of the equation.

6.5.1 The one-loop dressed case

Let us start our analysis from the one-loop dressed case, which corresponds to setting $C = 0$ in Eq. (6.73). Specifically, notice that, as $x \to 0$, this equation reduces to the following nonlinear constraint

$$m^2(0) = -\frac{3\pi}{4} \lambda\, F(0) \int_0^{\infty} \mathrm{d}y \; m^2(y) \mathcal{K}_1(y); \qquad \mathcal{K}_1(y) = \left[\mathcal{Z}^2(y)\right]', \tag{6.81}$$

where $\mathcal{Z}(y) = y\Delta(y)$ is the gluon dressing function. Note that the constraint of Eq. (6.81) is identical to that derived in [22]; remember, however, that the full one-loop equation for arbitrary momenta is different, for the reasons explained in section 6.2.

As explained in [22], the usefulness of Eq. (6.81) lies in the fact that, already at this level, one may recognize the difficulty in obtaining physical solutions (*i.e.*, positive definite in the entire momentum range), which can be ultimately traced down to the "wrong" sign in front of the equation. In addition, one may explore the conditions that might finally overcome this difficulty, without having to solve the integral equation in its full complexity. In particular, it is clear from Eq. (6.81) that, in order to have a possibility of obtaining physically meaningful solutions, the kernel $\mathcal{K}_1$ must display a "sufficiently deep" negative region, which might eventually counterbalance the overall minus sign; indeed, we have verified that it would be immediate to obtain positive-definite (and monotonically decreasing) solutions if we could reverse the overall sign of the equation (or, equivalently, the sign of the kernel). Thus, the existence of a negative region in the kernel is a necessary condition for obtaining physical solutions; a positive-definite kernel, would exclude immediately such a possibility. Of course, as we will see shortly, this condition is far from sufficient.

Specifically, using the lattice data for $\Delta(q^2)$ corresponding to a $SU(3)$ quenched lattice simulation [32], one can explicitly verify whether or not (and exactly how) the necessary condition described above is satisfied. These lattice data are plotted in Fig. 6.5 (left panel); on the same figure we also plot a fit, whose explicit functional form may be found in various recent articles [22,39,40]). On the right panel of Fig. 6.5 we then show the corresponding one-loop dressed kernel $\mathcal{K}_1$, calculated directly from the lattice data[1] and then also using the aforementioned fit. One clearly observes the zero crossing of the kernel (at $q^2 \sim 0.8$ GeV^2) and the corresponding negative region.

The propagator fit shown in Fig. 6.5 can be then used to construct the full kernel appearing in Eq. (6.73), when $C = 0$; the corresponding full integral equation can be then studied by means of the algorithm explained above (for the ghost dressing function F we use a continuous interpolator

[1] The kernel in this case is obtained by first calculating from the raw lattice data $(y_i, \Delta(y_i))$ the dressing function squared data $(y_i, \mathcal{Z}^2(y_i))$; next the derivative data are calculated as a simple first order central difference, *i.e.*, the data plotted are $(\frac{y_{i+1}+y_i}{2}, \frac{\mathcal{Z}^2(y_{i+1})-\mathcal{Z}^2(y_i)}{y_{i+1}-y_i})$. Finally, errors are calculated through error propagation.

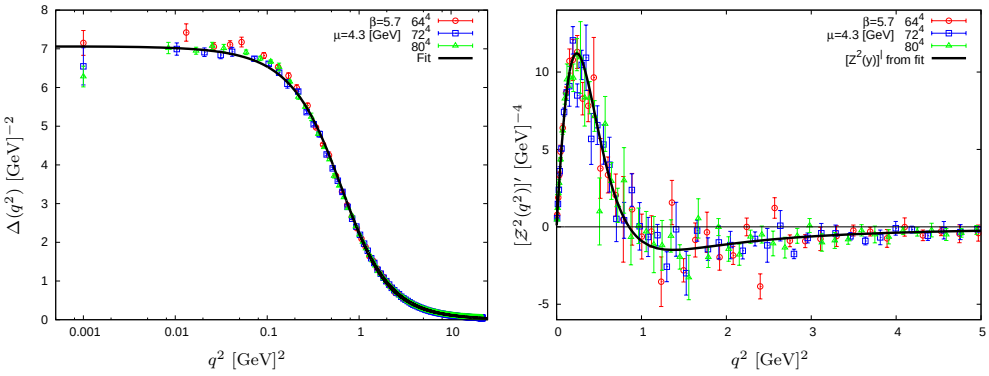

Fig. 6.5: (*Left panel.*) Lattice data for the (quenched) $SU(3)$ gluon propagator renormalized at $\mu = 4.3$ GeV, shown together with the log fit of [22, 39, 40]. (*Right panel.*) The one-loop dressed kernel derived from the lattice data, compared to the one obtained from the propagator fit.

of the corresponding $SU(3)$ lattice data). It turns out, however, that the solutions obtained have oscillatory behavior, and display large negative regions, ultimately voiding them of any physical meaning.

Evidently, the negative region furnished by the kernel is not sufficiently deep, or it is not located in the optimum momentum region, to counteract the effect of the overall minus sign. Clearly, if physical solutions are to be found, the full functional form of the kernel must be modified. As we will see in the next subsection, this type of appropriate modification is indeed implemented dynamically, when the two-loop corrections are included.

Finally, in order to avoid any confusion related to the conclusions of this subsection and the findings of [22], let us remind the reader that the equation solved in [22] does not coincide with the one solved here; therefore, the (non-monotonic) solutions found in [22], do not correspond to solutions of the present integral equation.

6.5.2 *The two-loop dressed case: finding physical solutions*

Let us now turn the two-loop dressed contributions back on, by setting $C > 0$. Considering again the $x \to 0$ limit first, one has in this case

$$m^2(0) = -\frac{3\pi}{4}\lambda\, F(0) \int_0^\infty \mathrm{d}y\, m^2(y)\mathcal{K}_2(y); \qquad \mathcal{K}_2(y) = \left\{[1 - 2CY(y)]\, \mathcal{Z}^2(y)\right\}'. \tag{6.82}$$

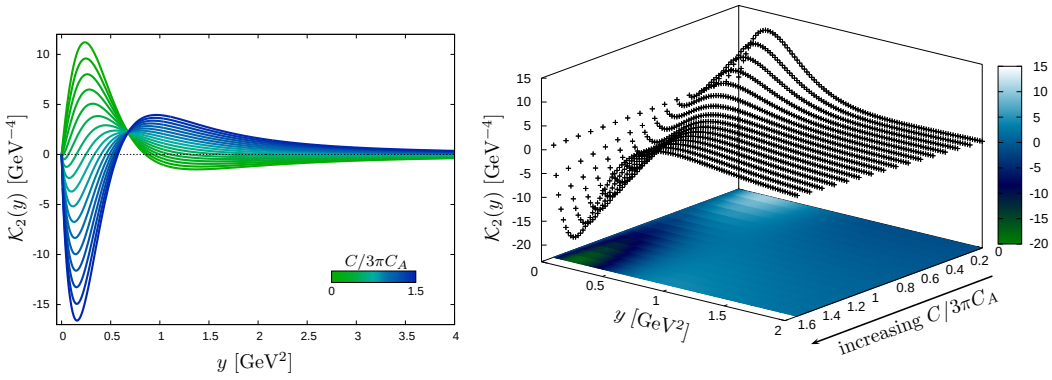

Fig. 6.6: Modification of the shape of the two-loop dressed kernel $\mathcal{K}_2(y)$ with varying C. As the latter parameter increases the kernel effectively reverses its sign showing a deep negative well in the low momenta region.

Since, as already mentioned, C will be treated as an independent parameter, one can study how the shape of the kernel $\mathcal{K}_2$ changes as C is varied. As can be seen in Fig. 6.6, when $C = 0$ one is back to the one-loop dressed kernel $\mathcal{K}_1$ of the previous subsection. As C increases $\mathcal{K}_2$ displays a less pronounced positive (respectively negative) peak in the small (respectively large) momenta region. Next, for $C \gtrsim 0.37$ a small negative region starts to appear in the IR, which rapidly becomes a deep negative well for $y \lesssim 0.6$, with $\mathcal{K}_2$ becoming positive for higher momenta[2]. Therefore, we see that the addition of the two-loop dressed contributions counteracts the effect of the overall minus sign of the integral equation, by effectively achieving a sign reversal of the kernel (roughly speaking, one has $\mathcal{K}_2 \approx -\mathcal{K}_1$). When this analysis is combined with the knowledge gathered from the one-loop dressed case, one concludes that there exists a critical value $\overline{C}$, such that, if $C > \overline{C}$ Eq. (6.82) will display at least one physical monotonically decreasing solution for a suitable value of the strong coupling α_s.

In order to see if the picture sketched above is confirmed when $x \neq 0$,

[2] It is also interesting to notice that all the curves meet at a common point y_*, which is determined by the general condition

$$\frac{\mathrm{d}}{\mathrm{d}y}\left[\log\left(\mathcal{Z}^2(y)\log\frac{y}{\mu^2}\right)\right]\Big|_{y=y_*} = 0,$$

with $y_* \simeq 0.67$ GeV^2.

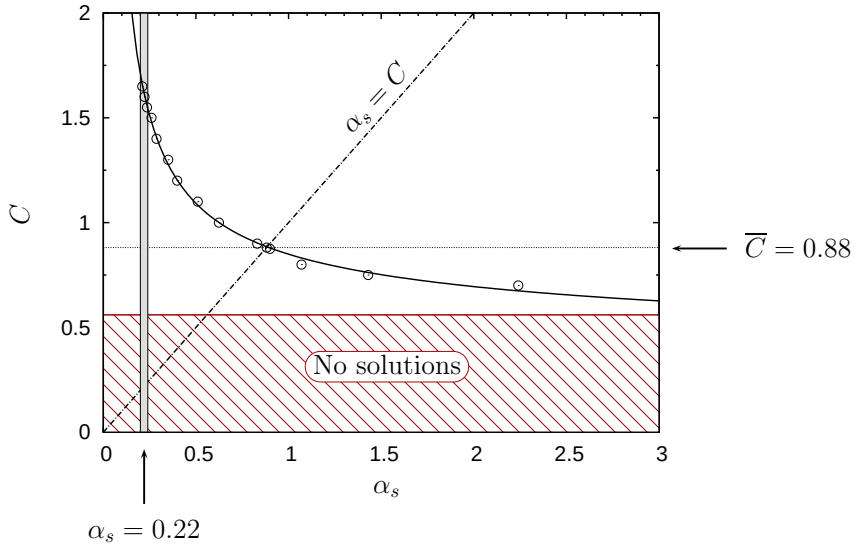

Fig. 6.7: The curve described by the set of the pairs (C, α_s) for which one finds physical solutions to the full mass equation (6.73). The curve starts from the critical value $\overline{C} \approx 0.56$ above which exactly one monotonically decreasing solution exists (below $\overline{C}$ there are no solutions). The value $C_* = \alpha_s (\approx 0.88)$ corresponds to the case in which Y is kept at its lowest order perturbative value. Finally, the gray vertical band represents the value for the quenched strong coupling obtained from the 4-loop MOM calculation of [?] renormalized at $\mu = 4.3$ GeV ($\alpha_s = 0.22$) with a customary 10% error; the matching values of C are between 1.55 – 1.65.

one can study numerically the solutions of the full mass equation (6.73) following the algorithm described at the beginning of the section (Fig. 6.7). Specifically, as shown in Fig. 6.7, there is a continuous curve formed by the pairs (C, α_s), for which one finds physical solutions. Indeed, for small values of C one has that all eigenvalues λ are either negative or complex, and no solution exists; this absence of solutions persists until the critical value $\overline{C} \approx 0.56$ is reached, after which one finds exactly one monotonically decreasing solution corresponding to the smallest positive eigenvalue λ_s (with bigger positive eigenvalues giving rise to oscillating non-physical solutions). However, for values up to $C \approx 0.8$ the coupling needed to get the corresponding running mass is of $\mathcal{O}(1)$, while for the quenched case the expected coupling from the 4-loop (momentum subtraction) calculation is $\alpha_s = 0.22$ at $\mu = 4.3$ GeV [?]. This latter value is obtained for $C \approx 1.55$ – 1.65, whereas for $C \approx 0.88$ one finds the solution to Eq. (6.73) for the lowest order perturbative value of the coefficient (6.76). In general one observes, as expected, that as C is increased, α_s decreases, *e.g.*, for $C = 1.1$, 1.3 and 1.5 one obtains solutions corresponding to the strong coupling values $\alpha_s \approx 0.51$, 0.35 and 0.26, respectively.

In Fig. 6.8 we plot the solutions for the most representative C values, *i.e.*, $C = 0.88$ and $C = 1.6$ (corresponding to, as already said, $\alpha_s \approx 0.88$ and 0.22 respectively); notice that we have used the linearity of the equation to normalize the solution in such a way that the mass at zero coincides with the IR saturating value found in lattice (Landau gauge) quenched simulations [34], or $m^2(0) = \Delta^{-1}(0) \approx 0.141$ GeV^2. As can be readily appreciated, the masses obtained display the basic qualitative features expected on general field-theoretic considerations and employed in numerous phenomenological studies; in particular, they are monotonically decreasing functions of the momentum, and vanish rather rapidly in the ultraviolet [7, 79, 80]. It would seem, therefore, that the all-order analysis presented here, puts the entire concept of the gluon mass, and a variety of fundamental properties ascribed to it, on a solid first-principle basis.

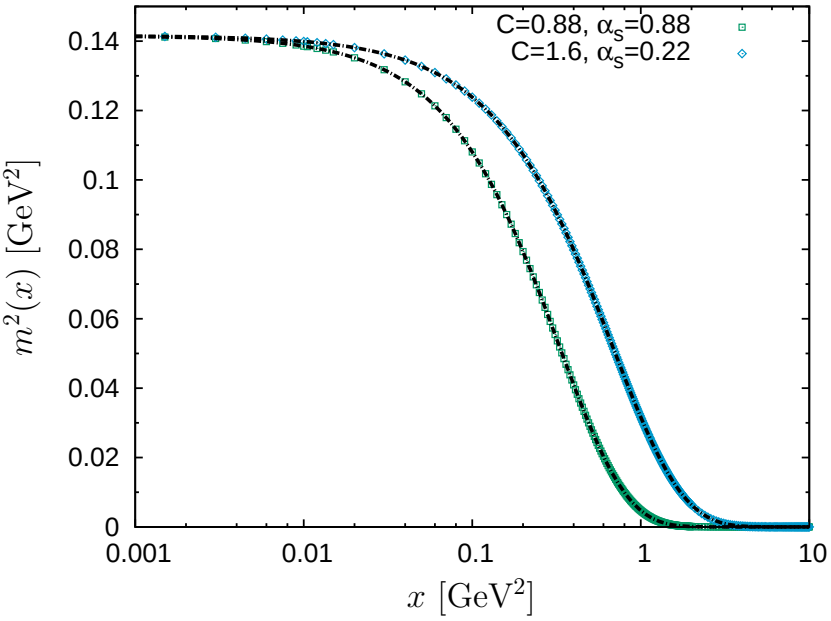

Fig. 6.8: Typical monotonically decreasing solution of the mass equation (6.73). The case shown have been obtained for the special values $C = 0.88$ and 1.6, corresponding value of the coupling $\alpha_s \approx 0.88$ and 0.22 respectively. The solutions have been normalized so that at zero they match the corresponding (Landau gauge) lattice value $\Delta^{-1}(0) \approx 0.141$ GeV^2.

7. MASSIVE GLUON PROPAGATOR IN THE MASSLESS BOUND-STATE FORMALISM.

As has been demonstrated in the previous chapter, the dynamical equation of the gluon mass in the Landau gauge may be derived from the SDE of the gluon propagator by postulating the existence of the pole vertices, and employing the WIs and STIs they satisfy, together with their totally longitudinal nature. The resulting integral equation makes no reference on the closed form of these vertices, nor on the actual dynamical ingredients composing them. However, the details of the actual dynamical formation of the bound-state poles, and subsequently of the pole vertices, as well as their exact closed form, transcend the limited purpose of obtaining a particular version of the gluon mass equation, and are of paramount importance for the self-consistency of the entire gluon mass generation scenario [81]. In fact, it would be highly desirable to establish a precise quantitative connection between the fundamental ingredients composing these vertices and the gluon mass itself.

The purpose of the present chapter is to dissect the pole vertices and scrutinize the field-theoretic properties of their constituents, within the context of the "massless bound-state formalism", first introduced in some early seminal contributions to this subject [15, 16, 61–63], and further developed in [64]. The final outcome of this analysis is an alternative, but completely equivalent, description of the dynamical gluon mass in terms of quantities appearing naturally in the physics of bound states, such as the "transition amplitude" and the "bound-state wave function". This new description makes manifest some of the salient physical properties of the gluon mass (e.g., positive-definiteness), and provides, in addition, a decisive confirmation of the self-consistency of the concepts and methodology employed.

Let us next present the general outline of the chapter, introducing some of the basic concepts, and commenting on the logical connections and delicate interplay between the various sections. Due to the complexity of the

concepts studied here, we will include some information about the preceding chapters, in order to realize a more self-contained description.

The starting point of our considerations is a brief review of the importance of the pole vertices for obtaining massive solutions out of the SDE for the gluon propagator, in a gauge invariant way, *i.e.*, preserving the form of the fundamental STIs of the theory (Section 7.1).

Within the massless bound-state formalism, the pole vertices are composed of three fundamental ingredients. (*i*) The nonperturbative transition amplitude, to be denoted by $I(q^2)$, which connects a single gluon to the massless excitation. (*ii*) The scalar massless excitation, whose propagator furnishes the pole i/q^2, and (*iii*) a set of "proper vertex functions" [62] (or "bound-state wave functions"), to be generically denoted by B, (with appropriate Lorentz and color indices), which connect the massless excitation to a number of gluons and/or ghosts. The quantity $I(q^2)$ is universal, in the sense that it appears in all possible pole vertices. Furthermore, it admits its own diagrammatic representation, which, in turn, involves the functions B. As a result, the dependence of the pole vertices on the Bs is quadratic (Section 7.2).

When inserted into the SDE for the gluon propagator, and all diagrams are kept (no truncation), the special structure of the pole vertices allows one to obtain a very concise relation between the gluon mass and the square of the transition amplitude, given in Eq. (7.30). This relation demonstrates that, unless $I(q^2)$ vanishes identically, the gluon mass obtained is positive-definite (Section 7.3).

If the above construction is repeated within the combined framework of the pinch technique (PT) [7, 23, 24, 44–46] and background field method (BFM) [47] (known as the "PT-BFM scheme" [42, 51, 52]), the relevant quantity to consider is the transition amplitude between a *background gluon* and the massless excitation, to be denoted by $\widetilde{I}(q^2)$ (all other ingredients remain identical). The mass of the propagator connecting a background (B) and a quantum gluon (Q) can then be expressed as the product of $I(q^2)$ and $\widetilde{I}(q^2)$ (an equivalent relation may be obtained from the background-background propagator). The additional fact that the PT-BFM gluon propagators are related to the conventional one by a set of powerful identities (known as Background-Quantum identities (BQIs) [54, 55]), allows one finally to relate $I(q^2)$ and $\widetilde{I}(q^2)$ as shown in Eq. (7.44) (Section 7.4).

Evidently, Eq. (7.44) has emerged as a self-consistency requirement between two different formulations of the SDE (conventional and PT-BFM),

which, in their untruncated version, must furnish the same physics. It would be very important, however, to establish the validity of Eq. (7.44) in a more direct, explicit way, by operating at the level of the pole vertices themselves, where $I(q^2)$ and $\widetilde{I}(q^2)$ make their primary appearance. To that end, we will carry out the explicit construction of the three-gluon pole vertex, both in the conventional and the BFM formalism, using as a sole input the WI and/or STIs they satisfy, and their totally longitudinal nature (subsection 7.5.1). The comparison of the two, after judicious identification of the parts that contribute to the corresponding gluon mass equations, reproduces precisely Eq. (7.44) (subsection 7.5.2).

It turns out that an even more fundamental derivation of Eq. (7.44) may be devised, which takes one back to the underpinnings of the PT-BFM connection: the BQIs, which are formally obtained within the Batalin-Vilkovisky (BV) formalism [56,57], can be alternatively derived through the diagrammatic rearrangements implemented by the PT. In the case of the SDE series containing regular (fully dressed) vertices, such a diagrammatic derivation amounts finally to the demonstration of the PT-BFM equivalence. From the operational point of view the standard PT construction boils down to the judicious exploitation of the rearrangements produced when certain longitudinal (pinching) momenta trigger the STIs satisfied by the aforementioned vertices; the required STIs are known from the formal machinery of the BV, or alternative formalisms. A priori, the implemenation of this procedure at the level of the diagrammatic representation of the $I(q^2)$ is thwarted by the fact that the pinching momenta will act on the B vertices (introduced above), whose STIs, however, are not formally known. Nonetheless, the explicit construction of the pole vertex, and the subsequent line of reasoning, furnish precisely the missing STI, and make the PT-driven diagrammatic construction possible An interesting by-product of this construction is the derivation of an integral constraint between the B-vertex functions containing ghost legs. When combined with the recent lattice findings on the infrared behavior of the ghost propagator, this constraint strongly suggests the individual vanishing of all ghost vertex functions (Section 7.6).

The diagrammatic evaluation of the transition amplitude furnishes Eq. (7.119), which express this fundamental ingredient of the bound-state formalism in terms of a double integral containing solely the vertex $B_{\mu\nu}$. Even though this vertex function is not known for general momenta, the powerful relation of Eq. (7.122), first derived in [64], relates its $g_{\mu\nu}$ form factor

to the gluon mass. This relation, in turn, allows one to recover the mass equation derived in [72], following a completely different methodology and formalism. The resulting exact coincidence reveals thus an impressive complementarity between two formally distinct methods (Section 7.7).

7.1 Getting massive solutions from the gluon SDE

In this section we review the general principles that allow the generation of massive solutions out of the gluon SDE, and study in detail the general structure of the special pole vertices that trigger this effect (for a different approach, see, e.g., [82]).

7.1.1 General principles

The full gluon propagator $\Delta^{ab}_{\mu\nu}(q) = \delta^{ab}\Delta_{\mu\nu}(q)$ in the Landau gauge is defined as

$$\Delta_{\mu\nu}(q) = -iP_{\mu\nu}(q)\Delta(q^2)\,, \tag{7.1}$$

where

$$P_{\mu\nu}(q) = g_{\mu\nu} - \frac{q_\mu q_\nu}{q^2}\,, \tag{7.2}$$

is the usual transverse projector, and the scalar cofactor $\Delta(q^2)$ is related to the (all-order) gluon self-energy $\Pi_{\mu\nu}(q) = P_{\mu\nu}(q)\Pi(q^2)$ through

$$\Delta^{-1}(q^2) = q^2 + i\Pi(q^2). \tag{7.3}$$

Alternatively, one may introduce the *inverse* of the gluon dressing function, $J(q^2)$, defined as [48]

$$\Delta^{-1}(q^2) = q^2 J(q^2)\,. \tag{7.4}$$

Let us consider the SDE for the gluon propagator in the conventional formulation of Yang-Mills (*i.e.*, linear R_ξ gauges)

$$\Delta^{-1}(q^2)P_{\mu\nu}(q) = q^2 P_{\mu\nu}(q) + i\Pi_{\mu\nu}(q), \tag{7.5}$$

with the self-energy given by

$$\Pi_{\mu\nu}(q) = \sum_{i=1}^{5}(a_i)_{\mu\nu}\,, \tag{7.6}$$

where the diagrams (a_i) are shown in Fig. 3.1. Note that the full (untruncated) self-energy is transverse, namely

$$q^\mu \Pi_{\mu\nu}(q) = \sum_{i=1}^{5} q^\mu (a_i)_{\mu\nu} = 0\,. \tag{7.7}$$

It turns out that, with the Schwinger mechanism turned off (*i.e.*, in the absence of massless poles in the vertices) the SDE leads to the conclusion that $\Delta^{-1}(0) = 0$, namely the absence of massive solutions.

In order to obtain massive solutions out of the above SDE, and preserve, at the same time, the gauge invariance intact, one must carry out the crucial substitution

$$\Gamma \longmapsto \Gamma' = \Gamma_m + V, \tag{7.8}$$

to all fully-dressed interaction vertices appearing in Eq. (7.5). The main characteristic of the vertices V, which sharply differentiates them from ordinary vertex contributions, is that they contain massless poles, originating from the contributions of bound-state excitations. Such dynamically generated poles are to be clearly distinguished from poles related to ordinary massless propagators, associated with elementary fields in the original Lagrangian. In addition, they are completely *longitudinally* coupled, *i.e.*, they satisfy conditions of the type (for the case of the three-gluon vertex)

$$P^{\alpha'\alpha}(q) P^{\mu'\mu}(r) P^{\nu'\nu}(p) V_{\alpha'\mu'\nu'}(q,r,p) = 0. \tag{7.9}$$

As for the vertices Γ_m, they are given by the same graphs as the Γ before, but with gluon propagators replaced by massive ones (see Eq. (7.12)), implementing simultaneously Eq. (7.8).

The new (massive) self-energy is then given by

$$\Pi_{\mu\nu}(q) = \sum_{i=1}^{5} (a_i')_{\mu\nu}, \tag{7.10}$$

where the "prime" indicates that the various fully-dressed vertices appearing inside the corresponding diagrams of the gluon self-energy have been replaced by their primed counterparts, as in Eq. (7.8). It is important to emphasize that, since the above replacement maintains the STIs of the theory unaltered, the transversality of the massive self-energy persists, *i.e.*,

$$\sum_{i=1}^{5} q^\mu (a_i')_{\mu\nu} = 0\,. \tag{7.11}$$

The appearance of massive solutions amounts effectively to the change (in Minkowski space)

$$\Delta^{-1}(q^2) = q^2 J(q^2) \longmapsto \Delta_m^{-1}(q^2) = q^2 J_m(q^2) - m^2(q^2), \tag{7.12}$$

with $m^2(0) \neq 0$ (of course, in Euclidean space, one must find $\Delta_m^{-1}(0) > 0$). The subscript "m" in J_m indicates that effectively one has now a mass inside the corresponding expressions: for example, whereas perturbatively $J(q^2) \sim \ln q^2$, after dynamical gluon mass generation has taken place, one has $J_m(q^2) \sim \ln(q^2 + m^2)$.

The actual evaluation of the relevant diagrams may be carried out by appealing to the basic global features of the V vertices, as deduced from the STIs and their complete longitudinality [72]. The final upshot is that the SDE may be schematically cast into the form (Minkowski space)

$$q^2 J_m(q^2) - m^2(q^2) = q^2 \left[1 + \mathcal{K}_1(q^2, m^2, \Delta_m)\right] + \mathcal{K}_2(q^2, m^2, \Delta_m), \tag{7.13}$$

such that $q^2 \mathcal{K}_1(q^2, m^2, \Delta_m) \to 0$, as $q^2 \to 0$, whereas $\mathcal{K}_2(q^2, m^2, \Delta_m) \neq 0$ in the same limit, precisely because it includes the term $1/q^2$ contained inside $V_{\alpha\mu\nu}(q, r, p)$. This form, in turn, gives rise to two coupled integral equations, an inhomogeneous equation for $J_m(q^2)$, and a homogeneous one for $m^2(q^2)$ (the latter is usually referred to as the "mass equation"), of the generic type

$$J_m(q^2) = 1 + \int_k \mathcal{K}_1(q^2, m^2, \Delta_m), \tag{7.14}$$

$$m^2(q^2) = -\int_k \mathcal{K}_2(q^2, m^2, \Delta_m). \tag{7.15}$$

Physically meaningful (i.e., positive definite and monotonically decreasing) solutions to an approximate version of the full mass equation have been recently presented in [72].

7.1.2 Structure of the vertices V

We will next consider the decomposition of the vertices V that emerges in a natural way, if one employs as a criterion the effect that the various components of V may have on the gluon SDE. For concreteness we will focus on the case $V_{\alpha\mu\nu}$; however, all basic arguments may be straighforwardly extended to any vertex of the type V.

Since the main function of the vertex $V_{\alpha\mu\nu}$ is to generate a mass term when inserted into the graph (a_1) of Fig. 3.1, it must contain components that do not vanish as $q \to 0$. To study this point in more detail, we first separate V into two distinct parts, namely

$$V_{\alpha\mu\nu}(q,r,p) = U_{\alpha\mu\nu}(q,r,p) + R_{\alpha\mu\nu}(q,r,p)\,, \tag{7.16}$$

defined as follows. U is the part of V that has its Lorentz index α saturated by the momentum q; thus, it contains necessarily the explicit q-channel massless excitation, namely the $1/q^2$ poles. It assumes the general form

$$U_{\alpha\mu\nu}(q,r,p) = \frac{q_\alpha}{q^2} C_{\mu\nu}(q,r,p), \tag{7.17}$$

where, due to Bose symmetry under the exchange $r \leftrightarrow p$, $\mu \leftrightarrow \nu$, $C_{\mu\nu}(q,r,p)$ must satisfy $C_{\nu\mu}(q,p,r) = -C_{\mu\nu}(q,r,p)$; as a result, $C_{\mu\nu}(0,-p,p) = 0$.

The term R contains everything else; in particular, the massless excitations in the other two kinematic channels, namely $1/r^2$ and $1/p^2$ (but not $1/q^2$) are assigned to R. Thus, for example, terms of the form $q_\alpha g_{\mu\nu}$ and $q_\alpha r_\mu p_\nu$ are assigned to $U_{\alpha\mu\nu}$, while terms of the type $p_\nu g_{\alpha\mu}$ and $r_\mu g_{\alpha\nu}$ belong to R. Evidently, $P^{\mu'\mu}(r)P^{\nu'\nu}(p)R_{\alpha\mu'\nu'}(q,r,p) = 0$. In addition, again due to Bose symmetry, we have that $R_{\alpha\mu\nu}(0,-p,p) = 0$.

Consider now the individual effect that U and R have when inserted into the gluon SDE, specifically the graph (a_1) of Fig. 3.1. Of course, it is expected, on general grounds, that R should not generate mass terms, because it does not contain poles of the type $1/q^2$; this is indeed what happens. If we work in the Landau gauge, any contribution from R vanishes for a simple kinematic reason, namely the above transversality condition satisfied by R. Away from the Landau gauge, R does not contribute to the mass equation Eq. (7.15) either, because $R_{\alpha\mu\nu}(0,-p,p) = 0$ and there is no $1/q^2$ term that could compensate this. Thus, R seems to contributes, in a natural way, to the equation for $J_m(q^2)$.

In fact, it is relatively straighforward to establish that, in the limit $q \to 0$, the SDE contribution generated by R vanishes as $\mathcal{O}(q^2)$ (or faster). Indeed, let us set $p = k$, the virtual integration momentum in the SDE diagram; given that $R_{\alpha\mu\nu}(0,-k,k) = 0$, a Taylor expansion of R around $q^2 = 0$ gives (suppressing indices)

$$R(q,-q-k,k) = 2(qk)R'(k^2) + \mathcal{O}(q^2)\,. \tag{7.18}$$

Now, the first term is odd in k, and therefore the corresponding integral vanishes. As a result, the term $2(qk)R'(k^2)$ must be multiplied by another

term proportional to (qk), coming from the rest of the terms (propagators, vertices etc) appearing in the integrand. Thus, the resulting contribution is of order $\mathcal{O}(q^2)$ (or higher), as announced. The importance of this property is related to the fact that, in order to arrive at Eq. (7.14), one must pull out of the corresponding integral equation a factor of q^2; had the integrand vanished slower than $\mathcal{O}(q^2)$, one would get a divergent contribution for $J_m(0)$, which would be physically unacceptable, given that $J_m(0)$ is inversely proportional to the infrared finite QCD effective charge.

Therefore, the only term that can contribute to the gluon mass equation is $U_{\alpha\mu\nu}(q,r,p)$; the precise contribution will depend, of course, on the exact form and behaviour of the cofactor $C_{\mu\nu}(q,r,p)$, as $q \to 0$. It is clear for instance, that if $C_{\mu\nu}(q,r,p)$ contains terms that behave as $\mathcal{O}(q^{1+c})$, with $c > 0$, as $q \to 0$, then these terms could not possibly trigger the Schwinger mechanism, because the effect of the pole would be counteracted by the positive powers of q. On the other hand, terms that vanish as $\mathcal{O}(q^{1-c})$, would give rise to divergent results; however, this latter possibility does not occur, again due to the Bose symmetry of V with respect to $p \leftrightarrow r$. Thus, the only terms of $C_{\mu\nu}$ relevant for gluon mass generation are those that vanish as $\mathcal{O}(q)$ $(c = 0)$.

These observations motivate the separation of $U_{\alpha\mu\nu}(q,r,p)$ into two parts, one that behaves as a constant, $\mathcal{O}(q^0)$, thus contributing to the mass equation (to be denoted by $\mathcal{U}_{\alpha\mu\nu}$), and one that vanishes as $\mathcal{O}(q^c)$, $c > 0$, and can be naturally reassigned to R (to be denoted by $\mathcal{U}'_{\alpha\mu\nu}$). In fact, due to the same reason explained above, namely, the absence of divergent contributions at the level of Eq. (7.14), we must have that $c \geq 1$; actually, the explicit construction presented in Section 7.5 [*e.g.* Eq. (7.71) and ensuing discussion], reveals that $c = 1$ Thus,

$$U_{\alpha\mu\nu}(q,r,p) = \underbrace{\mathcal{U}_{\alpha\mu\nu}(q,r,p)}_{\mathcal{O}(q^0)} + \underbrace{\mathcal{U}'_{\alpha\mu\nu}(q,r,p)}_{\mathcal{O}(q)} \tag{7.19}$$

Then, setting

$$\mathcal{R}_{\alpha\mu\nu}(q,r,p) = R_{\alpha\mu\nu}(q,r,p) + \mathcal{U}'_{\alpha\mu\nu}(q,r,p) \tag{7.20}$$

we arrive at the final separation

$$V_{\alpha\mu\nu}(q,r,p) = \underbrace{\mathcal{U}_{\alpha\mu\nu}(q,r,p)}_{m^2(q^2)} + \underbrace{\mathcal{R}_{\alpha\mu\nu}(q,r,p)}_{J_m(q^2)} \tag{7.21}$$

where the curly brackets below each term indicate in which equation [(7.14) or (7.15)] each term will contribute.

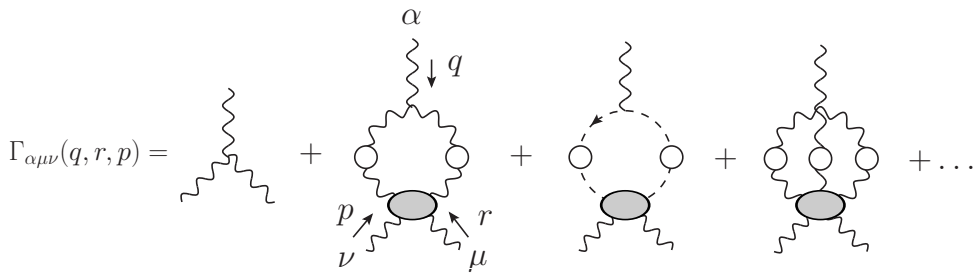

Fig. 7.1: The SDE for the Q^3 vertex $\Gamma_{\alpha\mu\nu}(q,r,p)$. Gray blobs denote the conventional 1PI (with respect to vertical cuts) multiparticle kernels.

7.2 Massless bound-state formalism

Whereas in the SDE approach outlined in the previous section one relies predominantly on the global properties of the vertices V, within the massless bound-state formalism one takes, instead, a closer look at the field-theoretic composition of these vertices, establishing fundamental relations between their internal ingredients and the gluon mass. This becomes possible thanks to the key observation that, since the fully dressed vertices appearing in the diagrams of Fig. 3.1 are themselves governed by their own SDEs, the appearance of such massless poles must be associated with very concrete modifications in the various structures composing them.

Let us begin by recalling that, in general, when setting up the usual SDE for any fully-dressed vertex contained in Eq. (7.5), a particular field (leg) is singled out, and is connected to the various multiparticle kernels through all elementary vertices of the theory involving this field (leg). The remaining legs enter into the various diagrams through the aforementioned multiparticle kernels, or, in terms of the standard skeleton expansions, through fully-dressed vertices (instead of tree-level ones). For example, in the case of the Q^3 three-gluon vertex $\Gamma_{\alpha\mu\nu}(q,r,p)$ we have (with a certain hindsight) identified the special leg to be the one entering into graph (a_1) of Fig. 3.1 from the right, carrying momentum q; the corresponding vertex SDE is shown in Fig. 7.1.

Now, when the Schwinger mechanism is turned off, the various multiparticle kernels appearing in the SDE for the Q^3 vertex have a complicated skeleton expansion, but their common characteristic is that they are *one-particle irreducible* with respect to cuts in the direction of the momentum

q. Thus, for example, diagram (a) of Fig. 7.2 is explicitly excluded from the (gray) four-gluon kernel (b), and the same is true for all other kernels.

When the Schwinger mechanism is turned on, the structure of the kernels is modified by the presence of the composite massless excitations, described by a propagator of the type i/q^2. For example, as shown in Fig. 7.2, the gray four-gluon kernel is converted into a black kernel, diagram (b'), which is the sum of two parts: (i) the term (b'_1), which corresponds to a kernel (gray striated) that is "regular" with respect to the q-channel, and (ii) the term (b'_2), which describes the exchange of the composite massless excitation between two gluons in the q-channel.

Thus, when the replacements of Eq. (7.12) and Eq. (7.8) are carried

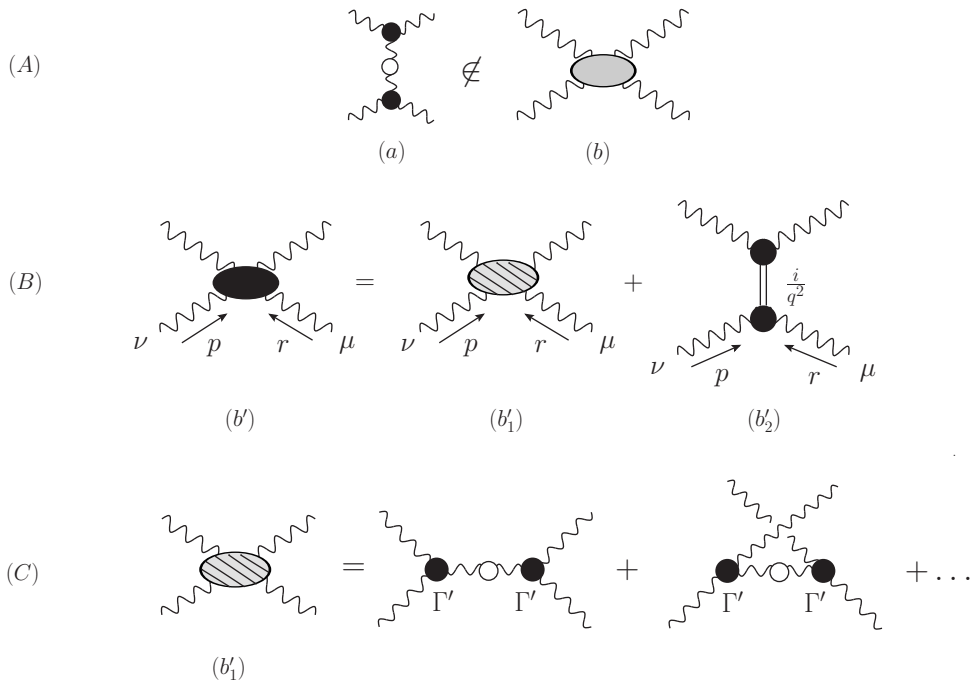

Fig. 7.2: (A) A diagram not included into the standard kernel. (B) The kernel with the Schwinger mechanism on: in addition to the "regular part" (b'_1) (gray striated), the massless excitation in the q-channel (b'_2) is added. (C) The part (b'_1) is obtained from the original (gray) kernel (b) by inserting massive gluon propagators into its diagrams, and carrying out the substitution Eq. (7.8) in the fully-dressed vertices of the skeleton expansion.

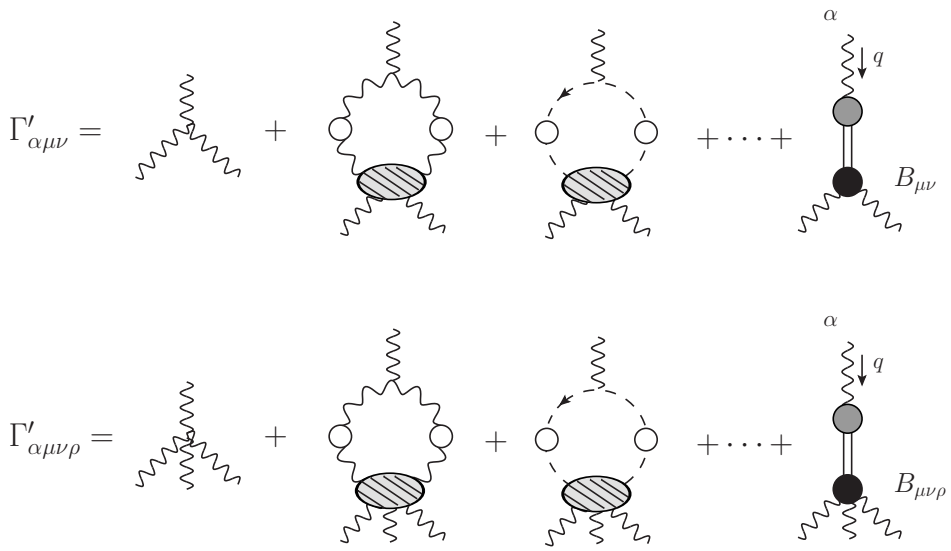

Fig. 7.3: Schwinger-Dyson equations for the full three and four gluon vertices in the presence of their pole parts. Note that (i) that the new SDE kernels are modified with respect to those appearing in Fig. 7.1; (ii) the last term in these SDEs corresponds to the $\mathcal{U}$ part of the pole vertices.

out, the SDE for the different interaction vertices in the presence of their pole parts will be given by expansions such as those shown in Fig. 7.3.

These modifications in the composition of the kernels give rise precisely to the vertices V mentioned earlier. A closer look at the structure of the terms comprising the last term in Fig .7.3 reveals that the Lorentz index α (of the leg carrying the momentum q) is saturated precisely by the momentum q. Similarly, Bose symmetry forces the same behavior on the other two channels, so that, in the end, we obtain a totally longitudinal structure, *i.e.*, Eq. (7.9). At this point we can make the nonperturbative pole manifest, and cast the last term of the three-gluon vertex in the form of Fig. 7.3, by setting

$$\mathcal{U}_{\alpha\mu\nu}(q,r,p) = I_\alpha(q)\frac{i}{q^2}B_{\mu\nu}(q,r,p), \tag{7.22}$$

where $I_\alpha(q)$ is the transition amplitude that mixes a quantum gluon with the massless excitation, i/q^2 corresponds to the propagator of the massless excitation, and B is an effective vertex describing the interaction between

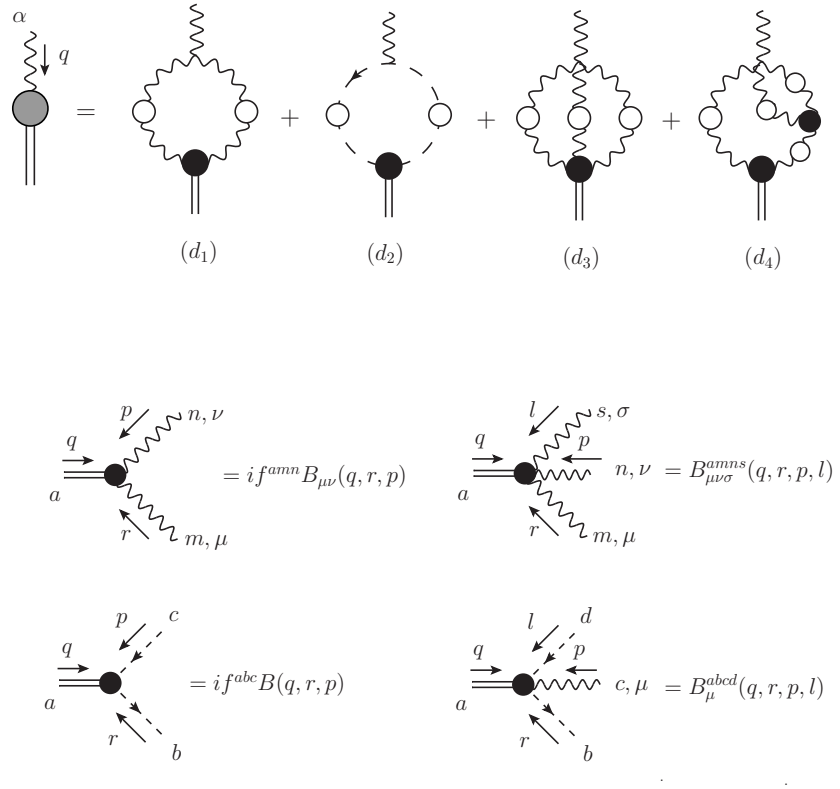

Fig. 7.4: Diagrammatic representation of the transition amplitude and the Feynman rules for the different effective vertices.

the massless excitation and gluons and/or ghosts. In the standard language used in bound-state physics, B represents the "bound-state wave function" (or "Bethe-Salpeter wave function"). Clearly, due to Lorentz invariance,

$$I_\alpha(q) = q_\alpha I(q^2), \tag{7.23}$$

and the scalar cofactor, to be referred as the "transition function", is simply given by

$$I(q^2) = \frac{q^\alpha}{q^2} I_\alpha(q). \tag{7.24}$$

Furthermore, notice that the transition amplitude $I_\alpha(q)$ is universal, in the

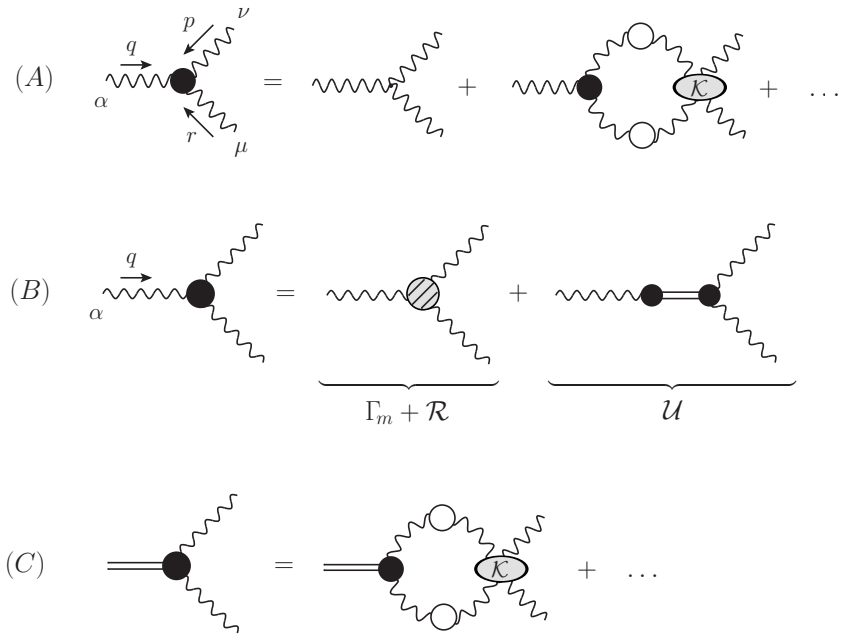

Fig. 7.5: Steps to be performed in order to derive the BSE which governs the dynamics of the effective B vertices.

sense that it constitutes a common ingredient of all V vertices, namely

$$\mathcal{U}_{\alpha\{\dots\}}(q,\dots) = I_\alpha(q)\frac{i}{q^2}B_{\{\dots\}}(q,\dots); \tag{7.25}$$

thus, the difference between the various $\mathcal{U}_{\alpha\{\dots\}}$ vertices is solely encoded into the structure of the wave functions $B_{\{\dots\}}$. The diagrammatic representation of the transition amplitude as well as the different effective vertices B are shown in Fig. 7.4. It is important to recognize that the $\mathcal{U}_{\alpha\{\dots\}}$ depend *quadratically* on the $B_{\{\dots\}}$, since $I_\alpha(q)$ depends linearly on them.

As has been explained in the literature, the dynamics of the B functions may be determined, at least in principle, from a set of homogeneous (coupled and nonlinear) integral equations, known as Bethe-Salpeter equations. This particular set of equations must admit nontrivial solutions, which, when properly adapted to the kinematic details of the problem at hand, will furnish the momentum dependence of the wave functions B.

The way to obtain this set of equations is by first rearranging the vertex SDE in such a way as to replace the bare vertex appearing in the original

expansion (e.g., Fig. 7.1) by a fully dressed one (Fig. 7.5, line A). At the same time, and as a consequence of this rearrangement, one must replace the standard SD kernel by the corresponding Bethe-Salpeter kernel (denoted by $\mathcal{K}$ in Fig. 7.5); the two kernels are diagrammatically different, and are formally related by a standard all-order formula [cite properly]. The next step is to separate the full vertex into the "regular" part, namely the part that behaves as a regular function in the limit $q \to 0$, and the pole part, $1/q^2$, as shown in Fig. 7.5, line B. Note that the full regular part is the sum of Γ_m and the term $\mathcal{R}$ coming from V, since neither of these two terms diverges in the aforementioned limit. Then, this separation is carried out on both sides of the equation; since the vertex on the rhs is now fully dressed, it too posesses a pole $1/q^2$. The final dynamical equation for B emerges by equating the coefficients multiplying the pole term on both sides, as seen in Fig. 7.5, line C. In the same way, the dynamical equation for the regular part is given by the remaining terms.

7.3 Relating the gluon mass with the transition amplitude

The aim of this section is to derive the fundamental formula that relates the effective gluon mass with the square of the transition amplitude.

To that end, let us go back to the SDE for the gluon propagator with the replacements given in Eqs.(7.8)-(7.12) already implemented, namely (Landau gauge)

$$[q^2 J_m(q^2) - m^2(q^2)]P_{\mu\nu}(q) = q^2 P_{\mu\nu}(q) + i\sum_{i=1}^{5}(a_i')_{\mu\nu}, \tag{7.26}$$

It turns out that the most expeditious way for deriving the gluon mass equation, and from it the desired relation between $m^2(q^2)$ and $I(q^2)$, is to identify, on both sides of Eq. (7.26), the cofactors of the tensorial structure $q_\mu q_\nu/q^2$ that survive the limit $q^2 \to 0$, and then set them equal to each other. In doing so, it is clear that the left-hand side (lhs) of Eq. (7.26) furnishes simply

$$[\text{lhs}]_{\mu\nu} = \frac{q_\mu q_\nu}{q^2} m^2(q^2). \tag{7.27}$$

On the other hand, the corresponding contribution from the righ-hand side (rhs) is directly related to the $\mathcal{U}$ part of the V vertices (see discussion in subsection 7.1.2), which, due to their very precise definition [see Eq. (7.25)], are all proportional to q_ν.

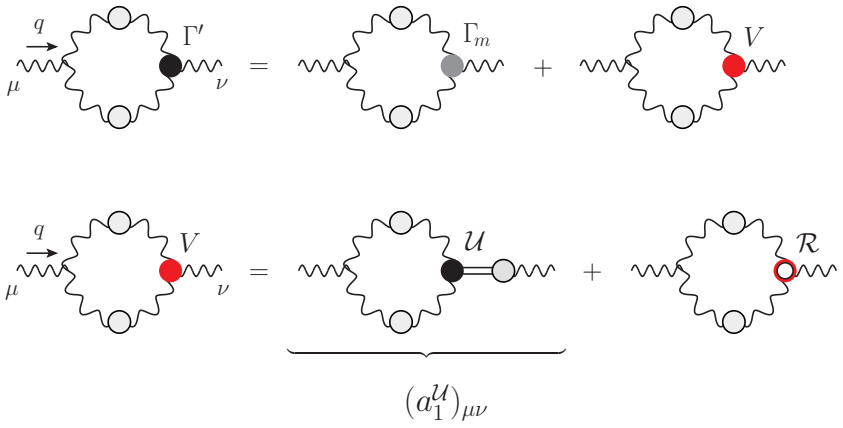

Fig. 7.6: Procedure for isolating the contribution of diagram (a_1') to the effective gluon mass.

The procedure described above is exemplified in Fig. 7.6 for the particular case of the diagram (a_1'). Specifically, in the first step one separates the regular part Γ_m from the pole part V of the full Q^3 vertex Γ'. In the second step the pole part V is written as the sum of the $\mathcal{U}$ part (containing the explicit q-channel massless excitation) and the $\mathcal{R}$ part. Finally, due to the special structure of the $\mathcal{U}$ part, this contribution is proportional to $q_\mu q_\nu/q^2$, and contributes to the rhs of the mass equation.

The next step is to carry out this procedure to the $\mathcal{U}$ parts of all diagrams, and determine the complete contribution to the rhs of the mass equation, as shown pictorially in Fig. 7.7. It is clear that from all diagrams containing the $\mathcal{U}$ parts (first line of Fig. 7.7) one may factor out the common quantity $I(q^2)$, since, as we have emphasized in the previous section, $I(q^2)$ is universal (second line of Fig. 7.7). Then, quite interestingly, the sum of the terms in the parenthesis is nothing else than the diagrammatic representation of $I(q^2)$, given in Fig. 7.4 (note that all combinatorial factors work out exactly).

So, applying this procedure for each one of the fully-dressed vertices appearing in the SDE Eq. (7.26), one can put together the contributions of the several $\mathcal{U}$ parts to the gluon self-energy, as shown in Fig. 7.7.

$$\sum_{i=1}^{5}(a_i^{\mathcal{U}})_{\mu\nu} = g^2 I_\mu(q)\left(\frac{i}{q^2}\right)I_\nu(-q) \tag{7.28}$$

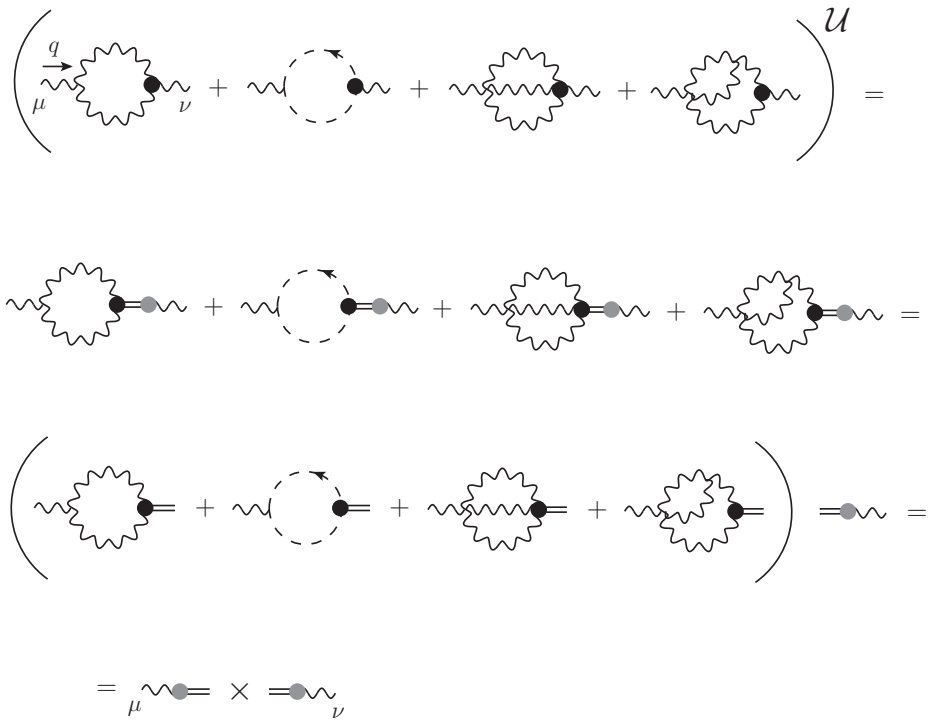

Fig. 7.7: General procedure for isolating the contributions of the right-hand side of Eq. (7.26) to the effective gluon mass. Note that the vertices appearing in this figure correspond to the $\mathcal{U}$ parts of the full vertices Γ'.

Then, using Eq. (7.23), together with the fact that $I_\nu(-q) = -I_\nu(q)$, one obtains the following result

$$[\text{rhs}]_{\mu\nu} = \frac{q_\mu q_\nu}{q^2} g^2 I^2(q^2). \tag{7.29}$$

Therefore, equating Eq. (7.27) with Eq. (7.29) we find that the effective gluon mass is related to the transition amplitude through the simple formula (Minkowski space)

$$m^2(q^2) = g^2 I^2(q^2). \tag{7.30}$$

This last formula may be passed to Euclidean space, using the standard conversion rules, together with the expression for $I(q^2)$ given in Eq. (7.121). In particular, the transition to the Euclidean space proceeds by using the

standard formulas that allow the conversion of the various Green's functions from the Minkowski momentum q^2 to the Euclidean $q_E^2 = -q^2 > 0$; specifically

$$\Delta_E(q_E^2) = -\Delta(-q_E^2); \quad m_E^2(q_E^2) = m^2(-q_E^2); \quad G_E(q_E^2) = G(-q_E^2); \quad \int_k = i\int_{k_E}. \tag{7.31}$$

As a consequence, we have $I_E(q_E^2) = -I(-q_E^2)$, so that

$$m_E^2(q_E^2) = g^2 I_E^2(q_E^2). \tag{7.32}$$

An immediate important implication of this last relation is that the gluon mass obtained is a positive-definite function for all values of the Euclidean momenta, as expected on physicsl grounds.

Let us finally mention that the transversality of the full gluon self-energy [see Eq. (7.11)] guarantees that if one were to consider the part of the mass equation proportional to $g_{\mu\nu}$, one would eventually obtain exactly the same relation given in Eq. (7.30). Note, however, that the corresponding derivation is far more subtle and laborious, and hinges crucially on the judicious use of a special integral identity (for a detailed treatment of this issue, see [72]).

7.4 The BQI of the transition amplitudes: SDE derivation

We will now repeat the construction of the last section using the SDEs of the PT-BFM formalism. Specifically, we will derive the relations analogous to Eq. (7.30), which, in conjunction with the BQIs connecting the conventional and PT-BFM gluon propagators, will furnish a nontrivial relation between the corresponding transition amplitudes.

7.4.1 General considerations

In the PT-BFM formalism the natural separation of the gluonic field into a "quantum" (Q) and a "background" (B) gives rise to an extended set of Feynman rules, and leads to an increase in the type of possible Green's functions that one may consider. In the case of the gluonic two-point function, in addition to the conventional QQ gluon propagator, Δ, two additional quantities appear: the QB propagator, $\widetilde{\Delta}$, mixing one quantum gluon with one background gluon, and the BB propagator, $\widehat{\Delta}$, with two

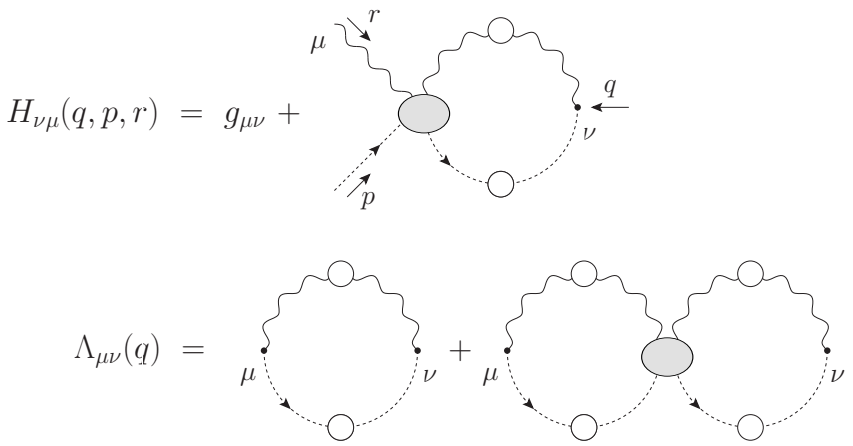

Fig. 7.8: Definitions and conventions of the auxiliary functions Λ and H.

background gluon legs. It turns out that these three propagators are related by the all order identities (referred to as BQIs)

$$\Delta(q^2) = [1 + G(q^2)]\widetilde{\Delta}(q^2) = [1 + G(q^2)]^2\widehat{\Delta}(q^2). \tag{7.33}$$

The function $G(q^2)$, whose role in enforcing these crucial relations is instrumental, is defined as the $g_{\mu\nu}$ form factor of a special two-point function, given by (see Fig. 7.8)

$$\begin{aligned}\Lambda_{\mu\nu}(q) &= -ig^2 C_A \int_k \Delta^\sigma_\mu(k) D(q-k) H_{\nu\sigma}(-q, q-k, k) \\ &= g_{\mu\nu} G(q^2) + \frac{q_\mu q_\nu}{q^2} L(q^2),\end{aligned} \tag{7.34}$$

where C_A denotes the Casimir eigenvalue of the adjoint representation (N for $SU(N)$), $d = 4-\epsilon$ is the space-time dimension, and we have introduced the integral measure

$$\int_k \equiv \frac{\mu^\epsilon}{(2\pi)^d} \int \mathrm{d}^d k, \tag{7.35}$$

with μ the 't Hooft mass. In addition, $D^{ab}(q^2) = \delta^{ab} D(q^2)$ is the ghost propagator, and $H_{\nu\sigma}$ is the gluon-ghost kernel. The dressed loop expansion of Λ and H is shown in Fig. 7.8. Notice that the standard ghost-gluon vertex Γ_μ is obtained from $H_{\nu\mu}$ simply through the contraction

$$q^\nu H_{\nu\mu}(q,p,r) = -\Gamma_\mu(r,q,p). \tag{7.36}$$

Finally, in the Landau gauge only, the form factors $G(q^2)$ and $L(q^2)$ are linked to the ghost dressing function

$$F(q^2) = q^2 D(q^2) \tag{7.37}$$

by means of the all-order relation [39, 58–60]

$$F^{-1}(q^2) = 1 + G(q^2) + L(q^2)\,, \tag{7.38}$$

which will be extensively used in the ensuing analysis.

Returning to Eq. (7.33), it is important to recognize that the two basic functions constituting the gluon propagators, namely $J_m(q^2)$and $m^2(q^2)$, satisfy Eq. (7.33) individually [65]. In particular, the corresponding masses are related by

$$\widehat{m}^2(q^2) = [1 + G(q^2)]\widetilde{m}^2(q^2) = [1 + G(q^2)]^2 m^2(q^2). \tag{7.39}$$

Finally, in order to obtain from the SDEs of the PT-BFM propagators a mass formula analogous to that of Eq. (7.30), one needs to introduce the appropriate transition amplitude connecting the background gluon with the massless excitation. This new transition amplitude, whose diagrammatic representation is shown in Fig. 7.9, allows us to write the $\widetilde{\mathcal{U}}$ part of the corresponding pole vertices in the BFM as

$$\widetilde{\mathcal{U}}_{\alpha\{\dots\}}(q,\dots) = \widetilde{I}_\alpha(q)\frac{i}{q^2}B_{\{\dots\}}(q,\dots). \tag{7.40}$$

Observe that only the transition amplitude is modified in this expression with respect to Eq. (7.25) when we go to the BFM. This is so because the only background field is the one carrying the momentum q, while all other fields are quantum (*i.e.*, they are common to the PT-BFM and conventional descriptions).

7.4.2 Relating the transition amplitudes through the SDEs of the PT-BFM

Consider the SDE for the QB propagator, connecting a quantum and a background field, given by the expression

$$\widetilde{\Delta}^{-1}(q^2)P_{\mu\nu}(q) = q^2 P_{\mu\nu}(q) + i\sum_{i=1}^{6}(a_i)_{\mu\nu}, \tag{7.41}$$

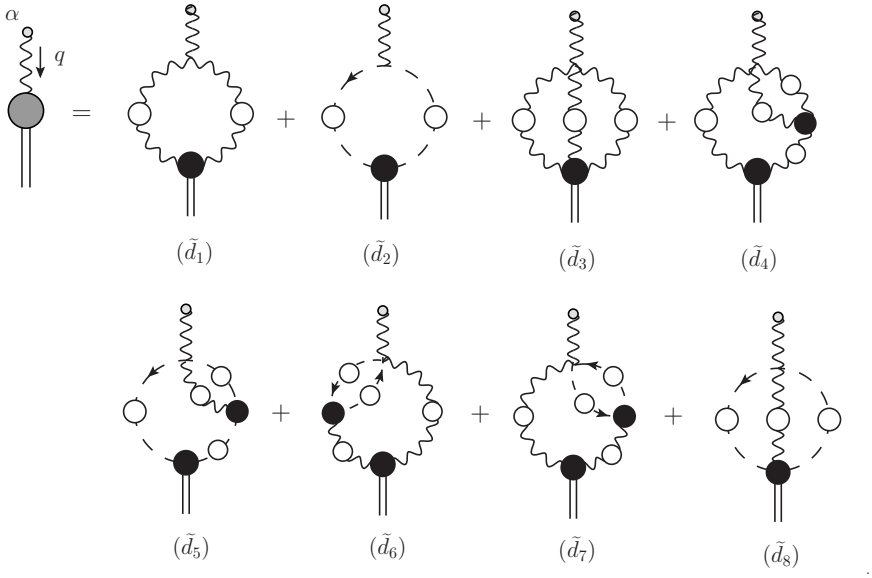

Fig. 7.9: Diagrammatic representation of the background transition amplitude.

with the diagrams (a_i) shown in Fig. 3.2. Note that the diagrams are separated into three blocks, each of which is individually transverse; this special property of "block-wise" transversality is particular to the PT-BFM scheme.

Let us now apply the diagrammatic procedure shown in Fig. 7.7 to the new set of diagrams appearing in this SDE. Evidently, the quantity to be factored out from all diagrams comprising the $\widetilde{\mathcal{U}}$-related part of the SDE is $\widetilde{I}(q^2)$. Then, it is easy to recognize that the (sub) diagrams composing the other factor coincide precisely with those shown in the first line of Fig. 7.4, thus giving rise to $I(q^2)$ again. Thus we arrive at the following expression for the mass of the QB propagator,

$$\widetilde{m}^2(q^2) = g^2 I(q^2)\widetilde{I}(q^2). \tag{7.42}$$

At this point one may use the BQI of Eq. (7.39) to replace $\widetilde{m}^2(q^2)$ in favor of $m^2(q^2)$ on the lhs of Eq. (7.42), namely

$$m^2(q^2) = \frac{g^2 I(q^2)\widetilde{I}(q^2)}{1+G(q^2)}. \tag{7.43}$$

Note that this last substitution is legitimate, because the corresponding SDEs have been considered in their full, untrancated version (all diagrams kept); therefore the masses obtained from them are the same exact quantities that satisfy the BQI.

Then, direct comparison with Eq. (7.30) furnishes the central relation

$$\widetilde{I}(q^2) = [1 + G(q^2)]I(q^2). \tag{7.44}$$

Interestingly enough, this relation emerges as a self-consistency requirement between the results obtained from two formally different, but physically equivalent, versions of the gluon SDE.

Furthermore, due to the special structure of Eq. (7.40), where only the transition amplitude knows if the q-leg is quantum or background, the result Eq. (7.44) implies that the part $\widetilde{\mathcal{U}}$ of the pole vertices must also satisfy the same BQI, namely (suppressing indices)

$$\widetilde{\mathcal{U}} = [1 + G(q^2)]\mathcal{U}. \tag{7.45}$$

Finally, let us consider for completeness the SDE for the BB propagator connecting two background gluons, given by the expression

$$\widehat{\Delta}^{-1}(q^2)P_{\mu\nu}(q) = q^2 P_{\mu\nu}(q) + i\sum_{i=1}^{10}(a_i)_{\mu\nu}, \tag{7.46}$$

where the diagrams (a_i) appearing on the rhs of the equation are shown in Fig. 3.3, arranged again into individually transverse blocks.

Repeating the procedure of Fig. 7.7 for this last SDE, we see that, as in the QB case, the common quantity to be factored out from all diagrams is again $\widetilde{I}(q^2)$. Then, the corresponding sum of (sub) diagrams coincides precisely with those of Fig. 7.9, thus giving rise to another $\widetilde{I}(q^2)$. As a result, one obtains

$$\widehat{m}^2(q^2) = g^2\widetilde{I}^2(q^2). \tag{7.47}$$

It should be easy to verify at this point that the direct use of Eq. (7.39) and subsequent comparison with Eq. (7.30) [or with Eq. (7.42)], furnishes again the result of Eq. (7.44).

7.5 Three-gluon pole vertex

In the previous section the basic relations Eq. (7.44) and Eq. (7.45) have been derived at the level of the SDEs, by appealing to the general properties

of the massless bound state formalism and the BQIs relating the gluon propagators in the PT-BFM formalism. In the next two subsections we will derive the same relations from the closed form of the pole part of the Q^3 vertex and the BQ^2 vertex. Specifically, in the first subsection we derive the closed form of these vertices [83], while in the next we isolate their $\mathcal{U}$ parts and carry out a direct comparison.

7.5.1 Explicit construction

As has been explained in detail in the recent literature, in order to preserve the gauge invariance of the theory in the presence of masses, the pole part of the BQ^2 vertex must satisfy the following WI and STIs,

$$\begin{aligned}
q^\alpha \widetilde{V}_{\alpha\mu\nu}(q,r,p) &= m^2(r^2)P_{\mu\nu}(r) - m^2(p^2)P_{\mu\nu}(p),\\
r^\mu \widetilde{V}_{\alpha\mu\nu}(q,r,p) &= F(r^2)[m^2(p^2)P^\mu_\nu(p)\widetilde{H}_{\mu\alpha}(p,r,q) - \widetilde{m}^2(q^2)P^\mu_\alpha(q)H_{\mu\nu}(q,r,p)],\\
p^\nu \widetilde{V}_{\alpha\mu\nu}(q,r,p) &= F(p^2)[\widetilde{m}^2(q^2)P^\nu_\alpha(q)H_{\nu\mu}(q,p,r) - m^2(r^2)P^\nu_\mu(r)\widetilde{H}_{\nu\alpha}(r,p,q)].
\end{aligned} \tag{7.48}$$

The quantity $\widetilde{H}$ is given by the same diagrammatic representation as that of H, shown in Fig. 7.8, but with the incoming gluon field replaced by a background one.

In the pole part of the Q^3 vertex, the background leg q_α becomes quantum, and the Abelian-like WI [first in Eq. (7.48)] is replaced by an STI, namely

$$q^\alpha V_{\alpha\mu\nu}(q,r,p) = F(q^2)[m^2(r^2)P^\alpha_\mu(r)H_{\alpha\nu}(r,q,p) - m^2(p^2)P^\alpha_\nu(p)H_{\alpha\mu}(p,q,r)]. \tag{7.49}$$

The STIs with respect to the other two legs are those of Eq. (7.48), but with the "tilded" quantities replaced by conventional ones.

The explicit closed form of the two pole vertices in question, $\widetilde{V}$ and V, may be determined from the STIs they satisfy, and the requirement of complete longitudinality, *i.e.*, the condition Eq. (7.9). Specifically, opening up the transverse projectors in Eq. (7.9), one can write the entire vertex in terms of its own divergences,

$$\begin{aligned}
\widetilde{V}_{\alpha\mu\nu}(q,r,p) &= \frac{q_\alpha}{q^2}q^\beta\widetilde{V}_{\beta\mu\nu} + \frac{r_\mu}{r^2}r^\rho\widetilde{V}_{\alpha\rho\nu} + \frac{p_\nu}{p^2}p^\sigma\widetilde{V}_{\alpha\mu\sigma} - \frac{q_\alpha r_\mu}{q^2r^2}q^\beta r^\rho\widetilde{V}_{\beta\rho\nu}\\
&- \frac{q_\alpha p_\nu}{q^2p^2}q^\beta p^\sigma\widetilde{V}_{\beta\mu\sigma} - \frac{r_\mu p_\nu}{r^2p^2}r^\rho p^\sigma\widetilde{V}_{\alpha\rho\sigma} + \frac{q_\alpha r_\mu p_\nu}{q^2r^2p^2}q^\beta r^\rho p^\sigma\widetilde{V}_{\beta\rho\sigma}.
\end{aligned} \tag{7.50}$$

Note that the last term will not contribute because if we apply the STI's,

$$q^\beta r^\rho p^\sigma \widetilde{V}_{\beta\rho\sigma}(q,r,p) = 0. \tag{7.51}$$

So, using Eq. (7.48) to evaluate the various terms, and after a straightforward rearrangement, we obtain the following expression for the pole part of the BQ^2 vertex,

$$\begin{aligned}\widetilde{V}_{\alpha\mu\nu}(q,r,p) &= \frac{q_\alpha}{q^2}[m^2(r^2) - m^2(p^2)]P^\rho_\mu(r)P_{\rho\nu}(p) \\ &+ D(r^2)[m^2(p^2)P^\rho_\nu(p)\widetilde{H}_{\rho\alpha}(p,r,q) - \widetilde{m}^2(q^2)P^\rho_\alpha(q)P^\sigma_\nu(p)H_{\rho\sigma}(q,r,p)]r_\mu \\ &+ D(p^2)[\widetilde{m}^2(q^2)P^\rho_\alpha(q)H_{\rho\mu}(q,p,r) - m^2(r^2)P^\rho_\mu(r)\widetilde{H}_{\rho\alpha}(r,p,q)]p_\nu.\end{aligned} \tag{7.52}$$

Applying the same procedure, but using now the STIs of Eq. (7.49), together with the condition of Eq. (7.9), we derive the closed expression for the pole part of the Q^3 vertex,

$$\begin{aligned}V_{\alpha\mu\nu}(q,r,p) &= D(q^2)[m^2(r^2)H_{\rho\sigma}(r,q,p) - m^2(p^2)H_{\sigma\rho}(p,q,r)]P^\rho_\mu(r)P^\sigma_\nu(p)q_\alpha \\ &+ D(r^2)[m^2(p^2)P^\rho_\nu(p)H_{\rho\alpha}(p,r,q) - m^2(q^2)P^\rho_\alpha(q)P^\sigma_\nu(p)H_{\rho\sigma}(q,r,p)]r_\mu \\ &+ D(p^2)[m^2(q^2)P^\rho_\alpha(q)H_{\rho\mu}(q,p,r) - m^2(r^2)P^\rho_\mu(r)H_{\rho\alpha}(r,p,q)]p_\nu.\end{aligned} \tag{7.53}$$

Let us discuss next certain issues related to the self-consistency of the previous vertex construction. Notice that, in order to obtain expressions Eq. (7.52) and Eq. (7.53), one must apply sequentially the WI and the STIs. In doing so, the Bose symmetry of both vertices is no longer explicit, and the result obtained is not manifestly symmetric under the exchange of the quantum gluon legs. Furthermore, seemingly different expressions are obtained, depending on which of the two momenta acts first on $\widetilde{V}$ or V. However, if one imposes the simple requirement of algebraic commutativity between the WI and the STIs satisfied by the three-gluon vertex, the Bose symmetry becomes manifest. For example, using Eq. (7.52) we can see that the elementary requirement

$$q^\alpha r^\mu \widetilde{V}_{\alpha\mu\nu}(q,r,p) = r^\mu q^\alpha \widetilde{V}_{\alpha\mu\nu}(q,r,p), \tag{7.54}$$

gives raise to the following identity

$$F(r^2)P^\mu_\nu(p)q^\alpha \widetilde{H}_{\mu\alpha}(p,r,q) = -r_\mu P^\mu_\nu(p). \tag{7.55}$$

A similar identity is obtained by imposing the requirement of Eq. (7.54) at the level of V, namely

$$F(r^2)P^{\mu}_{\nu}(p)q^{\alpha}H_{\mu\alpha}(p,r,q) = -F(q^2)P^{\mu}_{\nu}(p)r^{\alpha}H_{\mu\alpha}(p,q,r). \tag{7.56}$$

Quite remarkably, the identities Eq. (7.55) and Eq. (7.56) are a direct consequence of the WI and the STI that the kernels H and $\widetilde{H}$ satisfy, when they are contracted with the momentum of the background or quantum gluon leg, namely [65]

$$\begin{aligned} q^{\alpha}\widetilde{H}_{\mu\alpha}(p,r,q) &= -p_{\mu}F^{-1}(p^2) - r_{\mu}F^{-1}(r^2), \\ q^{\alpha}H_{\mu\alpha}(p,r,q) &= -F(q^2)[p_{\mu}F^{-1}(p^2)C(p,q,r) + r^{\alpha}F^{-1}(r^2)H_{\mu\alpha}(p,q,r)], \end{aligned} \tag{7.57}$$

where $C(q,p,r)$ is the auxiliary function that characterizes the four-ghost

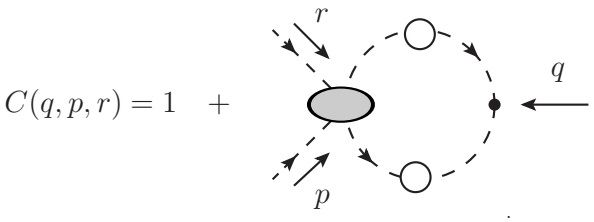

Fig. 7.10: Diagrammatic representation of the auxiliary function $C(q,p,r)$.

kernel (see Fig. 7.10). Indeed, use of Eq. (7.57) into Eq. (7.55) and Eq. (7.56), respectively, leads to a trivial identity. Conversely, one may actually derive Eq. (7.57) from Eq. (7.55) and Eq. (7.56); for example, starting with Eq. (7.55), and using also the identities [65]

$$\begin{aligned} p^{\mu}\widetilde{H}_{\mu\alpha}(p,r,q) &= r_{\alpha}F^{-1}(r^2) - \widetilde{\Gamma}_{\alpha}(q,p,r), \\ q^{\alpha}\widetilde{\Gamma}_{\alpha}(q,p,r) &= p^2F^{-1}(p^2) - r^2F^{-1}(r^2), \end{aligned} \tag{7.58}$$

one can easily reproduce Eq. (7.57).

Evidently, these constraints allow us to cast the pole part of the BQ^2-vertex into a manifestly Bose symmetric form with respect to the quantum legs,

$$\widetilde{V}_{\alpha\mu\nu}(q,r,p) = \frac{q_{\alpha}}{q^2}[m^2(r^2) - m^2(p^2)]P^{\rho}_{\mu}(r)P_{\rho\nu}(p) + \widetilde{S}_{\alpha\mu\nu}(q,r,p) - \widetilde{S}_{\alpha\nu\mu}(q,p,r), \tag{7.59}$$

with

$$\begin{aligned}\widetilde{S}_{\alpha\mu\nu}(q,r,p) &= D(r^2)m^2(p^2)P^{\rho}_{\nu}(p)\widetilde{H}_{\rho\alpha}(p,r,q)r_{\mu} \\ &- \frac{r_{\mu}}{2}D(r^2)\widetilde{m}^2(q^2)P^{\rho}_{\alpha}(q)[g^{\sigma}_{\nu}+P^{\sigma}_{\nu}(p)]H_{\rho\sigma}(q,r,p).\end{aligned} \tag{7.60}$$

Finally, for the pole part of the Q^3 vertex, the Bose symmetric expression reads

$$V_{\alpha\mu\nu}(q,r,p) = S_{\alpha\mu\nu}(q,r,p) - S_{\mu\alpha\nu}(r,q,p) - S_{\nu\mu\alpha}(p,r,q), \tag{7.61}$$

with

$$\begin{aligned}S_{\alpha\mu\nu}(q,r,p) &= \frac{q_{\alpha}}{2}D(q^2)m^2(r^2)P^{\rho}_{\mu}(r)[g^{\sigma}_{\nu}+P^{\sigma}_{\nu}(p)]H_{\rho\sigma}(r,q,p) \\ &- \frac{q_{\alpha}}{2}D(q^2)m^2(p^2)P^{\rho}_{\nu}(p)[g^{\sigma}_{\mu}+P^{\sigma}_{\mu}(r)]H_{\rho\sigma}(p,q,r).\end{aligned} \tag{7.62}$$

Note the fact that, as it should be, setting in Eqs.(7.59)-(7.61) the tree-level values $F = 1$ and $H_{\mu\nu} = g_{\mu\nu}$ for the ghost dressing function and the gluon-ghost kernel, respectively, one recovers the ansatz for the "abelianized" three-gluon vertex employed in [84].

7.5.2 Transition BQI from the pole vertices

We next identify from the explicit expressions for the BQ^2 and Q^3 pole vertices the terms $\widetilde{\mathcal{U}}$ and $\mathcal{U}$. To that end, and in complete accordance with the discussion presented in subsection 7.1.2, we apply a kinematic and a dynamical criterion, namely (i) collect all terms containing the tensorial structure q_{α}/q^2, and (ii) discard all terms that, when inserted into the SDE of the gluon self-energy, do not survive the $q \to 0$ limit. The final objective is to infer the validity of the BQI of Eq. (7.45), connecting $\widetilde{\mathcal{U}}$ and $\mathcal{U}$.

Applying criterion (i), and denoting by $\widetilde{U}$ and U the resulting expressions, it is straightforward to obtain from Eq. (7.59)

$$\begin{aligned}\widetilde{U}_{\alpha\mu\nu}(q,r,p) &= \frac{q_{\alpha}}{q^2}\Big\{m^2(r^2)P^{\rho}_{\mu}(r)P_{\rho\nu}(p) \\ &- \frac{r_{\mu}}{2}D(r^2)\widetilde{m}^2(q^2)[g^{\rho}_{\nu}+P^{\rho}_{\nu}(p)]\Gamma_{\rho}(p,q,r)\Big\} - \binom{r\leftrightarrow p}{\mu\leftrightarrow\nu},\end{aligned} \tag{7.63}$$

where Eq. (7.36) has been applied in order to relate the contractions of the auxiliary ghost functions H with the conventional gluon-ghost vertices Γ_ρ, and $\binom{r\leftrightarrow p}{\mu\leftrightarrow\nu}$ is obtained from the term that is shown explicitly after these exchanges. In addition, we get for the $\widetilde{R}$ part of the vertex

$$\begin{aligned}\widetilde{R}_{\alpha\mu\nu}(q,r,p) &= \frac{r_\mu}{r^2}F(r^2)\Big\{m^2(p^2)P^\rho_\nu(p)\widetilde{H}_{\rho\alpha}(p,r,q)\\ &- \frac{1}{2}\widetilde{m}^2(q^2)[g^\rho_\nu + P^\rho_\nu(p)]H_{\alpha\rho}(q,r,p)\Big\} - \binom{r\leftrightarrow p}{\mu\leftrightarrow\nu}.\end{aligned} \tag{7.64}$$

Similarly, from Eq. (7.61), and using the special STI Eq. (7.57), we obtain

$$\begin{aligned}U_{\alpha\mu\nu}(q,r,p) &= \frac{q_\alpha}{q^2}\Big\{F(q^2)m^2(r^2)H_{\rho\sigma}(r,q,p)P^\rho_\mu(r)P^\sigma_\nu(p)\\ &- \frac{r_\mu}{2}D(r^2)m^2(q^2)[g^\rho_\nu + P^\rho_\nu(p)]\Gamma_\rho(p,q,r)\Big\} - \binom{r\leftrightarrow p}{\mu\leftrightarrow\nu},\end{aligned} \tag{7.65}$$

and

$$\begin{aligned}R_{\alpha\mu\nu}(q,r,p) &= \frac{r_\mu}{r^2}F(r^2)\Big\{m^2(p^2)P^\rho_\nu(p)H_{\rho\alpha}(p,r,q)\\ &- \frac{1}{2}m^2(q^2)[g^\rho_\nu + P^\rho_\nu(p)]H_{\alpha\rho}(q,r,p)\Big\} - \binom{r\leftrightarrow p}{\mu\leftrightarrow\nu}.\end{aligned} \tag{7.66}$$

Let us now relax for a moment criterion (ii), and assume that $\widetilde{U}=\widetilde{\mathcal{U}}$ and $U=\mathcal{U}$, as well as $\widetilde{R}=\widetilde{\mathcal{R}}$ and $R=\mathcal{R}$. Let us further use Eq. (7.39), and substitute $m^2(q^2)=\widetilde{m}^2(q^2)[1+G(q^2)]^{-1}$ into Eq. (7.65). Then, employing Eq. (7.38) valid in the Landau gauge, dropping $L(q^2)$ since $L(0)=0$ [thus applying effectively criterion (ii)], it is relatively easy to establish that the (would-be) $\widetilde{\mathcal{U}}$ and $\mathcal{U}$ fail to satisfy Eq. (7.45) due to the presence of a very particular term. Specifically, if $H_{\rho\sigma}\to g_{\rho\sigma}$ in the first line of Eq. (7.65), then the BQI of Eq. (7.45) would be satisfied.

Therefore, write the $H_{\rho\sigma}(r,q,p)$ in Eq. (7.65) as

$$H_{\rho\sigma}(r,q,p) = g_{\rho\sigma} + H^Q_{\rho\sigma}(r,q,p), \tag{7.67}$$

where the $g_{\rho\sigma}$ corresponds to the tree-level value of $H_{\rho\sigma}$, and $H^Q_{\rho\sigma}$ contains the all-order quantum corrections; an exactly analogous expression holds

for $H_{\sigma\rho}(p,q,r)$, with $p \leftrightarrow r$. Note that in both cases the momentum q is carried by the ghost leg, see Fig. 7.11. Then, if we define the "genuine" $\mathcal{U}$ part as

$$\mathcal{U}_{\alpha\mu\nu}(q,r,p) = U_{\alpha\mu\nu}(q,r,p) - \mathcal{U}'_{\alpha\mu\nu}(q,r,p), \tag{7.68}$$

with

$$\mathcal{U}'_{\alpha\mu\nu}(q,r,p) = \frac{q_\alpha}{q^2} F(q^2) m^2(r^2) P^\rho_\mu(r) P^\sigma_\nu(p) H^Q_{\rho\sigma}(r,q,p) - \begin{pmatrix} r \leftrightarrow p \\ \mu \leftrightarrow \nu \end{pmatrix}. \tag{7.69}$$

it is clear that

$$\widetilde{\mathcal{U}}_{\alpha\mu\nu}(q,r,p) = [1 + G(q^2)]\mathcal{U}_{\alpha\mu\nu}(q,r,p). \tag{7.70}$$

The real justification for discarding $\mathcal{U}'_{\alpha\mu\nu}$ from $U_{\alpha\mu\nu}(q,r,p)$ is provided precisely by reinstating criterion (ii): the discarded term does not survive the limit $q \to 0$ when inserted into the corresponding gluon SDE.

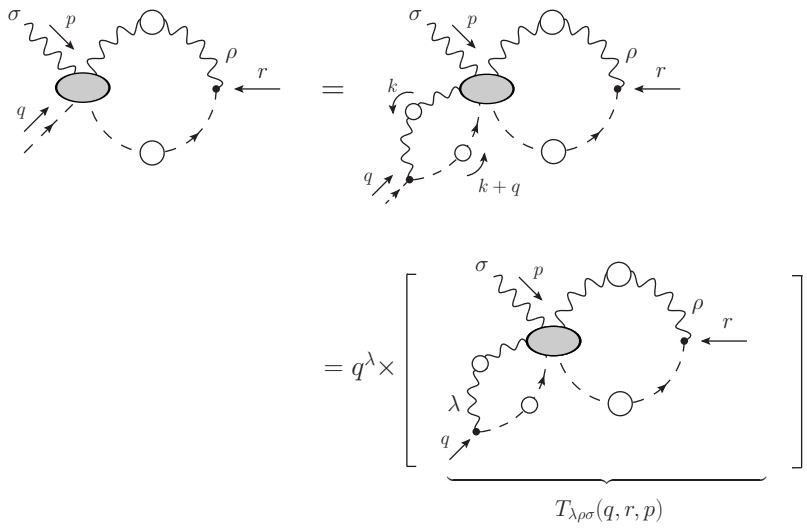

Fig. 7.11: Diagrammatic equality which allows to factorize out the momentum of the incoming ghost leg in the quantum corrections of the auxiliary ghost function H^Q.

To demonstrate that this is indeed so, note that in the Landau gauge $(k+q)^\lambda \Delta_{\lambda\sigma}(k) = q^\lambda \Delta_{\lambda\sigma}(k)$, and the momentum of the incoming ghost leg

factorizes out of the loop integrals. This observation allows us to cast H^Q in the form

$$H^Q_{\rho\sigma}(r,q,p) = q^\lambda T_{\lambda\rho\sigma}(q,r,p). \tag{7.71}$$

where T simply represents the rest of the diagram (see Fig. 7.11). If we assume now that T has a finite (non-divergent) value in the limit $q \to 0$, then

$$\lim_{q\to 0} H^Q_{\rho\sigma}(r,q,p) = \lim_{q\to 0} q^\lambda T_{\lambda\rho\sigma}(q,r,p) = 0. \tag{7.72}$$

So, using Eq. (7.71), the term given in Eq. (7.69) becomes

$$\mathcal{U}'_{\alpha\mu\nu}(q,r,p) = \frac{q_\alpha q^\lambda}{q^2} F(q^2) m^2(r^2) P^\rho_\mu(r) P^\sigma_\nu(p) T_{\lambda\rho\sigma}(q,r,p) - \begin{pmatrix} r \leftrightarrow p \\ \mu \leftrightarrow \nu \end{pmatrix}. \tag{7.73}$$

When $\mathcal{U}'_{\alpha\mu\nu}$ is written in this form, it is clear that its pole $1/q^2$ is actually compensated by $q_\alpha q^\lambda$, while the remaining terms cancel themselves when $r = -p$. Therefore, the entire term $\mathcal{U}'_{\alpha\mu\nu}$ vanishes as $q \to 0$, and should not be included in the $\mathcal{U}$ part of the Q^3 pole vertex.

Finally, returning to the identification $\widetilde{U} = \widetilde{\mathcal{U}}$, note that the expression in Eq. (7.63) does not get modified by the application of criterion (ii), because the above argument of discarding H^Q does not apply in this case. The reason for that is simply the channeling of the momenta in $H_{\rho\sigma}(q,r,p)$ and $H_{\rho\sigma}(q,p,r)$ (encoded into the gluon-ghost vertices Γ_ρ) is different from that of $H_{\rho\sigma}(r,q,p)$; the momentum entering in the ghost leg is no longer q, but rather r or p, and the corresponding H^Qs do not satisfy Eq. (7.72).

Let us now cast $\mathcal{U}_{\alpha\mu\nu}(q,r,p)$ and $\widetilde{\mathcal{U}}_{\alpha\mu\nu}(q,r,p)$ into their canonical form of Eq. (7.25) and Eq. (7.40), respectively, namely

$$\begin{aligned} \mathcal{U}_{\alpha\mu\nu}(q,r,p) &= -\frac{q_\alpha}{q^2} I(q^2) B_{\mu\nu}(q,r,p), \\ \widetilde{\mathcal{U}}_{\alpha\mu\nu}(q,r,p) &= -\frac{q_\alpha}{q^2} \widetilde{I}(q^2) B_{\mu\nu}(q,r,p); \end{aligned} \tag{7.74}$$

the minus sign comes from the extra imaginary factor appearing in the Feynman rule of the effective vertex, see Fig.7.4. The important point to recognize is that $B_{\mu\nu}(q,r,p)$ is common to both vertices, because the legs carrying r and p are quantum ones, and the difference induced due to the quantum or background nature of the leg carrying momentum q is entirely encoded into the form of the corresponding transition amplitudes, $I(q^2)$ and $\widetilde{I}(q^2)$, respectively. Then, Eq. (7.74) and Eq. (7.70) imply directly the validity of Eq. (7.44).

7.6 Diagrammatic demonstration of the BQI

It is well-known that the BQIs relating the conventional and BFM Green's functions are formally obtained by resorting to the powerful BV formalism. On the other hand, the PT (or its generalized version [24]) furnishes an equivalent diagrammatic derivation, which makes extensive use of the STIs satisfied by the kernels appearing in the SDEs of the Green's functions in question. In the previous sections the BQI relating the transition amplitudes $I(q^2)$ and $\widetilde{I}(q^2)$ has been obtained as a self-consistency requirement between two SDEs and from the corresponding BQI relating $\mathcal{U}$ and $\widetilde{\mathcal{U}}$ (sections 7.4 and 7.5, respectively). The objective of this section is to carry out a PT-guided demonstration of this particular BQI, through the systematic conversion of the set of Feynman diagrams defining one transition amplitude into the set defining the other (shown in Figs. 7.4 and 7.9). Essentially this conversion proceeds by allowing the longitudinal (pinching) momenta contained in the tree-level three-gluon vertex [graph $(\widetilde{d}_1)$] to act on the adjacent kernel; therefore, as we will see, a crucial ingredient for completing this construction is the knowledge of the STI satisfied by the effective vertex $B_{\mu\nu}$. In addition, the requirement that the BQI be diagrammatically exact imposes a strong constraint on the set of ghost diagrams that contribute to the transition amplitude, which may be translated (under mild assumptions) into the vanishing of the corresponding subset of B vertices.

Let us start by considering the diagram $(\widetilde{d}_1)$ of the background transition amplitude, shown in Fig. 7.12, whose contribution is given by

$$(\widetilde{d}_1)_\alpha = \frac{i}{2} C_A \int_k \widetilde{\Gamma}^{(0)}_{\alpha\mu\nu} \Delta^{\mu\sigma}(k+q) \Delta^{\nu\rho}(k) B_{\rho\sigma}. \tag{7.75}$$

In order to avoid notational clutter we will suppress the arguments of the momenta in the vertices, which can be easily recovered from the figures. We know that the tree-level vertex $\widetilde{\Gamma}^{(0)}_{\alpha\mu\nu}$ contains terms which are proportional to ξ^{-1}, so that one cannot take directly the limit $\xi = 0$ to work in the Landau gauge. Specifically, the tree-level part of the BQ^2 vertex is given by

$$\widetilde{\Gamma}^{(0)}_{\alpha\mu\nu}(q, -k-q, k) = \Gamma^{(0)}_{\alpha\mu\nu}(q, -k-q, k) - \frac{1}{\xi}\Gamma^{P}_{\alpha\mu\nu}(q, -k-, k), \tag{7.76}$$

where the purely longitudinal "pinch part" Γ^P reads

$$\Gamma^{P}_{\alpha\mu\nu}(q, -k-q, k) = g_{\alpha\mu} k_\nu + g_{\alpha\nu}(k+q)_\mu, \tag{7.77}$$

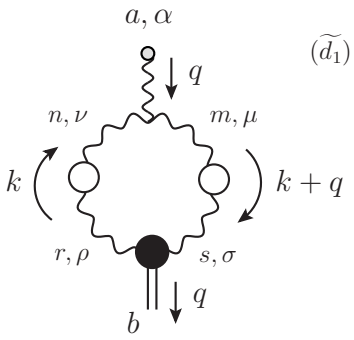

Fig. 7.12: One-loop dressed gluonic contribution to the background transition amplitude. The diagram has a symmetry factor 1/2 and we will factorize out $g\delta^{ab}$.

and

$$\Gamma^{(0)}_{\alpha\mu\nu}(q,-k-q,k) = -(2k+q)_\alpha g_{\mu\nu} + (k-q)_\mu g_{\alpha\nu} + (2q+k)_\nu g_{\alpha\mu} \quad (7.78)$$

is the tree-level value of the conventional three-gluon vertex. Using then the decomposition Eq. (7.76), we obtain from Eq. (7.75)

$$(\widetilde{d_1})_\alpha = (d_1)_\alpha - \frac{i}{2\xi} C_A \int_k \Gamma^P_{\alpha\mu\nu} \Delta^{\mu\sigma}(k+q) \Delta^{\nu\rho}(k) B_{\rho\sigma}. \quad (7.79)$$

Now, after the shifts $k+q \mapsto k$ and $k \mapsto -k$, and applying the antisymmetry property of the effective vertex, namely $B_{\rho\sigma} = -B_{\sigma\rho}$, the two contributions coming from the pinch part of the vertex in Eq. (7.79) sum up and cancel the symmetry factor, giving the result

$$(\widetilde{d_1})_\alpha = (d_1)_\alpha - \frac{i}{\xi} C_A \int_k k_\nu \Delta^{\nu\rho}(k) \Delta^\sigma_\alpha(k+q) B_{\rho\sigma}. \quad (7.80)$$

Therefore, employing the identity

$$\frac{1}{\xi} k_\nu \Delta^{\nu\rho}(k) = \frac{k^\rho}{k^2}, \quad (7.81)$$

the ξ^{-1} term cancels, and we can project Eq. (7.80) to the Landau gauge ($\xi = 0$)

$$(\widetilde{d_1})_\alpha = (d_1)_\alpha - i C_A \int_k \frac{k^\rho}{k^2} \Delta^\sigma_\alpha(k+q) B_{\rho\sigma}, \quad (7.82)$$

where the gluon propagator assumes its totally transverse form, *i.e.*, $\Delta_{\mu\nu}(k) = \Delta(k^2)P_{\mu\nu}(k)$.

At this point, in order to evaluate the extra term which appears in Eq. (7.82) when diagram $(\widetilde{d}_1)$ is projected to the Landau gauge, the knowledge of the STI satisfied by the effective vertex $B_{\rho\sigma}$ is required. Observe then that, if we compare Eq. (7.63) with Eq. (7.74), the following structure can be identified with the effective vertex $B_{\mu\nu}$,

$$\begin{aligned}\widetilde{I}(q^2)B_{\mu\nu}(q,r,p) &= -m^2(r^2)P^{\rho}_{\mu}(r)P_{\rho\nu}(p) \\ &+ \frac{r_\mu}{2}D(r^2)\widetilde{m}^2(q^2)[g^{\rho}_{\nu}+P^{\rho}_{\nu}(p)]\Gamma_{\rho}(p,q,r) - \binom{r\leftrightarrow p}{\mu\leftrightarrow\nu}.\end{aligned} \tag{7.83}$$

Now, contracting Eq. (7.83) with respect to the momentum r^μ, and breaking the transverse projector $P^{\rho}_{\nu}(p)$, we get

$$\begin{aligned}\widetilde{I}(q^2)r^{\mu}B_{\mu\nu}(q,r,p) &= F(r^2)\widetilde{m}^2(q^2)\Gamma_{\nu}(p,q,r) \\ &- \frac{p_\nu}{2p^2}\widetilde{m}^2(q^2)[F(r^2)p^{\rho}\Gamma_{\rho}(p,q,r)+F(p^2)r^{\rho}\Gamma_{\rho}(r,q,p)].\end{aligned} \tag{7.84}$$

Using then Eq. (7.36) together with the STI Eq. (7.57) satisfied by the gluon-ghost kernel, we can evaluate

$$\begin{aligned}F(r^2)p^{\rho}\Gamma_{\rho}(p,q,r) &= -F(r^2)p^{\rho}q^{\sigma}H_{\sigma\rho}(q,r,p) \\ &= F(r^2)F(p^2)D^{-1}(q^2)C(q,p,r) - F(p^2)r^{\rho}\Gamma_{\rho}(r,q,p).\end{aligned} \tag{7.85}$$

Applying this result and relating the mass of the mixed QB propagator with the transition amplitude through Eq. (7.42), we obtain from Eq. (7.84) the desired STI for the effective vertex $B_{\mu\nu}$,

$$r^{\mu}B_{\mu\nu}(q,r,p) = g^2I(q^2)F(r^2)\left[\Gamma_{\nu}(p,q,r) - \frac{1}{2}D(p^2)D^{-1}(q^2)C(q,p,r)p_{\nu}\right]. \tag{7.86}$$

Interestingly enough we observe that, in the Landau gauge, the four ghost kernel $C(q,p,r)$ will not contribute to the transition amplitude because it appears with the momentum p_ν, which is canceled by the transverse projector of the gluon propagator in Eq. (7.82).

Therefore, applying the STI Eq. (7.86) adapted to our kinematical configuration, *i.e.*, $r = -k$ and $p = k + q$, expression Eq. (7.82) becomes

$$\begin{aligned}(\widetilde{d_1})_\alpha &= (d_1)_\alpha + ig^2 C_A I(q^2) \int_k \Delta^\sigma_\alpha(k+q) D(k) \Gamma_\sigma \\ &= (d_1)_\alpha - ig^2 C_A I(q^2) q^\lambda \int_k \Delta^\sigma_\alpha(k+q) D(k) H_{\lambda\sigma}, \qquad (7.87)\end{aligned}$$

where in the second line Eq. (7.36) has been used to relate the gluon-ghost vertex with the contraction of the auxiliary ghost function. Looking at Eq. (7.87) one may recognize the auxiliary two-point function Eq. (7.34), and we get

$$(\widetilde{d_1})_\alpha = (d_1)_\alpha + I(q^2) q^\lambda \Lambda_{\alpha\lambda}(q) = (d_1)_\alpha + [G(q^2) + L(q^2)] I_\alpha(q). \qquad (7.88)$$

Finally, since $L(0) = 0$, we can drop this term and the following result is obtained

$$(\widetilde{d_1})_\alpha = (d_1)_\alpha + G(q^2) I_\alpha(q). \qquad (7.89)$$

Observe then that diagrams (d_3) and (d_4) in Fig.7.4 containing gluon loops can be converted automatically to background ones and be added to both sides of Eq. (7.89) in order to complete the transition amplitude. However, diagrams containing ghost loops only can be added if they satisfy the constraint

$$(d_2)_\alpha = [(\widetilde{d_2}) + (\widetilde{d_5}) + (\widetilde{d_8})]_\alpha. \qquad (7.90)$$

Note the fact that diagrams $(\widetilde{d_6})$ and $(\widetilde{d_7})$ are zero in the Landau gauge. So, if Eq. (7.90) holds, we can complete the transition amplitudes in both sides of Eq. (7.89) and obtain the BQI Eq. (7.44).

Let us next transform the diagrammatic constraint Eq. (7.90) into an integral identity for the effective vertices mixing the massless bound-state with ghosts, shown in Fig. 7.13. In the formulas that follow, color factors are shown explicitly, while the arguments of the momenta in the vertices are omitted as before. Consider first the diagram $(\widetilde{d_2})$, given by

$$(\widetilde{d_2})^{ab}_\alpha = -igC_A \delta^{ab} \int_k \widetilde{\Gamma}^{(0)}_\alpha D(k) D(k+q) B. \qquad (7.91)$$

Now, diagram $(\widetilde{d_5})$ gives the following contribution to the background transition amplitude,

$$(\widetilde{d_5})^{ab}_\alpha = g^3 C_A^2 \delta^{ab} \int_k \widetilde{\Gamma}^{(0)}_{\alpha\mu} D(k) D(k+q) B \int_l D(k+l) \Delta^{\mu\nu}(l) \Gamma_\nu. \qquad (7.92)$$

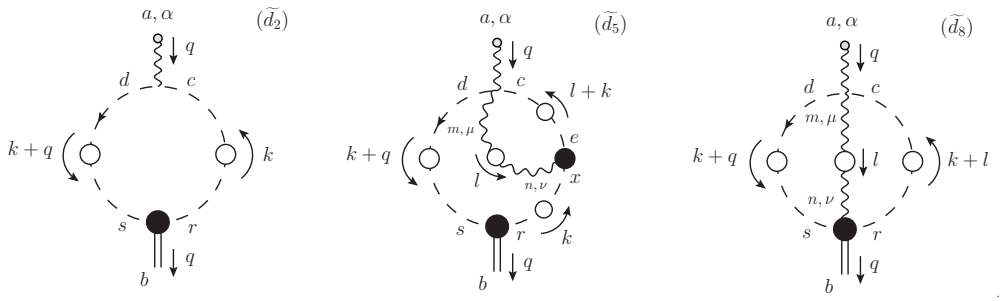

Fig. 7.13: Configuration for the diagrams of the BFM transition amplitude containing ghost loops. Observe that diagrams $(\widetilde{d}_6)$ and $(\widetilde{d}_7)$ appearing in Fig. 7.9 are zero in the Landau gauge.

Observe that in the Landau gauge, the internal gluon-ghost vertex Γ_ν cannot develop a pole part, since it should be longitudinally coupled and thus cancelled by the transverse projector of the gluon propagator. Therefore, only the regular part of this vertex survives in the diagram. So, using the conventional SDE of the ghost propagator written in the form,

$$g^2 C_A D(k) \int_l D(k+l)\Delta^{\mu\nu}(l)\Gamma_\nu = ik_\alpha[D(k) - D^{(0)}(k)], \tag{7.93}$$

we obtain from Eq. (7.92) the result

$$(\widetilde{d}_5)^{ab}_\alpha = igC_A\delta^{ab}\int_k k_\alpha[D(k) - D^{(0)}(k)]D(k+q)B. \tag{7.94}$$

The last diagram in Fig. 7.13 gives the contribution,

$$(\widetilde{d}_8)^{ab}_\alpha = g^2 f^{adx} f^{xcm}\int_k\int_l D(k+q)D(k+l)\Delta^\nu_\alpha(l)B^{bcmd}_\nu. \tag{7.95}$$

Finally, diagram (d_2) is obtained from the same configuration as diagram $(\widetilde{d}_2)$, but with the BFM gluon-ghost vertex replaced by a conventional one, *i.e.*,

$$(d_2)^{ab}_\alpha = -igC_A\delta^{ab}\int_k \Gamma^{(0)}_\alpha D(k)D(k+q)B. \tag{7.96}$$

Using all of these results we obtain from the constraint Eq. (7.90) the following integral identity which relates the effective vertices mixing the

massless excitation with ghosts,

$$iC_A\delta^{ab}\int_k \frac{k_\alpha}{k^2}D(k+q)B = gf^{adx}f^{xcm}\int_k\int_l D(k+q)D(k+l)\Delta^\nu_\alpha(l)B^{bcmd}_\nu. \tag{7.97}$$

The formalism give us this integral identity and, to go further, one should look at the Bethe-Salpeter equations satisfied by these effective vertices. However we can argue, invoking lattice results, that these effective vertices are zero. Consider then that we write the full BFM gluon-ghost vertex as the sum of a regular part and a pole part, like in Eq. (7.8),

$$\widetilde{\Gamma}'_\alpha(q,r,p) = \widetilde{\Gamma}_\alpha(q,r,p) + \widetilde{V}_\alpha(q,r,p). \tag{7.98}$$

It is known that the regular part of this vertex satisfies the following abelian-like WI,

$$q^\alpha\widetilde{\Gamma}_\alpha(q,r,p) = D^{-1}(r^2) - D^{-1}(p^2). \tag{7.99}$$

So, if we suppose that the pole part of this vertex triggers the Schwinger mechanism and generates in the ghost propagator and additional term $f(q^2)$, which is a deviation with respect to the massless ghost propagator, then the pole part must satisfy the following WI in order to preserve gauge invariance,

$$q^\alpha\widetilde{V}_\alpha(q,r,p) = f(p^2) - f(r^2). \tag{7.100}$$

If we solve this WI allowing the existence of a massless pole in the q-channel and also satisfying the totally longitudinally coupled condition

$$P^\beta_\alpha(q)\widetilde{V}_\beta(q,r,p) = 0, \tag{7.101}$$

we find the following expression for the pole part of the BFM gluon-ghost vertex

$$\widetilde{V}_\alpha(q,r,p) = \frac{q_\alpha}{q^2}[f(p^2) - f(r^2)]. \tag{7.102}$$

Note that this pole vertex only contains $\widetilde{\mathcal{U}}$ part and has not $\widetilde{\mathcal{R}}$ part. So, using the corresponding expression Eq. (7.40) for this vertex

$$\widetilde{V}_\alpha(q,r,p) = -\frac{q_\alpha}{q^2}\widetilde{I}(q^2)B(q,r,p), \tag{7.103}$$

and equating with Eq. (7.102), we obtain a relation between the effective vertex B and the mass-like term in the ghost propagator

$$\widetilde{I}(q^2)B(q,r,p) = f(r^2) - f(p^2). \tag{7.104}$$

Now, lattice results tell us that the ghost propagator in the Landau gauge behaves like a massless propagator, which means that $f = 0$. Therefore, since the transition amplitude is not zero, result Eq. (7.104) indicate us that $B = 0$. This is consistent with the integral identity Eq. (7.97) if we set $B_\nu = 0$. So, with this argument, we arrive to the conclusion that we can put to zero the effective vertices with ghost legs.

7.7 A decisive self-consistency check.

In this section we derive the full expression for the transition amplitude. Once obtained it, we show that the mass equation derived from the PT-BFM formalism can be reproduced from the full expression of the transition amplitude, providing a decisive self-consistency check and showing the compatibility and complementarity between the PT-BFM formalism and the bound-state formalism.

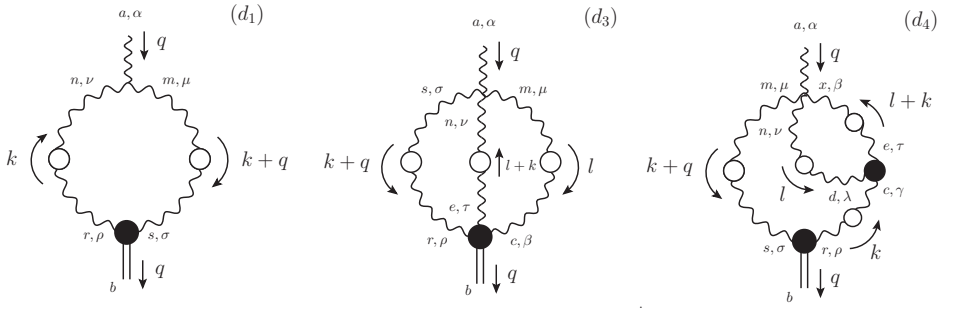

Fig. 7.14: Configuration for the diagrams of the transition amplitude containing gluon loops. The symmetry factors for the diagrams are $S(d_1, d_3, d_4) = (1/2, 1/6, 1/2)$ and we will factorize $g\delta^{ab}$.

According to the analysis of the previous section we have concluded that diagrams with ghost loops do not contribute to the transition amplitude. Furthermore, one may demonstrate that diagram (d_3) in Fig. 7.14, which contains the effective vertex $B_{\rho\tau\beta}$ mixing three quantum gluons with the bound state, is also zero in the Landau gauge. Effectively, with the configuration shown in Fig. 7.14, we can write down the contribution of this diagram,

$$(d_3)^{ab}_\alpha = \frac{1}{6}\int_k \int_l \Gamma^{(0)amns}_{\alpha\mu\nu\sigma} \Delta^{\sigma\rho}_{sr}(k+q)\Delta^{\nu\tau}_{ne}(l+k)\Delta^{\mu\beta}_{mc}(l)B^{brec}_{\rho\tau\beta}. \qquad (7.105)$$

As in the preceding sections, the arguments of the momenta in the vertices have been suppressed. Observe that, in order to evaluate this diagram in the Landau gauge, one should know how three transverse projectors act over the effective vertex $B_{\rho\tau\beta}$. Consider then the decomposition Eq. (7.21) for the BQ^3 pole vertex,

$$\widetilde{V}_{\lambda\rho\tau\beta}(q,r,p,l) = \widetilde{\mathcal{U}}_{\lambda\rho\tau\beta}(q,r,p,l) + \widetilde{\mathcal{R}}_{\lambda\rho\tau\beta}(q,r,p,l), \tag{7.106}$$

where, according with the discussion carry out in Section 7.1, the $\widetilde{\mathcal{R}}$ part of the vertex satisfies the transversality condition

$$P^{\sigma\rho}(r)P^{\nu\tau}(p)P^{\mu\beta}(l)\widetilde{\mathcal{R}}_{\lambda\rho\tau\beta}(q,r,p,l) = 0. \tag{7.107}$$

Thus, when Eq. (7.9) is applied for the case of the BQ^3 pole vertex, namely, four transverse projectors cancelling the vertex, we obtain from Eq. (7.106) the following result

$$\begin{aligned} P^{\sigma\rho}(r)P^{\nu\tau}(p)P^{\mu\beta}(l)\widetilde{\mathcal{U}}_{\alpha\rho\tau\beta}(q,r,p,l) &= \frac{q_\alpha}{q^2}P^{\sigma\rho}(r)P^{\nu\tau}(p)P^{\mu\beta}(l) \\ &\times\ q^\lambda \widetilde{V}_{\lambda\rho\tau\beta}(q,r,p,l). \end{aligned} \tag{7.108}$$

On the other hand Eq. (7.40) becomes for the $\widetilde{\mathcal{U}}$ part of this pole vertex,

$$\widetilde{\mathcal{U}}_{\alpha\rho\tau\beta}(q,r,p,l) = ig\frac{q_\alpha}{q^2}\widetilde{I}(q^2)B_{\rho\tau\beta}(q,r,p,l). \tag{7.109}$$

Therefore, applying three transverse projectors on Eq. (7.109) and equating the result with Eq. (7.108) we can relate the effective vertex $B_{\mu\nu\sigma}$ with the WI satisfied by the BQ^3 pole vertex,

$$\begin{aligned} ig\widetilde{I}(q^2)P^{\sigma\rho}(r)P^{\nu\tau}(p)P^{\mu\beta}(l)B_{\rho\tau\beta}(q,r,p,l) &= P^{\sigma\rho}(r)P^{\nu\tau}(p)P^{\mu\beta}(l) \\ &\times\ q^\lambda \widetilde{V}_{\lambda\rho\tau\beta}(q,r,p,l). \end{aligned} \tag{7.110}$$

Once the connection between the effective vertex $B_{\rho\tau\beta}$ and the WI satisfied by the BQ^3 pole vertex has been established through Eq. (7.110), following the same procedure outlined in Chapter 6 (see subsection 6.3.2), one arrives to the conclussion that the diagram (d_3) is zero.

So, the full transition amplitude will be given in the Landau gauge solely by the sum of diagrams (d_1) and (d_4). Thus, applying the conventions of Fig. 7.14, we obtain for diagram (d_1) the expression,

$$(d_1)_\alpha = \frac{i}{2}C_A\int_k \Gamma^{(0)}_{\alpha\mu\nu}\Delta^{\mu\sigma}(k+q)\Delta^{\nu\rho}(k)B_{\rho\sigma}. \tag{7.111}$$

One observes that the above integral has one free Lorentz index, which only can be saturated by the external momentum q. So, using the elementary WI for the tree-level three-gluon vertex,

$$q^\lambda \Gamma^{(0)}_{\lambda\mu\nu}(q,-k-q,k) = k^2 P_{\mu\nu}(k) - (k+q)^2 P_{\mu\nu}(k+q), \tag{7.112}$$

and after the appropriate shifts in the integrated momentum, we deduce in the Landau gauge the result,

$$(d_1)_\alpha = \frac{q_\alpha}{q^2} q^\lambda (d_1)_\lambda = iC_A \frac{q_\alpha}{q^2} \int_k k^2 \Delta^\rho_\mu(k) \Delta^{\mu\sigma}(k+q) B_{\rho\sigma}. \tag{7.113}$$

Now, diagram (d_4) contains the tree-level four-gluon vertex $\Gamma^{(0)}_{\alpha\mu\nu\beta}$. After the color algebra and using the standard Feynman rule for this vertex, we obtain for the prefactor of the diagram,

$$\frac{i}{2} g f^{bcm} f^{cxn} \Gamma^{(0)amnx}_{\alpha\mu\nu\beta} = \frac{3}{4} g^3 C_A^2 (g_{\alpha\nu} g_{\mu\beta} - g_{\alpha\beta} g_{\mu\nu}) \delta^{ab}. \tag{7.114}$$

Thus, we get in the Landau gauge the following expression,

$$(d_4)_\alpha = \frac{3}{4} g^2 C_A^2 (g_{\alpha\nu} g_{\mu\beta} - g_{\alpha\beta} g_{\mu\nu}) \int_k \Delta^{\mu\sigma}(k+q) \Delta^{\rho\gamma}(k) Y^{\nu\beta}_\gamma(k) B_{\rho\sigma}, \tag{7.115}$$

where we have defined the integral

$$Y^{\nu\beta}_\gamma(k) = \int_l \Delta^{\nu\lambda}(l) \Delta^{\beta\tau}(k+l) \Gamma_{\gamma\tau\lambda}. \tag{7.116}$$

Note that in the Landau gauge, the three-gluon vertex appearing in this integral only contains the regular part, since the transverse projectors of the gluon propagators trigger Eq. (7.9).

As before, the integral in Eq. (7.115) only can be saturated by the external momentum q. Moreover, due to the Bose symmetry of the three-gluon vertex is straightforward to show that the integral Eq. (7.116) is antisymmetric under the $\nu \leftrightarrow \beta$ exchange, and given also the antisymmetry of the prefactor under the same exchange, one can write

$$Y^{\nu\beta}_\gamma(k) = (k^\nu g^\beta_\gamma - k^\beta g^\nu_\gamma) Y(k^2) \quad ; \quad Y(k^2) = \frac{1}{d-1} \frac{k_\nu}{k^2} g^\gamma_\beta Y^{\nu\beta}_\gamma(k). \tag{7.117}$$

With these observations, Eq. (7.115) can be cast in the form

$$(d_4)_\alpha = \frac{q_\alpha}{q^2} q^\lambda (d_4)_\lambda = \frac{3}{2} g^2 C_A^2 \frac{q_\alpha}{q^2} \int_k [(kq) g_{\mu\gamma} + q_\mu q_\gamma] Y(k^2) \Delta^{\mu\sigma}(k+q) \Delta^{\rho\gamma}(k) B_{\rho\sigma}. \tag{7.118}$$

Employing now the results obtained for diagrams (d_1) and (d_4), we derive the complete expression of the transition amplitude in the Landau gauge [see Eq. (7.24)],

$$\begin{aligned} I(q^2) &= \frac{q^\alpha}{q^2}[(d_1)+(d_4)]_\alpha = \frac{i}{q^2}C_A\int_k k^2\Delta^\rho_\mu(k)\Delta^{\mu\sigma}(k+q)B_{\rho\sigma} \\ &+ \frac{3}{2}\frac{g^2C_A^2}{q^2}\int_k[(kq)g_{\mu\gamma}+q_\mu q_\gamma]Y(k^2)\Delta^{\mu\sigma}(k+q)\Delta^{\rho\gamma}(k)B_{\rho\sigma}. \end{aligned} \tag{7.119}$$

To proceed further, we decompose the effective vertex $B_{\rho\sigma}$ in the tensor basis

$$B_{\rho\sigma} = B_1 g_{\rho\sigma}+B_2 q_\rho q_\sigma+B_3(k+q)_\rho(k+q)_\sigma+B_4 k_\rho q_\sigma+B_5 k_\rho(k+q)_\sigma. \tag{7.120}$$

When this decomposition is inserted in Eq. (7.119), only the form factor B_1 survives, since in [64] was shown that $B_2 = 0$ and the rest of form factors are cancelled in the Landau gauge by the transverse projectors. Therefore, Eq. (7.119) becomes

$$\begin{aligned} I(q^2) &= \frac{i}{q^2}C_A\int_k k^2\Delta^\rho_\mu(k)\Delta^\mu_\rho(k+q)B_1 \\ &+ \frac{3}{2}\frac{g^2C_A^2}{q^2}\int_k[(kq)g_{\mu\gamma}+q_\mu q_\gamma]Y(k^2)\Delta^\mu_\rho(k+q)\Delta^{\rho\gamma}(k)B_1, \end{aligned} \tag{7.121}$$

which remarkably allows to express the full transition amplitude for a general momenta only in terms of the single form factor B_1. At this point we arrive at the crucial observation which enables us to relate the mass equation obtained in the context of the PT-BFM formalism with the bound-state formalism showing that, indeed both formalisms are consistent and connected between them. From Eq. (7.83) one may obtain, after identify the $g_{\mu\nu}$ component, a closed expression for the form factor B_1 in terms of the gluon mass, namely

$$\widetilde{I}(q^2)B_1(q,r,p) = m^2(p^2) - m^2(r^2). \tag{7.122}$$

Using this result together with the BQI Eq. (7.44), we obtain from Eq. (7.121) and after a straightforward rearrangement, the following expression for the

square of the transition amplitude,

$$\begin{aligned} I^2(q^2) &= \frac{iC_A}{1+G(q^2)}\frac{1}{q^2}\int_k m^2(k)[(k+q)^2-k^2]\Delta^{\rho}_{\mu}(k)\Delta^{\mu}_{\rho}(k+q) \\ &\times \left\{1+\frac{3}{4}ig^2C_A[Y(k+q)+Y(k)]\right\} - \frac{3}{4}\frac{g^2C_A}{1+G(q^2)}\frac{1}{q^2}(q^2g_{\mu\gamma}-2q_\mu q_\gamma) \\ &\times \int_k m^2(k)[Y(k+q)-Y(k)]\Delta^{\mu}_{\rho}(k+q)\Delta^{\rho\gamma}(k). \end{aligned} \tag{7.123}$$

Thus, using the mass formula Eq. (7.30) to relate the square of the transtion amplitude with the gluon mass in the r.h.s of Eq. (7.123), we recover exactly the full mass equation derived in [72], following a considerably different methodology and formalism.

7.8 Massless bound state formalism VS SDE.

As has become clear throughout this chapter, the gluon mass generation mechanism admits a self-consistent description in the framework of the massless bound state formalism. The fundamental ingredients appearing in this formalism, namely, the transition amplitude I and the B vertices, have been related with the effective gluon mass through a very precise equations, Eq. (7.30) and Eq. (7.122). Furthermore, it has been demonstrated in Section 7.7 that the full mass equation satisfied by the gluon mass may be exactly recovered from Eq. (7.121) using the aforementioned equations. Thus, providing two equivalent formalisms for the description of the dynamically generated gluon mass.

Although equivalents, the study of the gluon mass features in both formalisms proceeds in a rather different form. When the mass equation is derived from the SDE of the gluon propagator following the procedure established in [72] and pictorially summarized in Fig. 6.4, the final answer can be written generically as

$$m^2(q^2) = \int_k \mathcal{K}_{SD}(q,k)m^2(k^2). \tag{7.124}$$

In this expression, the quantity $\mathcal{K}_{SD}$ represents the kernel which contains the one and two-loop dressed contributions to the mass equation. Specifically, the two-loop dressed contribution to that kernel, shown in line A of Fig. 7.15, depends on the integral $Y(k^2)$ defined in Eq. (7.117), containing a fully-dressed three-gluon vertex and two dressed gluon propagators.

Therefore, in this approach, the solutions of Eq. (7.124) are controlled by the approximations realized over such structure. Particularly, in Fig. 7.15, we also show the approximation employed in [72], where the internal gluon propagators and the three-gluon vertex are given by their tree-level values.

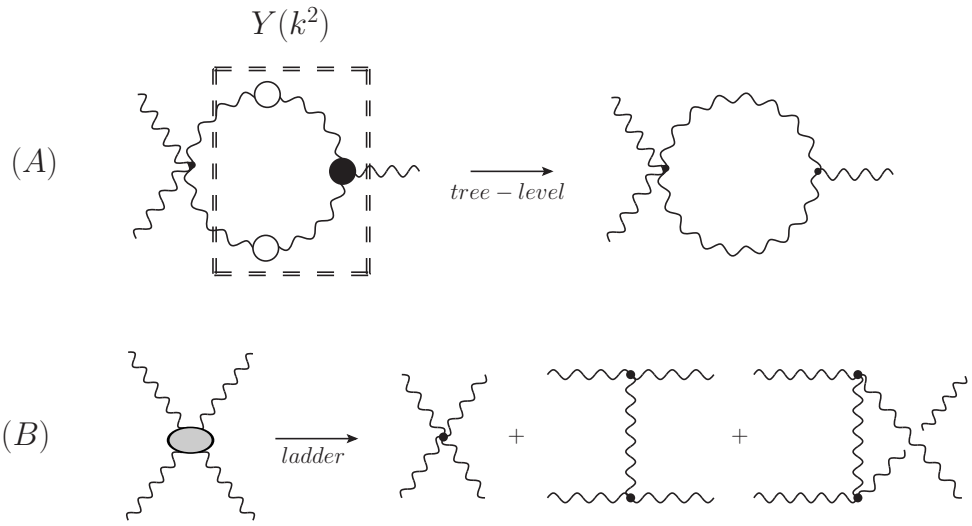

Fig. 7.15: (A) Two-loop dressed contribution to the kernel $\mathcal{K}_{SD}$ of the mass equation and the approximation used in [72]. (B) The kernel $\mathcal{K}_{BS}$ of the BSE satisfied by B_1' and the approximation used in [64].

In what concerns to the bound state formalism, after carrying out the appropriate Taylor expansions, Eq. (7.122) gives in the limit $q \to 0$ the following exact relation for the derivative of the effective gluon mass (Euclidean space)

$$[m^2(p^2)]' = -\widetilde{I}(0)B_1'(p^2). \tag{7.125}$$

Note that this relation was obtained previously in [64] using the WI satisfied by the pole part of the three-gluon vertex. Now, Eq. (7.125) can be integrated giving the result

$$m^2(q^2) = m^2(0) - \widetilde{I}(0)\int_0^{q^2} dx B_1'(x). \tag{7.126}$$

So, in the bound state formalism, the behaviour of the gluon mass is characterized by Eq. (7.126), which in turn depends on the value $\widetilde{I}(0)$ of the transition amplitude and the derivative $B_1'(x)$. These latter quantities are

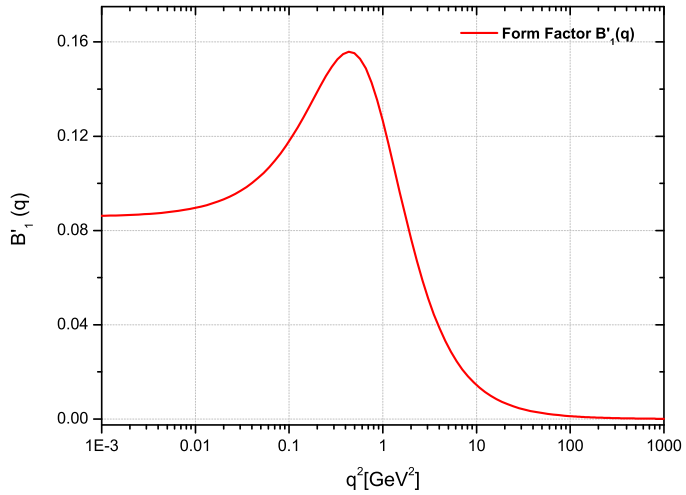

Fig. 7.16: The numerical solution $B_1'(q^2)$ obtained from Eq. (7.128) with $\alpha_s = 0.492$.

determined as follows. First, using the BQI Eq. (7.44) as well as Eq. (7.38) and Eq. (7.30), one obtains

$$\widetilde{I}(0) = F^{-1}(0)I(0) = F^{-1}(0)\sqrt{\frac{m^2(0)}{g^2}} = F^{-1}(0)\sqrt{\frac{\Delta^{-1}(0)}{4\pi\alpha_s}}, \qquad (7.127)$$

which allow us to estimate $\widetilde{I}(0)$ using the values of the ghost dressing function and the gluon propagator at zero momentum, treating α_s as a parameter. Finally, the derivative $B_1'(q^2)$ satisfies its own BSE [see Fig. 7.5 and discussion below], which can be cast in the form

$$B_1'(q^2) = \int_k \mathcal{K}_{BS}(q,k)B_1'(k^2). \qquad (7.128)$$

Here, $\mathcal{K}_{BS}$ corresponds to the BS kernel, shown in line B of Fig. 7.15. Note that, due to the fact that Eq. (7.128) is homogeneous and linear, if $B_1'(q^2)$ is a solution then the function $cB_1'(q^2)$ is also a solution, for any real constant c. The arbitrariness in the constant c is completely eliminated applying Eq. (7.127) as a constraint for a selected value of α_s. Following the above procedure and using the ladder approximation for the BS kernel, shown in Fig. 7.15, we represent in Fig. 7.16 the solution of Eq. (7.128) obtained in [64].

Thus, one has available two different equations, Eq. (7.124) and Eq. (7.126), and formalisms for describe the gluon mass. The fact that both are equivalents and must furnish the same physical description, provides an impressive framework for study the dynamical mass generation mechanism in pure Yang-Mills theories.

8. CONCLUSIONS (CONCLUSIONES).

Throughout this thesis we have established the appropriate framework for the study of the gluon mass generation mechanism in pure Yang-Mills theories. It has been proved rigorously that the gauge-invariant generation of a gluon mass relies on the existence of massless bound-state excitations, which trigger the Schwinger mechanism. We have demonstrated that the presence of these excitations in the skeleton expansions of the fully dressed vertices of the theory induces longitudinally coupled pole structures, giving rise to purely nonperturbative components, the pole vertices V. The fundamental and basic dynamical ingredients of these pole vertices have been exhaustively analyzed and related with the effective gluon mass. Furthermore, the special properties of these new nonperturbative vertices have been exploited to derive the all-order equation governing the evolution of the momentum-dependent gluon mass, which supports monotonically decreasing solutions for the gluon mass.

Without any doubt, the fundamental piece that makes possible the entire construction, are the nonperturbative vertices V, containing the massless poles necessary for triggering the Schwinger mechanism. From the point of view of dynamical mass generation, the appearance of poles in off shell Green's functions is required, once the generation of a gauge-boson mass is energetically favored. In such case (and in the absence of fundamental scalars), these poles will assume the role of Nambu-Goldstone bosons, and their presence is necessary for maintaining all the original STIs intact. Unfortunately, no such proof exists for pure Yang-Mills. A proof along these lines would entail the minimization of an appropriate functional, such as the Cornwall-Jackiw-Tomboulis (CJT) effective potential [4], showing that the generation of a mass, or the formation of the related condensate, lowers the vacuum energy. Note that this is indeed true in $d = 3$ [85], where it was shown that the formation of a gluon condensate, which is interconnected with the gluon mass, minimizes the action (see also [86]).

As has been emphasized in the literature [87, 88], the generation of a

gluon mass is intimately connected with a variety of other related phenomena, and most importantly with the center vortex picture of confinement [89–91]. Once the mass generation mechanism takes place, a possible effective low-energy field theory which incorporates the gluon mass is the gauged non-linear sigma model, known as "massive gauge-invariant $SU(N)$ Yang-Mills" [87]. The corresponding Lagrangian density is

$$\mathcal{L}_{MYM} = \frac{1}{2}G_{\mu\nu}^2 - m^2 Tr[A_\mu - g^{-1}U(\theta)\partial_\mu U^{-1}(\theta)]^2, \tag{8.1}$$

where the gauge field is given by

$$A_\mu(x) = \frac{1}{2i}\sum_{a=1}^{N^2-1}\lambda_a A_\mu^a(x), \tag{8.2}$$

the λ_a are the $SU(N)$ generators (with $Tr\{\lambda_a\lambda_b\} = 2\delta_{ab}$), and the $N \times N$ unitary matrix

$$U(\theta) = \exp\left[\frac{i}{2}\lambda_a\theta^a(x)\right] \tag{8.3}$$

describes the scalar fields $\theta_a(x)$. Note that $\mathcal{L}_{MYM}$ is locally gauge invariant under the combined gauge transformation

$$A'_\mu(x) = V(\omega)A_\mu(x)V^{-1}(\omega) - g^{-1}(\partial_\mu V)V^{-1}, \quad U(\theta') = V(\omega)U(\theta), \tag{8.4}$$

for any group matrix $V \in SU(N)$, where $\omega^a(x)$ are the group parameters. One might think that, by employing Eq. (8.4), the fields θ_a can always be continuously transform to zero, but this is not so if the fields θ_a contain vortices[1]. To use the $\mathcal{L}_{MYM}$ in Eq. (8.1), one solves the equation of motion for U in terms of the gauge potentials and substitutes the result in the equations for the gauge potential. One then finds that this model admits vortex solutions [87], with a long-range pure gauge term in their potentials, which endows them with a topological quantum number corresponding to the center of the gauge group [Z_N for $SU(N)$], and might, in turn, account for quark confinement and gluon screening [88, 93]. Specifically, center vortices of thickness $\sim m^{-1}$, where m is the induced mass of the gluon, may form a condensate when their entropy (per unit size) becomes larger than their action. This condensation would then furnish an area law to

[1] Vortices are solitonic solutions of the equations of motion for the Lagrangian Eq. (8.1), which contain Dirac strings that cannot be gauged away, e.g. [92].

the fundamental representation Wilson loop, thus confining quarks [94]. On the other hand, the adjoint potential between two quarks, studied in an extensive series of works [95–97], would show a roughly linear regime followed by string breaking [98] when the potential energy is about $2m$, corresponding to gluon screening [7, 87].

Fianlly, must be observed that $\mathcal{L}_{MYM}$ is not renormalizable, and breaks down in the ultraviolet. This breakdown simply reflects the fact that the gluon mass m in Eq. (8.1) is assumed to be constant, while, as has been established in this thesis, the SDEs furnish a momentum-dependent gluon mass, vanishing at large q^2.

It would seem, therefore, that a profound, and yet largely unexplored, connection exists between gluon mass generation and confinement.

8. Conclusiones.

A lo largo de esta tesis se ha establecido el apropiado formalismo para el estudio del mecanismo de generación de masa gluónica en teorías puras de Yang-Mills. Se ha probado rigurosamente que la generación de masa gluónica de una manera invariante gauge se basa en la existencia de estados ligados excitados no masivos, los cuales activan el mecanismo Schwinger. También se ha demostrado que la presencia de dichas excitaciones induce nuevas estructuras con polos, acopladas longitudinalmente en los vértices de la teoría, dando lugar a componentes puramente no perturbativas que hemos llamado vértices polo V. Los ingredientes fundamentales y básicos de este tipo de vértices polo han sido extensamente analizados y relacionados con la masa gluónica efectiva. Más aún, las propiedades especiales de estos nuevos vértices no perturbativos se han empleado para derivar la ecuación exacta a todos órdenes que gobierna la evolución de la masa gluónica con la energía y se ha demostrado que la ecuación resultante admite soluciones monotónicamente decrecientes para la masa gluónica.

Sin lugar a dudas, la pieza fundamental que hace posible esta construcción son los vértices no perturbativos V, que contienen los polos necesarios para activar el mecanismo de Schwinger. Desde el punto de vista de la generación dinámica de masa, la aparición de polos en las funciones de Green es requerida una vez que la generación de la masa del bosón de gauge es energéticamente favorable. En tal caso, y en ausencia de campos escalares fundamentales, estos polos asumen el papel de los bosones de Nambu-Goldstone y su presencia es necesaria para mantener todas las STIs de la teoría intactas. Desgraciadamente, hasta el momento no existe ninguna prueba rigurosa de que la generación de masa sea energéticamente favorable en las teorías de Yang-Mills puras. Una demostración de este fenómeno podría involucrar la minimización de un funcional apropiado, como por ejemplo el potencial efectivo de Cornwall-Jackiw-Tomboulis (CJT) [4]. Dicha minimización debería entonces probar que la generación de una masa, o la formación del correspondiente condensado, disminuye la energía del vacío. De hecho, esto se cumple en dimensión $d = 3$ [85] donde fue demostrado que la formación de un condensado de gluones, que a su vez está relacionado con la masa gluónica, minimiza la acción de la teoría (consultar también [86]).

Como se ha enfatizado ampliamente en la literatura [87, 88], la generación de una masa gluónica está íntimamente conectada con una gran variedad de fenómenos no perturbativos y, en particular, con la imagen de

confinamiento proporcionada por una clase especial de vórtices [89–91]. De hecho, una vez que el mecanismo de generación de masa ha tenido lugar, es posible construir una teoría efectiva válida en el rango de bajas energías, la cual incorpora de manera natural la masa gluónica. Este tipo de teorías, conocidas como modelos sigma no lineales o teorías $SU(N)$ gauge invariantes masivas de Yang-Mills [87], están caracterizadas por una densidad Lagrangiana del tipo

$$\mathcal{L}_{MYM} = \frac{1}{2}G_{\mu\nu}^2 - m^2 Tr[A_\mu - g^{-1}U(\theta)\partial_\mu U^{-1}(\theta)]^2, \tag{8.5}$$

donde el campo gauge viene dado por

$$A_\mu(x) = \frac{1}{2i}\sum_{a=1}^{N^2-1}\lambda_a A_\mu^a(x), \tag{8.6}$$

las matrices λ_a son los generadores del grupo $SU(N)$, con $Tr\{\lambda_a\lambda_b\} = 2\delta_{ab}$, y las matrices unitarias de tamaño $N \times N$

$$U(\theta) = \exp\left[\frac{i}{2}\lambda_a\theta^a(x)\right] \tag{8.7}$$

describen los campos escalares $\theta_a(x)$. Se observa entonces que la densidad Lagrangiana $\mathcal{L}_{MYM}$ es localmente invariante gauge bajo las transformaciones de gauge combinadas

$$A'_\mu(x) = V(\omega)A_\mu(x)V^{-1}(\omega) - g^{-1}(\partial_\mu V)V^{-1}, \quad U(\theta') = V(\omega)U(\theta), \tag{8.8}$$

para cada matriz $V \in SU(N)$, siendo $\omega^a(x)$ los parámetros del grupo. Se podría pensar entonces que empleando Eq. (8.8), los campos θ_a siempre pueden ser deformados a cero, pero esto no es posible si los campos θ_a contienen vórtices[2]. Para emplear la densidad lagrangian $\mathcal{L}_{MYM}$ dada en Eq. (8.5), se resuelven en primer lugar las ecuaciones de movimiento de U en función de los potenciales gauge y, seguidamente, se sustituye el resultado en las propias ecuaciones de movimiento del potencial. Cuando esta tarea se lleva a cabo, se descubre que este modelo admite soluciones de tipo vórtice [87]. Estos vórtices son muy característicos ya que contienen en sus potenciales un término gauge puro de largo alcance que dota a los

[2] Los vórtices son soluciones solitónicas de las ecuaciones de movimiento clásicas para la densidad Lagrangiana Eq. (8.5). Dichas soluciones contienen cuerdas de Dirac que no pueden hacerse desaparecer mediante transformaciones de gauge, e.g. [92].

vórtices de un número cuántico topológico relacionado con el centro del grupo gauge [Z_N for $SU(N)$]. Dicho número topológico está relacionado con el confinamiento de quarks y el apantallamiento de gluones [88,93]. Específicamente, esta clase de vórtices de espesor $\sim m^{-1}$, siendo m la masa gluónica inducida, pueden formar un condensado cuando su entropía excede el valor de su acción. Esta condensación debería entonces proporcionar una ley de área para la representación fundamental del lazo de Wilson, confinando por tanto a los quarks [94]. Por otra parte, el potencial adjunto entre dos quarks, estudiado en una gran serie de trabajos [95–97], debería mostrar en esta imagen de confinamiento un régimen lineal con la distancia de separación entre quarks seguido de un proceso de ruptura de cuerda [98] cuando la energía potencial ronda el valor $2m$, correspondiente al apantallamiento de gluones [7, 87].

Por último, debe observarse que la densidad lagrangiana $\mathcal{L}_{MYM}$ no es renormalizable y falla en el ultravioleta. Este fallo simplemente refleja el hecho de que la masa gluónica m en Eq. (8.5) se considera constante mientras que, como se ha establecido en esta tesis, la masa gluónica depende de la energía y se desvanece en el régimen de altas energías.

Parece, por tanto, que existe una profunda y todavía inexplorada conexión entre el mecanismo de generación de masa gluónica y el problema de confinamiento.

APPENDIX

A. THE QCD LAGRANGIAN.

The QCD Lagrangian density is given by

$$\mathcal{L} = \mathcal{L}_{\rm I} + \mathcal{L}_{\rm GF} + \mathcal{L}_{\rm FPG}. \tag{A.1}$$

$\mathcal{L}_{\rm I}$ represents the gauge invariant $SU(3)$ Lagrangian, namely

$$\mathcal{L}_{\rm I} = -\frac{1}{4} F^a_{\mu\nu} F_a^{\mu\nu} + \bar{\psi}^i_f (i\gamma^\mu \mathcal{D}_\mu - m)_{ij} \psi^j_f, \tag{A.2}$$

where $a = 1, \ldots, 8$ (respectively $i, j = 1, 2, 3$) is the color index for the adjoint (respectively fundamental) representation, while f is the flavor index. The field strength is

$$F^a_{\mu\nu} = \partial_\mu A^a_\nu - \partial_\nu A^a_\mu + g f^{abc} A^b_\mu A^c_\nu, \tag{A.3}$$

and the covariant derivative is defined as

$$(\mathcal{D}_\mu)_{ij} = \partial_\mu (\mathbb{I})_{ij} - ig A^a_\mu (t^a)_{ij}, \tag{A.4}$$

with g the (strong) coupling constant. Finally, the $SU(N)$ generators t^a satisfy the commutation relations

$$[t^a, t^b] = i f^{abc} t^c, \tag{A.5}$$

with f^{abc} the totally antisymmetric $SU(N)$ structure constants.

At the classical level, $\mathcal{L}_{\rm I}$ is invariant under the (infinitesimal) local gauge transformations

$$\delta A^a_\mu = -\frac{1}{g} \partial_\mu \theta^a + f^{abc} \theta^b A^c_\mu; \quad \delta \psi^i_f = -i\theta^a (t^a)_{ij} \psi^j_f; \quad \delta \bar{\psi}^i_f = -i\theta^a \bar{\psi}^j_f (t^a)_{ji}, \tag{A.6}$$

where $\theta^a(x)$ are the local infinitesimal parameters corresponding to the $SU(N)$ generators t^a. However, in order to quantize the theory, the gauge invariance needs to be broken; this is achieved through a gauge fixing function $\mathcal{F}^a$, giving rise to the gauge fixing Lagrangian $\mathcal{L}_{\rm GF}$ and its associated

Faddeev-Popov ghost term $\mathcal{L}_{\rm FPG}$. The usual linear R_ξ gauges, correspond to the covariant choice

$$\mathcal{F}^a_{R_\xi} = \partial^\mu A^a_\mu. \tag{A.7}$$

In this case one has

$$\begin{aligned} \mathcal{L}_{\rm GF} &= \frac{1}{2\xi}(\partial^\mu A^a_\mu)^2, \\ \mathcal{L}_{\rm FPG} &= \partial^\mu \bar{c}^a \partial_\mu c^a + g f^{abc}(\partial^\mu \bar{c}^a) A^b_\mu c^c, \end{aligned} \tag{A.8}$$

and the Feynman rules for this choice can be seen in Fig. A.1.

m,μ ∿∿∿ n,ν	$-i\frac{\delta^{mn}}{k^2}\left[g_{\mu\nu}-(1-\xi)\frac{k_\mu k_\nu}{k^2}\right]$	$i\Delta^{mn}_{\mu\nu}(k)$
m ⋯⋯▸⋯⋯ n	$i\frac{\delta^{mn}}{k^2}$	$iD^{mn}(k)$
i,f ——▸—— j,f'	$i\frac{\delta^{ij}\delta^{\mathrm{ff}'}}{k^\mu\gamma_\mu - m_\mathrm{f}}$	$iS^{\mathrm{ff}'}_{ij}(k)$
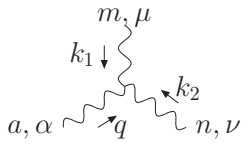	$gf^{amn}\left[g_{\mu\nu}(k_1-k_2)_\alpha + g_{\alpha\nu}(k_2-q)_\mu + g_{\alpha\mu}(q-k_1)_\nu\right]$	$i\Gamma_{A^a_\alpha A^m_\mu A^n_\nu}(k_1,k_2)$
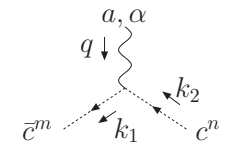	$gf^{amn}k_{1\alpha}$	$i\Gamma_{c^n A^a_\alpha \bar{c}^m}(q,-k_1)$
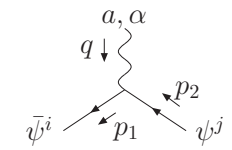	$ig\gamma^\alpha(t^a)_{ij}$	$i\Gamma_{\psi^j A^a_\alpha \bar{\psi}^i}(q,-p_1)$
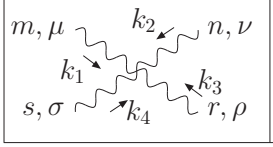	$-ig^2\left[f^{mse}f^{ern}(g_{\mu\rho}g_{\nu\sigma}-g_{\mu\nu}g_{\rho\sigma}) + f^{mne}f^{esr}(g_{\mu\sigma}g_{\nu\rho}-g_{\mu\rho}g_{\nu\sigma}) + f^{mre}f^{esn}(g_{\mu\sigma}g_{\nu\rho}-g_{\mu\nu}g_{\rho\sigma})\right]$	$\Gamma_{A^m_\mu A^n_\nu A^r_\rho A^s_\sigma}(k_2,k_3,k_4)$

Fig. A.1: Feynman rules for QCD in the R_ξ gauges. The first two columns show the lowest order Feynman diagrams and rule respectively, while the last one shows the corresponding all-order Green's function.

B. THE BACKGROUND FIELD METHOD.

In the background field method (BFM) [25, 47] one splits the gauge field appearing in the Lagrangian into a classical background field, $\widehat{A}^a_\mu$, and a fluctuating quantum field, A^a_μ, i.e.,

$$A^a_\mu \longmapsto \widehat{A}^a_\mu + A^a_\mu. \tag{B.1}$$

Then, one defines the so called covariant background field derivative as

$$\widehat{\mathcal{D}}^{ab}_\mu = \delta^{ab}\partial_\mu + g f^{amb}\widehat{A}^m_\mu, \tag{B.2}$$

so that the (covariant) gauge fixing function in this case is given by

$$\widehat{\mathcal{F}}^a = (\widehat{\mathcal{D}}^\mu A_\mu)^a = \partial^\mu A^a_\mu + g f^{abc}\widehat{A}^b_\mu A^\mu_c. \tag{B.3}$$

With this choice the gauge fixing term is given by

$$\mathcal{L}^{\rm BFM}_{\rm GF} = \frac{1}{2\xi_Q}(\widehat{\mathcal{F}}^a)^2, \tag{B.4}$$

where ξ_Q is the gauge fixing parameter of the quantum gauge field, whereas the associated Faddeev-Popov term becomes

$$\begin{aligned}\mathcal{L}^{\rm BFM}_{\rm FPG} &= \partial^\mu\bar{c}^a\partial_\mu c^a + g f^{abc}(\partial^\mu\bar{c}^a)A^b_\mu c^c + g f^{abc}(\partial^\mu\bar{c}^a)\widehat{A}^b_\mu c^c \\ &- g f^{abc}\bar{c}^a\widehat{A}^b_\mu(\partial^\mu c^c) - g^2 f^{abe}f^{cde}\bar{c}^a\widehat{A}^b_\mu(A^\mu_c + \widehat{A}^\mu_c)c^d.\end{aligned} \tag{B.5}$$

Notice the appearance of a modified ghost sector respect to the usual linear R_ξ gauges. Specifically, the interaction between ghosts and background gluons are very characteristic, consisting of a symmetric $\widehat{A}c\bar{c}$ ghost vertex and a completely new, four particle vertex, $\widehat{A}Ac\bar{c}$. The corresponding Feynman rules are listed below, in Fig. B.1. But, the crucial feature that makes the BFM such an advantageous way of quantizing gauge theories is the following. With the choice of the gauge fixing function Eq. (B.3), even

after the gauge-fixing procedure, the Lagarangian is still invariant under the following (infinitesimal) gauge transformations of the background field,

$$\delta\widehat{A}^a_\mu = -\frac{1}{g}\partial_\mu\widehat{\theta}^a + f^{abc}\widehat{\theta}^b\widehat{A}^c_\mu. \tag{B.6}$$

Notice that the (infinitesimal) parameter of the gauge transformation above has been denoted by $\widehat{\theta}$, because it is different from the one appearing in the gauge transformations of the quantum field A.

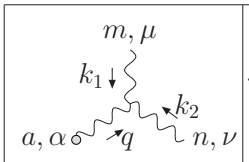	$gf^{amn}\left[g_{\mu\nu}(k_1-k_2)_\alpha + g_{\alpha\nu}(k_2-q+\frac{1}{\xi}k_1)_\mu + g_{\alpha\mu}(q-k_1-\frac{1}{\xi}k_2)_\nu\right]$	$i\Gamma_{\widehat{A}^a_\alpha A^m_\mu A^n_\nu}(k_1,k_2)$
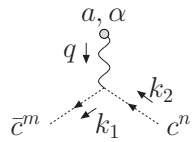	$gf^{amn}(k_1+k_2)_\alpha$	$i\Gamma_{c^n\widehat{A}^a_\alpha\bar{c}^m}(q,-k_1)$
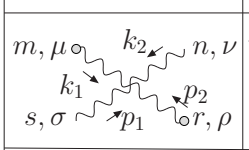	$-ig^2\left[f^{mse}f^{ern}(g_{\mu\rho}g_{\nu\sigma}-g_{\mu\nu}g_{\rho\sigma}+\frac{1}{\xi}g_{\mu\sigma}g_{\nu\rho}) + f^{mne}f^{esr}(g_{\mu\sigma}g_{\nu\rho}-g_{\mu\rho}g_{\nu\sigma}-\frac{1}{\xi}g_{\mu\nu}g_{\rho\sigma}) + f^{mre}f^{esn}(g_{\mu\sigma}g_{\nu\rho}-g_{\mu\nu}g_{\rho\sigma})\right]$	$\Gamma_{\widehat{A}^m_\mu A^n_\nu \widehat{A}^r_\rho A^s_\sigma}(k_2,p_2,p_1)$
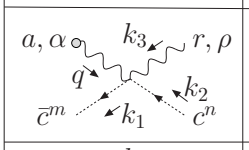	$-ig^2 g_{\alpha\rho}f^{mae}f^{ern}$	$\Gamma_{c^n\widehat{A}^a_\alpha A^r_\rho\bar{c}^m}(q,k_3,-k_1)$
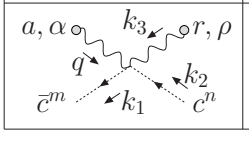	$-ig^2 g_{\alpha\rho}(f^{mae}f^{ern}+f^{mre}f^{ean})$	$\Gamma_{c^n\widehat{A}^a_\alpha\widehat{A}^r_\rho\bar{c}^m}(q,k_3,-k_1)$

Fig. B.1: Feynman rules for QCD in the BFM gauge. We only include those rules which are different from the R_ξ ones to lowest order. A gray circle on a gluon line indicates a background field.

So, the whole Lagrangian retains (background) gauge invariance with respect to the $\widehat{A}$ field. As a consequence, the background field only appears in external lines because the $\widehat{A}$ propagator is not defined. The gauge symmetry is, however, explicitly broken by the quantum field A, which enters only in loops.

BIBLIOGRAPHY

[1] H. D. Politzer, "Asymptotic Freedom: An Approach to Strong Interactions," Phys. Rept. **14** (1974) 129.

[2] F. J. Dyson, "The S matrix in quantum electrodynamics," Phys. Rev. **75** (1949) 1736.

[3] J. S. Schwinger, "On the Green's functions of quantized fields. 1.," Proc. Nat. Acad. Sci. **37** (1951) 452.

[4] J. M. Cornwall, R. Jackiw and E. Tomboulis, "Effective Action for Composite Operators," Phys. Rev. D **10** (1974) 2428.

[5] W. J. Marciano and H. Pagels, "Quantum Chromodynamics: A Review," Phys. Rept. **36** (1978) 137.

[6] K. D. Lane, "Asymptotic Freedom and Goldstone Realization of Chiral Symmetry," Phys. Rev. D **10** (1974) 2605.

[7] J. M. Cornwall, "Dynamical Mass Generation in Continuum QCD," Phys. Rev. D **26** (1982) 1453.

[8] J. S. Schwinger, "Gauge Invariance and Mass," Phys. Rev. **125** (1962) 397.

[9] J. S. Schwinger, "Gauge Invariance and Mass. 2.," Phys. Rev. **128** (1962) 2425.

[10] P. W. Higgs, "Broken Symmetries and the Masses of Gauge Bosons," Phys. Rev. Lett. **13** (1964) 508.

[11] P. W. Higgs, "Broken symmetries, massless particles and gauge fields," Phys. Lett. **12** (1964) 132.

[12] F. Englert and R. Brout, "Broken Symmetry and the Mass of Gauge Vector Mesons," Phys. Rev. Lett. **13** (1964) 321.

[13] G. S. Guralnik, C. R. Hagen and T. W. B. Kibble, "Global Conservation Laws and Massless Particles," Phys. Rev. Lett. **13** (1964) 585.

[14] P. W. Higgs, "Spontaneous Symmetry Breakdown without Massless Bosons," Phys. Rev. **145** (1966) 1156.

[15] E. Eichten and F. Feinberg, "Dynamical Symmetry Breaking of Nonabelian Gauge Symmetries," Phys. Rev. D **10** (1974) 3254.

[16] E. C. Poggio, E. Tomboulis and S. -H. H. Tye, "Dynamical Symmetry Breaking in Nonabelian Field Theories," Phys. Rev. D **11** (1975) 2839.

[17] Y. Nambu, "Quasiparticles and Gauge Invariance in the Theory of Superconductivity," Phys. Rev. **117** (1960) 648.

[18] J. Goldstone, "Field Theories with Superconductor Solutions," Nuovo Cim. **19** (1961) 154.

[19] J. Goldstone, A. Salam and S. Weinberg, "Broken Symmetries," Phys. Rev. **127** (1962) 965.

[20] Y. Nambu and G. Jona-Lasinio, "Dynamical Model Of Elementary Particles Based On An Analogy With Superconductivity. Ii," Phys. Rev. **124** (1961) 246.

[21] Y. Nambu and G. Jona-Lasinio, "Dynamical Model of Elementary Particles Based on an Analogy with Superconductivity. 1.," Phys. Rev. **122** (1961) 345.

[22] A. C. Aguilar, D. Binosi and J. Papavassiliou, "The dynamical equation of the effective gluon mass," Phys. Rev. D **84** (2011) 085026 [arXiv:1107.3968 [hep-ph]].

[23] D. Binosi and J. Papavassiliou, "Pinch Technique: Theory and Applications," Phys. Rept. **479** (2009) 1 [arXiv:0909.2536 [hep-ph]].

[24] A. Pilaftsis, "Generalized pinch technique and the background field method in general gauges," Nucl. Phys. B **487**, 467 (1997) [hep-ph/9607451].

[25] L. F. Abbott, "Introduction to the Background Field Method," Acta Phys. Polon. B **13** (1982) 33.

[26] A. C. Aguilar, D. Binosi and J. Papavassiliou, "Gluon and ghost propagators in the Landau gauge: Deriving lattice results from Schwinger-Dyson equations," Phys. Rev. D **78** (2008) 025010 [arXiv:0802.1870 [hep-ph]].

[27] A. C. Aguilar, D. Binosi and J. Papavassiliou, "Unquenching the gluon propagator with Schwinger-Dyson equations," Phys. Rev. D **86** (2012) 014032 [arXiv:1204.3868 [hep-ph]].

[28] J. Skullerud and A. Kizilersu, "Quark gluon vertex from lattice QCD," JHEP **0209** (2002) 013 [hep-ph/0205318].

[29] C. Alexandrou, P. De Forcrand and E. Follana, "The Laplacian gauge gluon propagator in SU(N(c))," Phys. Rev. D **65** (2002) 117502 [hep-lat/0203006].

[30] C. Alexandrou, P. de Forcrand and E. Follana, "The Gluon propagator without lattice Gribov copies on a finer lattice," Phys. Rev. D **65** (2002) 114508 [hep-lat/0112043].

[31] C. Alexandrou, P. de Forcrand and E. Follana, "The Gluon propagator without lattice Gribov copies," Phys. Rev. D **63** (2001) 094504 [hep-lat/0008012].

[32] I. L. Bogolubsky, E. M. Ilgenfritz, M. Muller-Preussker and A. Sternbeck, "The Landau gauge gluon and ghost propagators in 4D SU(3) gluodynamics in large lattice volumes," PoS LAT **2007** (2007) 290 [arXiv:0710.1968 [hep-lat]].

[33] P. O. Bowman, U. M. Heller, D. B. Leinweber, M. B. Parappilly, A. Sternbeck, L. von Smekal, A. G. Williams and J. -b. Zhang, "Scaling behavior and positivity violation of the gluon propagator in full QCD," Phys. Rev. D **76** (2007) 094505 [hep-lat/0703022 [HEP-LAT]].

[34] I. L. Bogolubsky, E. M. Ilgenfritz, M. Muller-Preussker and A. Sternbeck, "Lattice gluodynamics computation of Landau gauge Green's functions in the deep infrared," Phys. Lett. B **676** (2009) 69 [arXiv:0901.0736 [hep-lat]].

[35] O. Oliveira and P. J. Silva, "The Lattice infrared Landau gauge gluon propagator: The Infinite volume limit," PoS LAT **2009** (2009) 226 [arXiv:0910.2897 [hep-lat]].

[36] A. Cucchieri and T. Mendes, "What's up with IR gluon and ghost propagators in Landau gauge? A puzzling answer from huge lattices," PoS LAT **2007** (2007) 297 [arXiv:0710.0412 [hep-lat]].

[37] A. Cucchieri and T. Mendes, "Constraints on the IR behavior of the gluon propagator in Yang-Mills theories," Phys. Rev. Lett. **100** (2008) 241601 [arXiv:0712.3517 [hep-lat]].

[38] A. Cucchieri and T. Mendes, "Landau-gauge propagators in Yang-Mills theories at beta = 0: Massive solution versus conformal scaling," Phys. Rev. D **81** (2010) 016005 [arXiv:0904.4033 [hep-lat]].

[39] A. C. Aguilar, D. Binosi and J. Papavassiliou, "QCD effective charges from lattice data," JHEP **1007** (2010) 002 [arXiv:1004.1105 [hep-ph]].

[40] A. C. Aguilar and J. Papavassiliou, "Chiral symmetry breaking with lattice propagators," Phys. Rev. D **83** (2011) 014013 [arXiv:1010.5815 [hep-ph]].

[41] A. C. Aguilar, A. A. Natale and P. S. Rodrigues da Silva, "Relating a gluon mass scale to an infrared fixed point in pure gauge QCD," Phys. Rev. Lett. **90** (2003) 152001 [hep-ph/0212105].

[42] A. C. Aguilar and J. Papavassiliou, "Gluon mass generation in the PT-BFM scheme," JHEP **0612** (2006) 012 [hep-ph/0610040].

[43] A. C. Aguilar and J. Papavassiliou, "Gluon mass generation without seagull divergences," Phys. Rev. D **81** (2010) 034003 [arXiv:0910.4142 [hep-ph]].

[44] J. M. Cornwall and J. Papavassiliou, "Gauge Invariant Three Gluon Vertex in QCD," Phys. Rev. D **40** (1989) 3474.

[45] D. Binosi and J. Papavassiliou, "The Pinch technique to all orders," Phys. Rev. D **66** (2002) 111901 [hep-ph/0208189].

[46] D. Binosi and J. Papavassiliou, "Pinch technique selfenergies and vertices to all orders in perturbation theory," J. Phys. G G **30** (2004) 203 [hep-ph/0301096].

[47] L. F. Abbott, "The Background Field Method Beyond One Loop," Nucl. Phys. B **185** (1981) 189.

[48] J. S. Ball and T. -W. Chiu, "Analytic Properties Of The Vertex Function In Gauge Theories. 2.," Phys. Rev. D **22** (1980) 2550 [Erratum-ibid. D **23** (1981) 3085].

[49] C. Becchi, A. Rouet and R. Stora, "Renormalization of Gauge Theories," Annals Phys. **98** (1976) 287.

[50] C. Becchi, A. Rouet and R. Stora, "Renormalization of the Abelian Higgs-Kibble Model," Commun. Math. Phys. **42** (1975) 127.

[51] D. Binosi and J. Papavassiliou, "Gauge-invariant truncation scheme for the Schwinger-Dyson equations of QCD," Phys. Rev. D **77** (2008) 061702 [arXiv:0712.2707 [hep-ph]].

[52] D. Binosi and J. Papavassiliou, "New Schwinger-Dyson equations for non-Abelian gauge theories," JHEP **0811** (2008) 063 [arXiv:0805.3994 [hep-ph]].

[53] J. S. Ball and T. -W. Chiu, "Analytic Properties of the Vertex Function in Gauge Theories. 1.," Phys. Rev. D **22** (1980) 2542.

[54] P. A. Grassi, T. Hurth and M. Steinhauser, "Practical algebraic renormalization," Annals Phys. **288** (2001) 197 [hep-ph/9907426].

[55] D. Binosi and J. Papavassiliou, "Pinch technique and the Batalin-Vilkovisky formalism," Phys. Rev. D **66** (2002) 025024 [hep-ph/0204128].

[56] I. A. Batalin and G. A. Vilkovisky, "Relativistic S Matrix of Dynamical Systems with Boson and Fermion Constraints," Phys. Lett. B **69** (1977) 309.

[57] I. A. Batalin and G. A. Vilkovisky, "Gauge Algebra and Quantization," Phys. Lett. B **102** (1981) 27.

[58] P. A. Grassi, T. Hurth and A. Quadri, "On the Landau background gauge fixing and the IR properties of YM Green functions," Phys. Rev. D **70** (2004) 105014 [hep-th/0405104].

[59] A. C. Aguilar, D. Binosi, J. Papavassiliou and J. Rodriguez-Quintero, "Non-perturbative comparison of QCD effective charges," Phys. Rev. D **80** (2009) 085018 [arXiv:0906.2633 [hep-ph]].

[60] A. C. Aguilar, D. Binosi and J. Papavassiliou, "Indirect determination of the Kugo-Ojima function from lattice data," JHEP **0911** (2009) 066 [arXiv:0907.0153 [hep-ph]].

[61] R. Jackiw and K. Johnson, "Dynamical Model of Spontaneously Broken Gauge Symmetries," Phys. Rev. D **8** (1973) 2386.

[62] R. Jackiw, "Dynamical Symmetry Breaking," In *Erice 1973, Proceedings, Laws Of Hadronic Matter*, New York 1975, 225-251 and M I T Cambridge - COO-3069-190 (73,REC.AUG 74) 23p

[63] J. M. Cornwall and R. E. Norton, "Spontaneous Symmetry Breaking Without Scalar Mesons," Phys. Rev. D **8** (1973) 3338.

[64] A. C. Aguilar, D. Ibanez, V. Mathieu and J. Papavassiliou, "Massless bound-state excitations and the Schwinger mechanism in QCD," Phys. Rev. D **85** (2012) 014018 [arXiv:1110.2633 [hep-ph]].

[65] D. Binosi and J. Papavassiliou, "Gauge invariant Ansatz for a special three-gluon vertex," JHEP **1103** (2011) 121 [arXiv:1102.5662 [hep-ph]].

[66] A. Salam, "Renormalizable electrodynamics of vector mesons," Phys. Rev. **130**, 1287 (1963);

[67] A. Salam and R. Delbourgo, "Renormalizable electrodynamics of scalar and vector mesons. II," Phys. Rev. **135**, B1398 (1964);

[68] R. Delbourgo and P. C. West, "A Gauge Covariant Approximation To Quantum Electrodynamics," J. Phys. A **10**, 1049 (1977);

[69] R. Delbourgo and P. C. West, "Infrared Behavior Of A Gauge Covariant Approximation," Phys. Lett. B **72**, 96 (1977).

[70] A. Kizilersu and M. R. Pennington, "Building the Full Fermion-Photon Vertex of QED by Imposing Multiplicative Renormalizability of the Schwinger-Dyson Equations for the Fermion and Photon Propagators," Phys. Rev. D **79**, 125020 (2009); [arXiv:0904.3483 [hep-th]].

[71] A. Bashir, A. Kizilersu and M. R. Pennington, "The non-perturbative three-point vertex in massless quenched QED and perturbation theory constraints," Phys. Rev. D **57**, 1242 (1998). [arXiv:hep-ph/9707421].

[72] D. Binosi, D. Ibanez and J. Papavassiliou, "The all-order equation of the effective gluon mass," Phys. Rev. D **86** (2012) 085033 [arXiv:1208.1451 [hep-ph]].

[73] J. Rodriguez-Quintero, "The low-momentum ghost dressing function and the gluon mass," PoS LC **2010** (2010) 023 [arXiv:1011.1392 [hep-ph]].

[74] D. Dudal, J. A. Gracey, S. P. Sorella, N. Vandersickel and H. Verschelde, "A Refinement of the Gribov-Zwanziger approach in the Landau gauge: Infrared propagators in harmony with the lattice results," Phys. Rev. D **78** (2008) 065047 [arXiv:0806.4348 [hep-th]].

[75] P. Boucaud, J. P. Leroy, A. Le Yaouanc, J. Micheli, O. Pene and J. Rodriguez-Quintero, "On the IR behaviour of the Landau-gauge ghost propagator," JHEP **0806** (2008) 099 [arXiv:0803.2161 [hep-ph]].

[76] C. D. Roberts and A. G. Williams, "Dyson-Schwinger equations and their application to hadronic physics," Prog. Part. Nucl. Phys. **33** (1994) 477 [hep-ph/9403224].

[77] W. H. Press, S. A. Teukolsky, W. T. Vetterling and B. P. Flannery, "Numerical Recipes in FORTRAN: The Art of Scientific Computing," ISBN-9780521430647.

[78] J. C. R. Bloch, "Two loop improved truncation of the ghost gluon Dyson-Schwinger equations: Multiplicatively renormalizable propagators and nonperturbative running coupling," Few Body Syst. **33** (2003) 111 [hep-ph/0303125].

[79] M. Lavelle, Phys. Rev. D **44** (1991) 26.

[80] A. C. Aguilar and J. Papavassiliou, "Power-law running of the effective gluon mass," Eur. Phys. J. A **35** (2008) 189 [arXiv:0708.4320 [hep-ph]].

[81] D. Ibanez and J. Papavassiliou, "Massive gluon propagator in the massless bound-state formalism," In preparation.

[82] C. S. Fischer, A. Maas and J. M. Pawlowski, "On the infrared behavior of Landau gauge Yang-Mills theory," Annals Phys. **324**, 2408 (2009).

[83] D. Ibanez, "Explicit construction of the pole part of the three-gluon vertex," PoS QCD **-TNT-II** (2011) 025 [arXiv:1112.5081 [hep-ph]].

[84] J. M. Cornwall and W. -S. Hou, "Extension Of The Gauge Technique To Broken Symmetry And Finite Temperature," Phys. Rev. D **34**, 585 (1986).

[85] J. M. Cornwall, "Exact zero momentum sum rules in d = 3 gauge theory," Nucl. Phys. B **416** (1994) 335.

[86] J. Alexandre and N. E. Mavromatos, "A Lorentz-Violating Alternative to Higgs Mechanism?," Phys. Rev. D **84** (2011) 105013 [arXiv:1108.3983 [hep-ph]].

[87] J. M. Cornwall, "Quark Confinement and Vortices in Massive Gauge Invariant QCD," Nucl. Phys. B **157** (1979) 392.

[88] J. M. Cornwall, "Center vortices and confinement versus screening," Phys. Rev. D **57** (1998) 7589 [hep-th/9712248].

[89] J. Greensite, "The Confinement problem in lattice gauge theory," Prog. Part. Nucl. Phys. **51** (2003) 1 [hep-lat/0301023].

[90] J. Greensite, K. Langfeld, S. Olejnik, H. Reinhardt and T. Tok, "Color Screening, Casimir Scaling, and Domain Structure in G(2) and SU(N) Gauge Theories," Phys. Rev. D **75** (2007) 034501 [hep-lat/0609050].

[91] D. Ibanez, "Topological aspects of confinement," Master thesis (2009), Department of Theoretical Physics (University of Valencia).

[92] H. Reinhardt, "Topology of center vortices," Nucl. Phys. B **628** (2002) 133 [hep-th/0112215].

[93] C. W. Bernard, "Adjoint Wilson Lines And The Effective Gluon Mass," Nucl. Phys. B **219** (1983) 341.

[94] K. G. Wilson, "Confinement of Quarks," Phys. Rev. D **10** (1974) 2445.

[95] J. Greensite, B. Lucini and A. Patella, "k-string tensions and the 1/N expansion," Phys. Rev. D **83** (2011) 125019 [arXiv:1101.5344 [hep-th]].

[96] J. Greensite and S. Olejnik, "Constituent Gluon Content of the Static Quark-Antiquark State in Coulomb Gauge," Phys. Rev. D **79** (2009) 114501 [arXiv:0901.0199 [hep-lat]].

[97] P. Gonzalez, V. Vento and V. Mathieu, "Non Perturbative One Gluon Exchange Potential from Dyson-Schwinger Equations," arXiv:1207.4314 [hep-ph].

[98] J. Greensite and C. B. Thorn, "Gluon chain model of the confining force," JHEP **0202** (2002) 014 [hep-ph/0112326].